



NRL/MR/6730--14-9572

Comparison of Fresh and Aged TNT with Multiwavelength Raman Spectroscopy

ROBERT LUNSFORD
JACOB GRUN

*Laser Plasma Branch
Plasma Physics Division*

PRATIMA KUNAPAREDDY

*Research Support Instruments
Lanham, Maryland*

December 4, 2014

Approved for public release; distribution is unlimited.

REPORT DOCUMENTATION PAGE				Form Approved OMB No. 0704-0188	
Public reporting burden for this collection of information is estimated to average 1 hour per response, including the time for reviewing instructions, searching existing data sources, gathering and maintaining the data needed, and completing and reviewing this collection of information. Send comments regarding this burden estimate or any other aspect of this collection of information, including suggestions for reducing this burden to Department of Defense, Washington Headquarters Services, Directorate for Information Operations and Reports (0704-0188), 1215 Jefferson Davis Highway, Suite 1204, Arlington, VA 22202-4302. Respondents should be aware that notwithstanding any other provision of law, no person shall be subject to any penalty for failing to comply with a collection of information if it does not display a currently valid OMB control number. PLEASE DO NOT RETURN YOUR FORM TO THE ABOVE ADDRESS.					
1. REPORT DATE (DD-MM-YYYY) 04-12-2014		2. REPORT TYPE Memorandum		3. DATES COVERED (From - To) Jan 2010 – Jan 2013 and Mar 2013 – Sept 2014	
4. TITLE AND SUBTITLE Comparison of Fresh and Aged TNT with Multiwavelength Raman Spectroscopy				5a. CONTRACT NUMBER	
				5b. GRANT NUMBER N0001410AF00002	
				5c. PROGRAM ELEMENT NUMBER	
6. AUTHOR(S) Robert Lunsford, Jacob Grun, and Pratima Kunapareddy ¹				5d. PROJECT NUMBER	
				5e. TASK NUMBER	
				5f. WORK UNIT NUMBER	
7. PERFORMING ORGANIZATION NAME(S) AND ADDRESS(ES) Naval Research Laboratory 4555 Overlook Avenue, SW Washington, DC 20375-5320				8. PERFORMING ORGANIZATION REPORT NUMBER NRL/MR/6730--14-9572	
9. SPONSORING / MONITORING AGENCY NAME(S) AND ADDRESS(ES) Office of Naval Research One Liberty Center 875 North Randolph Street, Suite 1425 Arlington, VA 22203-1995				10. SPONSOR / MONITOR'S ACRONYM(S) ONR	
				11. SPONSOR / MONITOR'S REPORT NUMBER(S)	
12. DISTRIBUTION / AVAILABILITY STATEMENT Approved for public release; distribution is unlimited.					
13. SUPPLEMENTARY NOTES ¹ Research Support Instruments, 4325 Forbes Blvd., Lanham, MD 20706					
14. ABSTRACT Differences in the Raman signatures of fresh and environmentally aged explosives could allow a warfighter who has identified the presence of trace amounts of explosives to ascertain if the material detected is the remnant of a previous event that has been exposed to the environment for a period of time or is an indication of a current threat. To determine if environmental exposure alters Raman signatures, we examined the signatures of fresh and artificially aged TNT at multiple illumination wavelengths between 420 and 620 nanometers. While the macroscopic differences (such as peak height and line ratios) between the Raman signatures of the fresh and aged samples are either too small or not reproducible enough to use for differentiation, we find that by utilizing an algorithm based on the Pearson correlation coefficient, differentiation can be made between the fresh and aged variants at an accuracy of 82%.					
15. SUBJECT TERMS Raman spectroscopy TNT Multiple wavelength					
16. SECURITY CLASSIFICATION OF:			17. LIMITATION OF ABSTRACT Unclassified Unlimited	18. NUMBER OF PAGES 56	19a. NAME OF RESPONSIBLE PERSON Robert Lunsford
a. REPORT Unclassified Unlimited	b. ABSTRACT Unclassified Unlimited	c. THIS PAGE Unclassified Unlimited			19b. TELEPHONE NUMBER (include area code) (202) 404-4354

Introduction

Raman spectroscopy has been shown⁽¹⁻⁴⁾ as an effective diagnostic for detection of explosives in the environment. This detection has also been shown to be effective at trace levels^(5,6) and in complex backgrounds⁽⁷⁻⁹⁾. In addition studies have been done⁽¹⁰⁻¹²⁾ on the environmental decomposition of explosives demonstrating that there are chemical changes which occur due to exposure to the elements. If differentiable these variations in the Raman signatures of fresh and environmentally aged explosives could allow a warfighter who has identified the presence of trace amounts of explosives to ascertain if the material detected is the remnant of a previous event which has been exposed to the environment for a period of time or is an indication of a current threat. To determine if environmental exposure can detectably alter the Raman signatures of an explosive we examine the spectra of fresh and artificially aged TNT.

Raman signatures were obtained on the SWOrRD (Swept Wavelength Optical resonance Raman Detector) system at the US Naval Research Laboratory. The samples were measured at a series of illumination wavelengths ranging from 420nm and 620nm in 10 nm intervals. These individual Raman signatures were processed to remove noise and correct for fluorescence and then combined to create a multi-wavelength signature as shown in Figure 1. The explosives were measured in multiple batches as well as at multiple points on each sample.

Our examination shows that by utilizing a specific set of signal processing routines and an algorithm based on the Pearson correlation coefficient, correct differentiation between the fresh and aged variants of TNT could be made 82% of the time.

To conclude the project, the samples were sent to the Swedish Defense Research Agency for chemical testing and analysis^(22, 23). The samples were examined by several standard analytic techniques¹³ such as Fourier Transform Infra-Red analysis (FT-IR), Gas Chromatograph and Liquid Chromatograph Mass Spectroscopy (GC-MS, LC-MS), High Performance Liquid Chromatography (HPLC), Nuclear Magnetic Resonance (NMR), Thermogravimetric Analysis (TGA), and Differential Scanning Calorimetry (DSC). The results of these tests show that there are some slight differences inherent in the chemical structure between the fresh and aged variants. This is particularly true of UV aging which had the greater effect on the sample of the two aging processes tested.

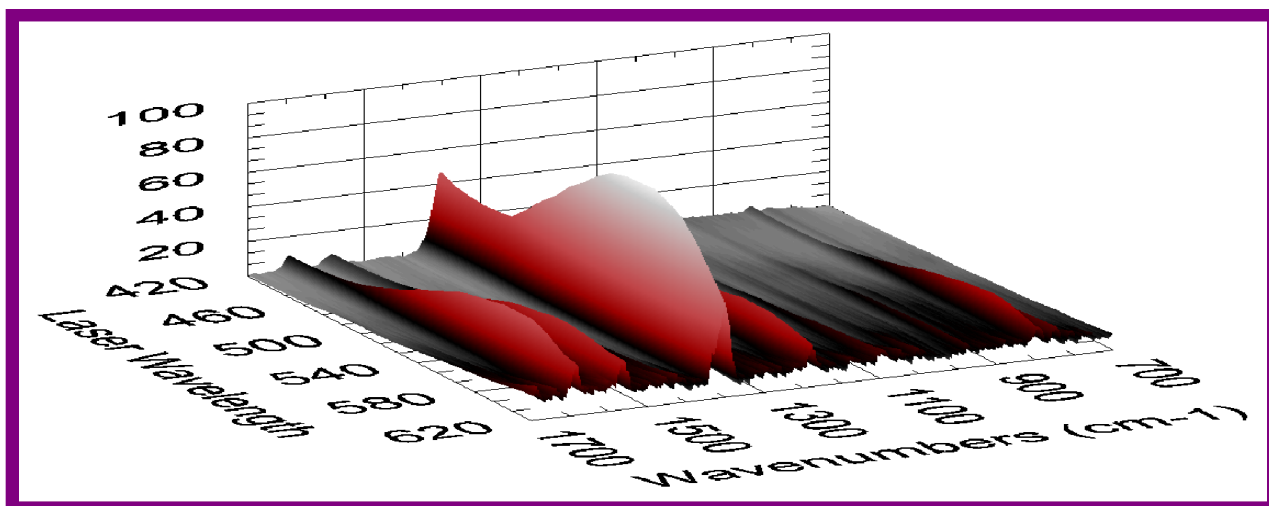
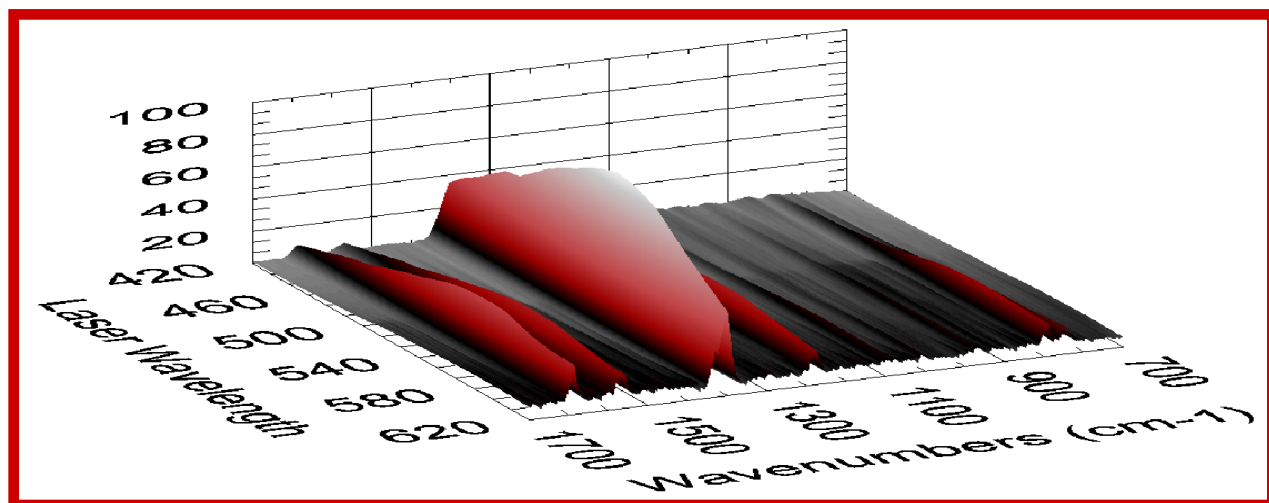
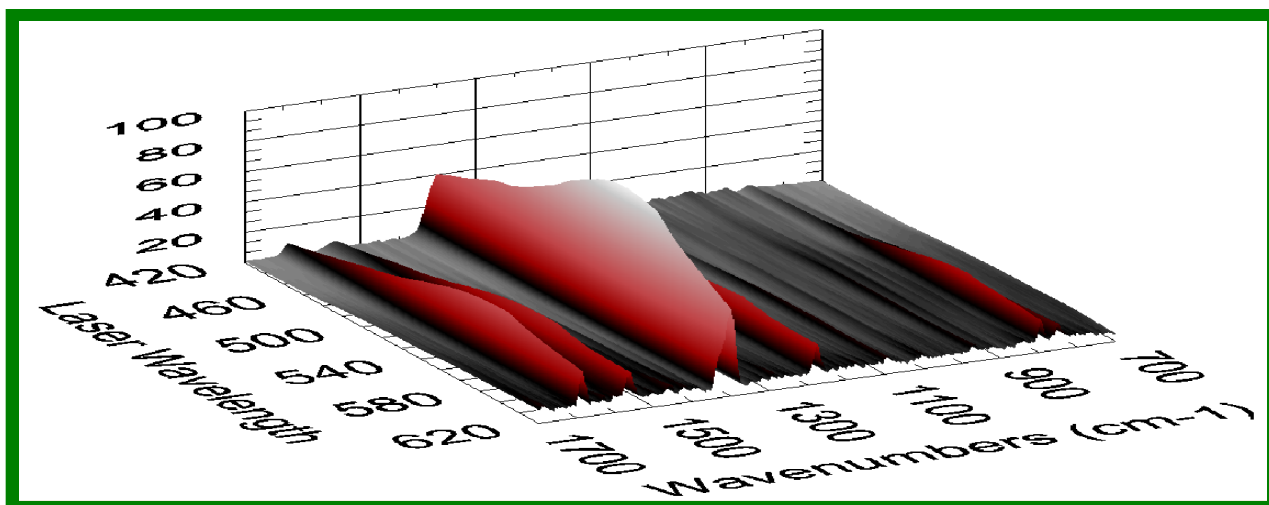


Figure 1: Multiwavelength Raman Signatures for TNT : A series of Raman spectra taken at sequential laser illumination wavelengths are combined to form a single 2-dimensional structure which can then be analyzed along either the Laser Wavelength or Wavenumber axis. The top spectrum is the signature of Fresh TNT, the second is Heat Aged TNT and the third is UV Aged TNT.

SWOrRD System

The experiment is performed with the Swept Wavelength Optical resonant Raman Detector (SWOrRD) at the U.S. Naval Research Laboratory⁽¹⁴⁻¹⁷⁾. SWOrRD is a spectroscopy system capable of rapidly acquiring the spectral signatures of both solid, liquid and gaseous samples illuminated by a range of laser wavelengths. The SWOrRD apparatus includes a tunable OPO (optical parametric oscillator) pumped by Q-switched frequency-tripled Nd:YAG diode-pumped solid state laser. The laser generates 5 ns pulses at a 1 kHz pulse repetition rate and is wavelength selectable in bands between 210nm and 350 nm, 420 nm and 700 nm, and 710nm and 2100 nm in steps as small as 0.1nm. The average laser power incident on the sample ranges from 10 mW in the ultraviolet to 50 mW in the visible and is measured before and during each acquisition thus allowing spectra acquired at different laser wavelengths to be scaled to a single common energy on target.

Samples were initially tested at laser wavelengths ranging from 220nm to 280 nm. However the large absorption of bulk TNT in the UV resulted in poor data quality. Because of this, we switched to visible illumination wavelengths between 420nm to 620nm. To acquire signatures, the samples are placed on a brass plate and illuminated with the SWOrRD laser from above. Light scattered from the illuminated sample is collected at an angle of 90 degrees with respect to incident laser beam and is focused onto the entrance slit of an Acton double spectrometer consisting of two 0.5 meter stages with a selection of gratings. A Pixus CCD camera, back illuminated and coated for enhanced UV response provides detection of the dispersed light. Data acquisition, laser tunability and spectrograph operation are computer controlled. Between acquisition of the new 2D signatures the sample is repositioned so that a new area is illuminated by the laser spot.

Explosive preparation

The Trinitrotoluene (TNT) samples used in this experiment were purified in-house at the US Naval Surface Warfare Center (NSWC) and are part of NSWC's standards and analytic reference material stock. The TNT was split into three classes which consisted of Fresh, Heated and UV Aged. To simulate thermal ageing, a bulk sample of each explosive was inserted into an aluminum block calorimeter and heated using an oil bath to 75°C and maintained at that temperature for two weeks. This process is an abbreviated version of a typical ageing protocol for solid explosives^(18,19), in which samples are held at elevated temperatures (usually 50, 60, or 70 °C) for periods of 8-12 months. UV ageing was accomplished by exposing the samples for two weeks with a 15 Watt, 254 nm, Cole Parmer ultraviolet

lamp at a distance of 12.7 cm. (Since our experiment is designed to show proof of principle we did not attempt to determine an equivalent age of our samples in ambient conditions.) The explosives were then cut into smaller pieces and shipped to the US Naval Research Lab. Upon arrival the explosives were subdivided into four separate sets of fresh, heated and UV aged samples which were measured for this experiment. Each crystal is measured between five and ten times at multiple points on the sample to create an equivalent number of multi-wavelength signatures for each explosive and aging condition. The samples were single crystals of explosive measuring approximately 1.5 mm in diameter and all weighed less than 2 milligrams. The fresh and heat-aged TNT samples were white in appearance, while the UV aged sample had a brownish tint.

For batch 1 the fresh, heated and UV aged samples were each measured 4 times per sample at wavelengths ranging from 420 to 580 nm in 10 nm steps, producing 12 two dimensional signals which contain 204 individual single wavelength Raman Signatures. In batch 2 the fresh, heated and UV aged samples were each measured 8, 6, and 6 times respectively at wavelengths ranging from 420 to 620 nm in 10 nm steps. Likewise in batch 3 the fresh, heated and UV aged samples were each measured 5, 5, and 4 times respectively at wavelengths ranging from 420 to 620 nm in 10 nm steps. In this batch the UV Aged TNT sample was significantly degraded by the ageing process thus resulting in a poor signal. Finally in batch 4 the fresh, heated and UV aged samples were each measured 24, 20, and 10 times respectively. We chose to conduct our measurements in this batch on the upper register of the wavelength regime to record greater signal fidelity at these wavelengths, so while the dataset does range from 420 to 620 nm for some signatures, most were recorded from 500nm – 620nm with an increased laser illumination time. This limited range was applied to the entire UV Aged data set.

Data Analysis

After acquisition each multiwavelength measurement is processed using an NRL developed Matlab based toolbox. Within this automated toolbox random noise is removed and the spectra are adjusted to compensate for laser power variation and wavenumber drift. In addition the raw spectra are filtered with a 1.2 kHz low pass Fourier filter to remove high-frequency noise and a 50 Hz high pass Fourier filter to remove the baseline. The spectra are then aligned and assembled to form a contour map of the functional form $I = f(x,y)$ where x and y are the excitation wavelength and the Stokes Raman wavenumber shift respectively. We refer to this as a multi-wavelength or two-dimensional (2D) Raman signature.

When examining the 2D signature, we find that the overall intensity of the signature can vary by as much as a factor of 10 based upon where on the sample the measurement is made. We speculate that this is caused by differences in the average surface orientation presented to the laser. To remove this variation we have normalized the 2-dimensional spectra by setting the highest global point in each signature equal to unity. This procedure maintains the overall shape of the two dimensional spectrum while removing differences due to disparate overall intensity.

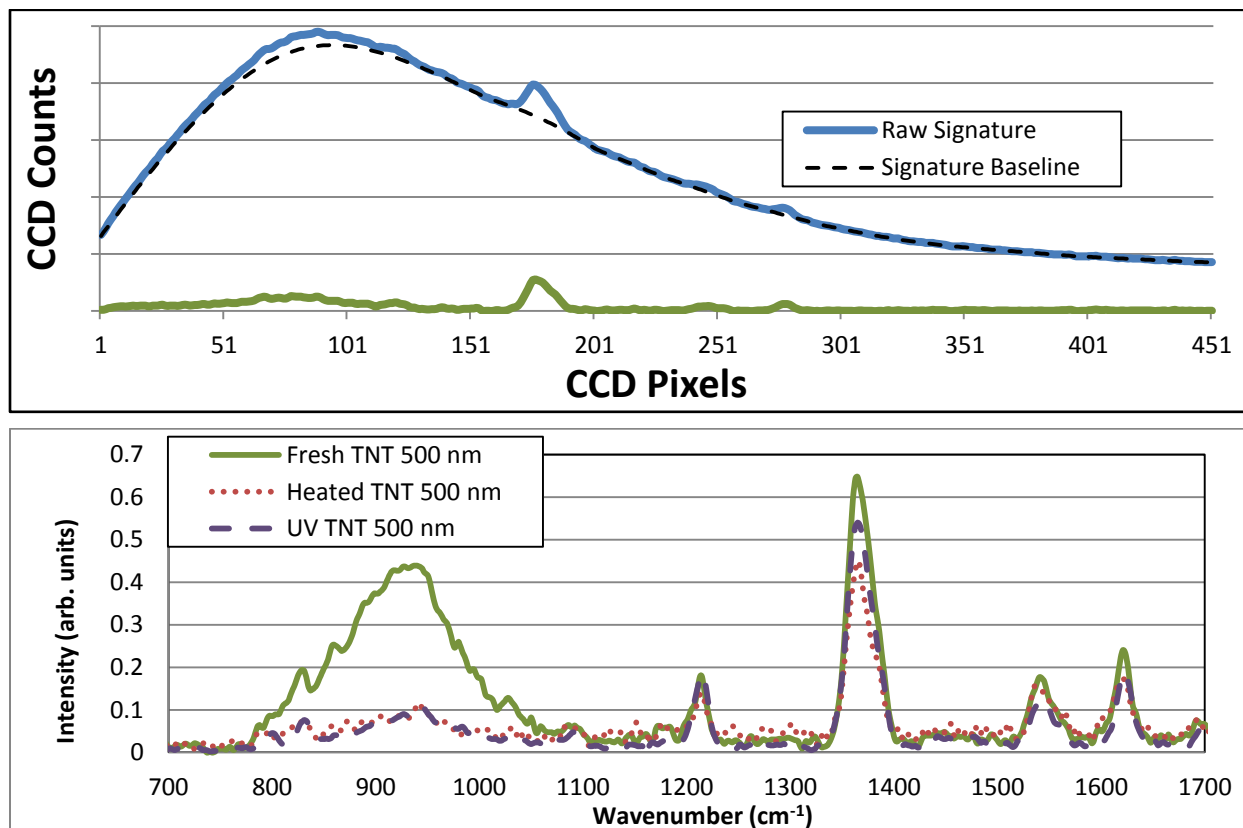


Figure 2: Removal of the baseline from the signature. The unprocessed Raman signature (top blue curve) sits atop a broad feature which is a combination of fluorescence and specular scattering. The majority of the feature is removed through Fourier filtering (black dotted line) leaving primarily the Raman signal (green line) however the automated filter is deliberately kept modest to refrain from attenuating the Raman peaks. This feature was later removed by a user monitored baseline subtraction algorithm. The lower figure displays this remnant feature for Fresh, Heated and UV aged TNT at a single laser wavelength. This feature can be seen here at approximately 950 cm^{-1}

After this post acquisition processing there was often the remnant of a broad feature which was not completely removed by the baseline subtraction algorithm. This feature is thought to be the result of a combination of fluorescence and specular scattering from the target sample. This effect can be seen in

Figure 2 where the fresh signature exhibits a broad peak stretching from 850 cm^{-1} to 1200 cm^{-1} . We arrived at this conclusion after noting that while there is a baseline fluorescence present in each sample, the overall shape of the baseline curve can vary significantly as the laser surface interaction is changed due to the variational geometry between the laser beam and the crystal surface. We noted a difference in the baseline intensity between the fresh and aged TNT and believe it to be due to the well known^(20,21) discoloration that occurs with TNT as it ages.

While these broad spectral features remain fairly reproducible during the examination of a single explosive batch they can vary greatly from batch to batch. To mitigate these effects we have developed an algorithm which allows for line by line removal of these remnants with guidance from an operator. This a-priori knowledge of the location of pertinent Raman lines which should remain unaffected allows full removal of the remaining baseline artifacts.

To determine if the explosive was fresh or aged we began by examining the ratios of several primary peaks within the TNT Raman signature. Differences within these ratios could be used as an easy metric to determine if an explosive was fresh or aged. Although some differences were observed, these differences were not reproducible across different batches. We also examined the behavior of the most prominent Raman lines as the illumination wavelength was adjusted. We find that the 2D behavior of the system, while consistent from shot to shot within a single sample batch could not be replicated over the full range of experiments. These results are catalogued by batch in the enclosed appendices. To remove this variability from the final identification process we have normalized the most prominent peak at each illumination wavelength to unity prior to crating a two dimensional signature, thus "flattening" the 2D spectrum.

To ascertain if there are less obvious underlying differences between the samples we examined the correlation between a sample's two-dimensional signature and the signatures of an average of the Fresh, Heated and UV Aged signatures. The Pearson correlation coefficient (r) of the signatures is determined by comparing the covariance of the signature of the mixture (\mathbf{X}) to the signatures of each chemical (\mathbf{Y}). Here N refers to the size of the signature array and is determined by the number of the illumination laser wavelengths times the number of wavenumbers in the recorded spectrum.

$$\text{Eq 1:} \quad r = \frac{\sum \mathbf{XY} - \frac{\sum \mathbf{X} \sum \mathbf{Y}}{N}}{\sqrt{\left(\left(\sum \mathbf{X}^2 - \frac{(\sum \mathbf{X})^2}{N} \right) \left(\sum \mathbf{Y}^2 - \frac{(\sum \mathbf{Y})^2}{N} \right) \right)}}$$

Single Signature Name	Fresh Correlation	Heated Correlation	UV Correlation	Average Difference
FreshTNTVis_01_24_2013_Run1b_FinalData.txt	0.9948	0.9947	0.9917	0.0016
FreshTNTVis_01_24_2013_Run2b_FinalData.txt	0.9849	0.9831	0.9826	0.0021
FreshTNTVis_01_24_2013_Run3b_FinalData.txt	0.9895	0.9879	0.9857	0.0027
FreshTNTVis_01_24_2013_Run4b_FinalData.txt	0.9908	0.9885	0.9857	0.0037
FreshTNTVis_01_24_2013_Run5b_FinalData.txt	0.9892	0.9872	0.9869	0.0021
FreshTNTVis_01_24_2013_Run6b_FinalData.txt	0.988	0.9837	0.9817	0.0053
FreshTNTVis_01_09_2013_FinalData.txt	0.9893	0.9935	0.9856	
FreshTNTVis_01_09_2013_Run2_FinalData.txt	0.9764	0.9754	0.9646	0.0064
FreshTNTVis_01_09_2013_Run3_FinalData.txt	0.9869	0.9915	0.9862	
FreshTNTVis_01_08_2013_FinalData.txt	0.9782	0.9757	0.9699	0.0054
FreshTNTVis_01_08_2013_Run2_FinalData.txt	0.9691	0.962	0.9553	0.0105
FreshTNTVis_01_08_2013_Run3_FinalData.txt	0.9819	0.9799	0.9745	0.0047
FreshTNTVis_01_08_2013_Run4_FinalData.txt	0.8588	0.8394	0.8272	0.0255
FreshTNTVis_01_08_2013_Run5_FinalData.txt	0.9429	0.9318	0.917	0.0185
FreshTNTVis_01_04_2013_FinalData.txt	0.9899	0.9878	0.986	0.0030
FreshTNTVis_01_04_2013_Run10_FinalData.txt	0.8602	0.8415	0.832	0.0235
FreshTNTVis_01_04_2013_Run2_FinalData.txt	0.9872	0.9847	0.9831	0.0033
FreshTNTVis_01_04_2013_Run3_FinalData.txt	0.9816	0.9774	0.9744	0.0057
FreshTNTVis_01_04_2013_Run4_FinalData.txt	0.9849	0.9811	0.9774	0.0057
FreshTNTVis_01_04_2013_Run5_FinalData.txt	0.9838	0.9807	0.976	0.0054
FreshTNTVis_01_04_2013_Run6_FinalData.txt	0.9796	0.9753	0.9744	0.0048
FreshTNTVis_01_04_2013_Run7_FinalData.txt	0.9863	0.9818	0.9788	0.0060
FreshTNTVis_01_04_2013_Run8_FinalData.txt	0.9815	0.9774	0.9697	0.0080
FreshTNTVis_01_04_2013_Run9_FinalData.txt	0.9612	0.9513	0.94	0.0156
FreshTNTVis_10_02_2012_FinalData.txt	0.9732	0.972	0.967	0.0037
FreshTNTVis_10_02_2012_Run2_FinalData.txt	0.9791	0.9787	0.974	0.0027
FreshTNTVis_10_02_2012_Run3_FinalData.txt	0.9228	0.9113	0.9052	0.0146
FreshTNTVis_10_02_2012_Run4_FinalData.txt	0.9623	0.9535	0.9446	0.0133
FreshTNTVis_10_02_2012_Run5_FinalData.txt	0.9571	0.9478	0.9384	0.0140
FreshTNT_vis_07_20_2011_FinalData.txt	0.9238	0.9253	0.9258	
FreshTNT_vis_07_20_2011_Run10_FinalData.txt	0.9798	0.9788	0.9728	0.0040
FreshTNT_vis_07_20_2011_Run3_FinalData.txt	0.943	0.9413	0.937	0.0038
FreshTNT_vis_07_20_2011_Run4_FinalData.txt	0.9505	0.9442	0.9334	0.0117
FreshTNT_vis_07_20_2011_Run5_FinalData.txt	0.9241	0.924	0.9208	0.0017
FreshTNT_vis_07_20_2011_Run7_FinalData.txt	0.9745	0.9747	0.9711	
FreshTNT_vis_07_20_2011_Run8_FinalData.txt	0.9675	0.9672	0.9617	0.0031
FreshTNT_vis_07_20_2011_Run9_FinalData.txt	0.9702	0.969	0.9644	0.0035
Fresh_TNT_exVis2_10_21_2010_FinalData.txt	0.983	0.987	0.9866	
Fresh_TNT_exVis3_10_21_2010_FinalData.txt	0.9722	0.9746	0.976	
Fresh_TNT_exVis4_10_21_2010_FinalData.txt	0.935	0.9376	0.9334	
Fresh_TNT_exVis_10_21_2010_FinalData.txt	0.9859	0.9907	0.9892	
Average Correlation	0.966363415	0.963195122	0.958239024	
Standard Deviation of Correlation	0.031361878	0.035172141	0.037156567	

Table 1.1 Fresh TNT Correlation Coefficients. Green background indicates correct identification and red incorrect identification.

Single Signature Name	Fresh Correlation	Heated Correlation	UV Correlation	Average Difference
HeatedTNTVis_01_16_2013_Run10b_FinalData.txt	0.9736	0.9736	0.9652	0.0042
HeatedTNTVis_01_16_2013_Run1b_FinalData.txt	0.9827	0.9858	0.98	0.0045
HeatedTNTVis_01_16_2013_Run2b_FinalData.txt	0.9759	0.9776	0.9676	0.0059
HeatedTNTVis_01_16_2013_Run3b_FinalData.txt	0.983	0.9855	0.9802	0.0039
HeatedTNTVis_01_16_2013_Run4b_FinalData.txt	0.981	0.9824	0.9763	0.0038
HeatedTNTVis_01_16_2013_Run5b_FinalData.txt	0.9867	0.988	0.9818	0.0037
HeatedTNTVis_01_16_2013_Run6b_FinalData.txt	0.9854	0.9867	0.98	0.0040
HeatedTNTVis_01_16_2013_Run7b_FinalData.txt	0.9879	0.9887	0.981	0.0042
HeatedTNTVis_01_16_2013_Run8b_FinalData.txt	0.9855	0.9872	0.981	0.0040
HeatedTNTVis_01_16_2013_Run9b_FinalData.txt	0.9677	0.9705	0.9581	0.0076
HeatedTNTVis_01_15_2013_FinalData.txt	0.9895	0.9943	0.9884	0.0053
HeatedTNTVis_01_15_2013_Run10_FinalData.txt	0.9883	0.9913	0.9843	0.0050
HeatedTNTVis_01_15_2013_Run2_FinalData.txt	0.977	0.9777	0.9628	0.0078
HeatedTNTVis_01_15_2013_Run3_FinalData.txt	0.9869	0.9917	0.9848	0.0059
HeatedTNTVis_01_15_2013_Run4_FinalData.txt	0.9822	0.9829	0.9723	0.0057
HeatedTNTVis_01_15_2013_Run5_FinalData.txt	0.988	0.993	0.9871	0.0055
HeatedTNTVis_01_15_2013_Run6_FinalData.txt	0.9814	0.9858	0.9757	0.0072
HeatedTNTVis_01_15_2013_Run7_FinalData.txt	0.9844	0.9894	0.9831	0.0056
HeatedTNTVis_01_15_2013_Run8_FinalData.txt	0.9866	0.9913	0.9839	0.0061
HeatedTNTVis_01_15_2013_Run9_FinalData.txt	0.9849	0.9909	0.9855	0.0057
HeatedTNTVis_10_02_2012_FinalData.txt	0.971	0.9716	0.9676	0.0023
HeatedTNTVis_10_02_2012_Run2_FinalData.txt	0.9706	0.9695	0.9631	
HeatedTNTVis_10_02_2012_Run3_FinalData.txt	0.9572	0.9554	0.9477	
HeatedTNTVis_10_02_2012_Run4_FinalData.txt	0.9356	0.9296	0.919	
HeatedTNTVis_10_02_2012_Run5_FinalData.txt	0.9862	0.9868	0.9815	0.0030
HeatedTNT_vis_07_19_2011_FinalData.txt	0.6643	0.6838	0.6728	0.0153
HeatedTNT_vis_07_19_2011_Run2_FinalData.txt	0.9229	0.9322	0.9234	0.0091
HeatedTNT_vis_07_19_2011_Run3_FinalData.txt	0.9258	0.9359	0.9266	0.0097
HeatedTNT_vis_07_19_2011_Run4_FinalData.txt	0.9652	0.9682	0.9577	0.0068
HeatedTNT_vis_07_19_2011_Run5_FinalData.txt	0.9093	0.911	0.8974	0.0077
HeatedTNT_vis_07_19_2011_Run6_FinalData.txt	0.9284	0.9342	0.9262	0.0069
HeatedTNT_exVis2_10_21_2010_FinalData.txt	0.9745	0.9819	0.978	0.0056
HeatedTNT_exVis3_10_21_2010_FinalData.txt	0.9531	0.9642	0.9691	
HeatedTNT_exVis4_10_21_2010_FinalData.txt	0.9823	0.9879	0.9826	0.0054
HeatedTNT_exVis_10_21_2010_FinalData.txt	0.9842	0.9906	0.9876	0.0047
Average Correlation	0.962548571	0.966202857	0.95884	
Standard Deviation of Correlation	0.056184472	0.053567722	0.054725562	

Table 1.2 Heated TNT Correlation Coefficients. . Green background indicates correct identification and red incorrect identification.

Single Signature Name	Fresh Correlation	Heated Correlation	UV Correlation	Average Difference
UVTNTVis_01_23_2013_Run10b_FinalData.txt	0.9513	0.9471	0.951	
UVTNTVis_01_23_2013_Run1b_FinalData.txt	0.986	0.9838	0.9842	
UVTNTVis_01_23_2013_Run2b_FinalData.txt	0.9828	0.9819	0.9791	
UVTNTVis_01_23_2013_Run3b_FinalData.txt	0.987	0.9863	0.9853	
UVTNTVis_01_23_2013_Run4b_FinalData.txt	0.9888	0.9878	0.9891	0.0008
UVTNTVis_01_23_2013_Run5b_FinalData.txt	0.9833	0.9815	0.9837	0.0013
UVTNTVis_01_23_2013_Run6b_FinalData.txt	0.9554	0.9521	0.9576	0.0039
UVTNTVis_01_23_2013_Run7b_FinalData.txt	0.9619	0.9616	0.9678	0.0061
UVTNTVis_01_23_2013_Run8b_FinalData.txt	0.9816	0.9784	0.9792	
UVTNTVis_01_23_2013_Run9b_FinalData.txt	0.9652	0.9649	0.9709	0.0059
UVTNTVis_10_03_2012_FinalData.txt	0.9614	0.9622	0.9654	0.0036
UVTNTVis_10_03_2012_Run2_FinalData.txt	0.9095	0.9073	0.9162	0.0078
UVTNTVis_10_03_2012_Run3_FinalData.txt	0.7418	0.7396	0.7585	0.0178
UVTNTVis_10_03_2012_Run4_FinalData.txt	0.7251	0.7201	0.7369	0.0143
UVTNT_vis_07_07_2011_FinalData.txt	0.9817	0.9845	0.9856	0.0025
UVTNT_vis_07_07_2011_Run2_FinalData.txt	0.9838	0.9857	0.986	0.0012
UVTNT_vis_07_07_2011_Run3_FinalData.txt	0.9812	0.9835	0.9813	
UVTNT_vis_07_07_2011_Run4_FinalData.txt	0.9781	0.98	0.9807	0.0017
UVTNT_vis_07_07_2011_Run5_FinalData.txt	0.9854	0.9881	0.9903	0.0035
UVTNT_vis_07_07_2011_Run6_FinalData.txt	0.9766	0.9786	0.9836	0.0060
UVTNT_exVis2_10_21_2010_FinalData.txt	0.8651	0.8775	0.9071	0.0358
UVTNT_exVis3a_10_21_2010_FinalData.txt	0.93	0.9414	0.957	0.0213
UVTNT_exVis4_10_21_2010_FinalData.txt	0.9303	0.9405	0.9553	0.0199
UVTNT_exVis_10_21_2010_FinalData.txt	0.9042	0.9161	0.9363	0.0262
Average Correlation	0.9415625	0.9429375	0.949504167	
Standard Deviation of Correlation	0.071539267	0.071717506	0.06606763	

Table 1.3 UV aged correlation coefficients. . Green background indicates correct identification and red incorrect identification.

We compare the signature to the average on a wavelength by wavelength basis and then compile the correlation coefficient scores into a single global number to represent the correlation percentage between the unknown sample and the average. In this manner each sample is compared to the average signature of the Fresh, Heated and UV Aged Samples. The largest score is then considered the selection.

The results of these calculations are contained in tables 1.1 - 1.3. The correct detections are highlighted in green and the incorrect detections are denoted with a red block background. These determinations are made regardless of the proximity of the next closest correlation factor. Correlation factors are carried to the fourth decimal place to ensure that there are no duplicate correlation scores. For

fresh TNT the correct detection was made 33 out of 41 times. For Heated TNT the correct detection was made 31 out of 35 times, and for UV aged TNT the algorithm was correct 18 out of 24 times. Overall the algorithm was able to correctly discern a fresh from aged sample 82 out of 100 times.

Chemical Analysis

To determine if there were physical changes to the samples resultant from the artificial ageing program a portion of the fresh and aged samples were sent to the Swedish Defense Research Institute^(22, 23) for chemical analysis. The samples were examined by Fourier Transform Infra-Red analysis (FT-IR), Gas Chromatograph and Liquid Chromatograph Mass Spectroscopy (GC-MS, LC-MS), High Performance Liquid Chromatography (HPLC), Nuclear Magnetic Resonance (NMR), Thermogravimetric Analysis (TGA), and Differential Scanning Calorimetry (DSC). The HPLC, GC-MS, NMR, and DSC did not show any difference between the fresh and aged materials while the FT-IR, LC-MS, and TGA showed minute differences consistent with the level of sample variation seen by the swept wavelength Raman spectroscopy.

Conclusion

Examining the multi-wavelength Raman signatures of a single explosive and comparing these to an average of the signatures by utilizing a Pearson correlation algorithm we find that multi-wavelength Raman spectroscopy can distinguish fresh from artificially aged explosives a majority of the time. We have also determined that while 2D line shape and peak ratios are different for the different classes of explosive (Fresh, Heated, UV Aged) these differences are not greater than the variations in signature observed over the course of several experimental batches and therefore cannot be utilized for identification with this system at this level of artificial ageing. Thus the differences due to artificial environmental ageing are minute and may not be suitable for the rigorous distinguishability needed for field application. This conclusion is borne out by the minor variations observed during chemical analysis.

Acknowledgement

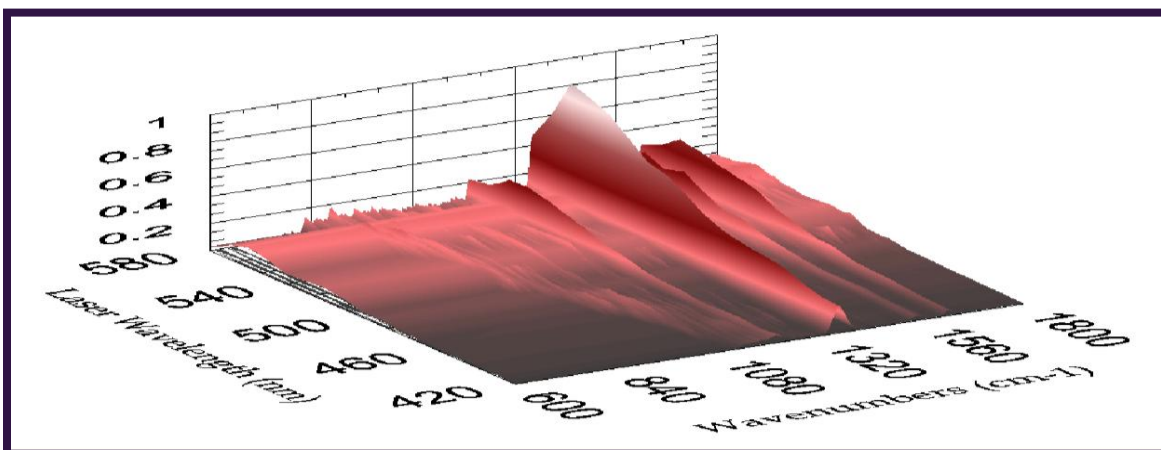
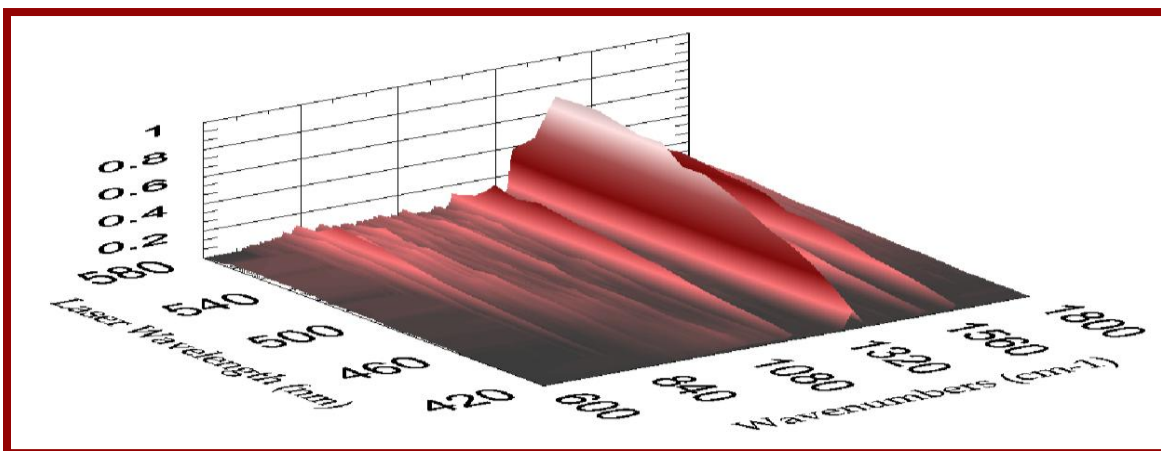
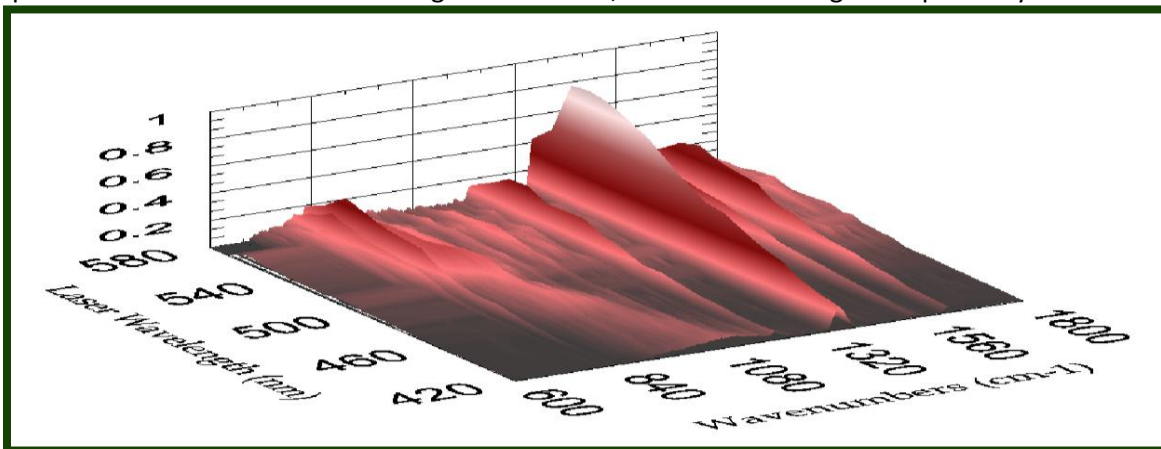
Special thanks to Dr. Jared Gump formerly of the US NSWC for preparation and ageing of the explosives

- 1) J.C. Carter, S.M. Angel, M. Lawrence-Snyder, J. Scaffidi, R.E. Whipple, J.G. Reynolds, "Standoff Detection of High Explosive Materials at 50 Meters in Ambient Light Conditions Using a Small Raman Instrument" *Appl. Spectrosc.* 59, 769 (2005)
- 2) D. D. Tuschel, A. V. Mikhonin, B. E. Lemoff, S. A. Asher, "Deep Ultraviolet Resonance Raman Excitation Enables Explosives Detection" *Appl. Spectrosc.* 64, 425 (2010)
- 3) L. Nagli, M. Gaft, Y. Flegler, M. Rosenbluh, "Absolute Raman cross-section of some explosives: Trend to UV" *Optical Materials.* 30, 1747 (2008)
- 4) I.R. Lewis, N.W. Daniel Jr, N.C. Chaffin, P.R. Griffiths, M.W. Tungol "Raman spectroscopic studies of explosive materials: towards a fieldable explosives detector" *Spectrochimica Acta Part A* 51, 1985 (1995)
- 5) E. M. Ali, H. G. Edwards, M. D. Hargreaves, I. J. Scowen, "Detection of explosives on human nail using confocal Raman microscopy" *J Raman Spectrosc.* 40, 144 (2009)
- 6) S. Botti, L. Cantarini, A. Palucci, "Surface-enhanced Raman spectroscopy for trace-level detection of explosives" *J. Raman Spectrosc.* 41, 866 (2010)
- 7) M.T. Bremer, P.J. Wrzesinski, N. Butcher, V.V. Lozovoy, M Dantus, "Highly selective standoff detection and imaging of trace chemicals in a complex background using single-beam coherent anti-Stokes Raman scattering" *Appl Phys Letters* 99, 101109 (2011)
- 8) E. M. Ali, H. G. Edwards, I. J. Scowen, "Raman spectroscopy and security applications: the detection of explosives and precursors on clothing" *J Raman Spectrosc.* 40, 2009 (2009)
- 9) E.D. Emmons, A. Tripathi, J.A. Guicheteau, S.D. Christensen, A.W. Fountain, "Raman Chemical Imaging of Explosive-Contaminated Fingerprints" *Appl Spectrosc.* 63, 1197 (2009)
- 10) T Junk, W. J. Catallo, "Environmental transformation products of 2,4,6-trinitrotoluene" *Chemical Speciation and Bioavailability*, 10, 47 (1998)
- 11) S. Taylor, J.H. Lever, J. Fadden, N. Perron, B. Packer, "Simulated rainfall-driven dissolution of TNT, Trional, Comp B and Octol particles" *Chemosphere* 75, 1074 (2009)

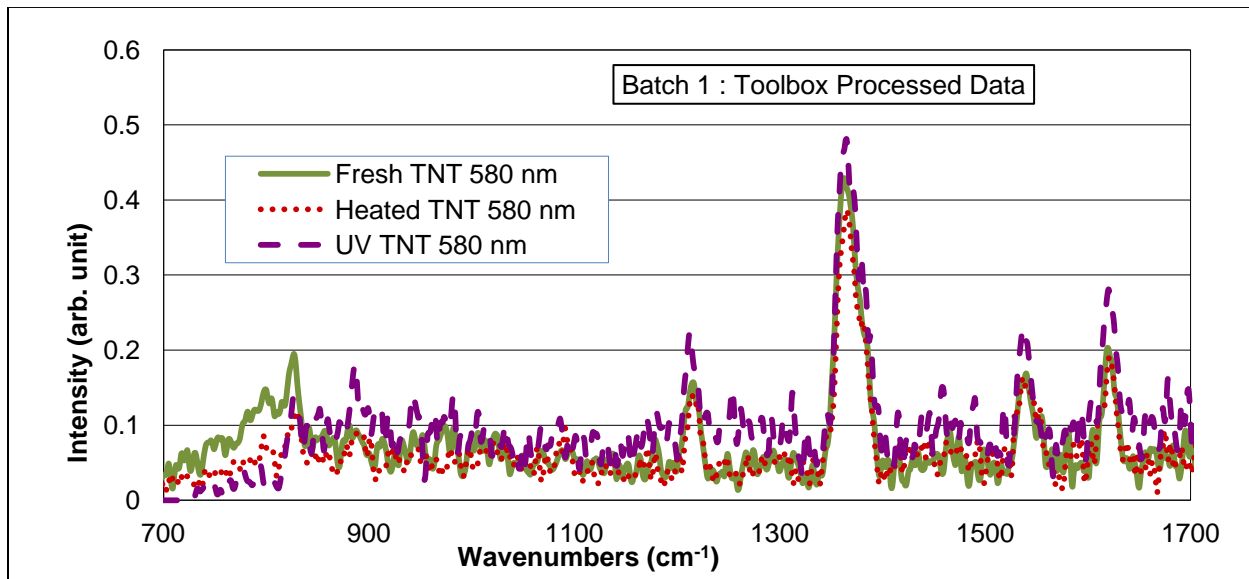
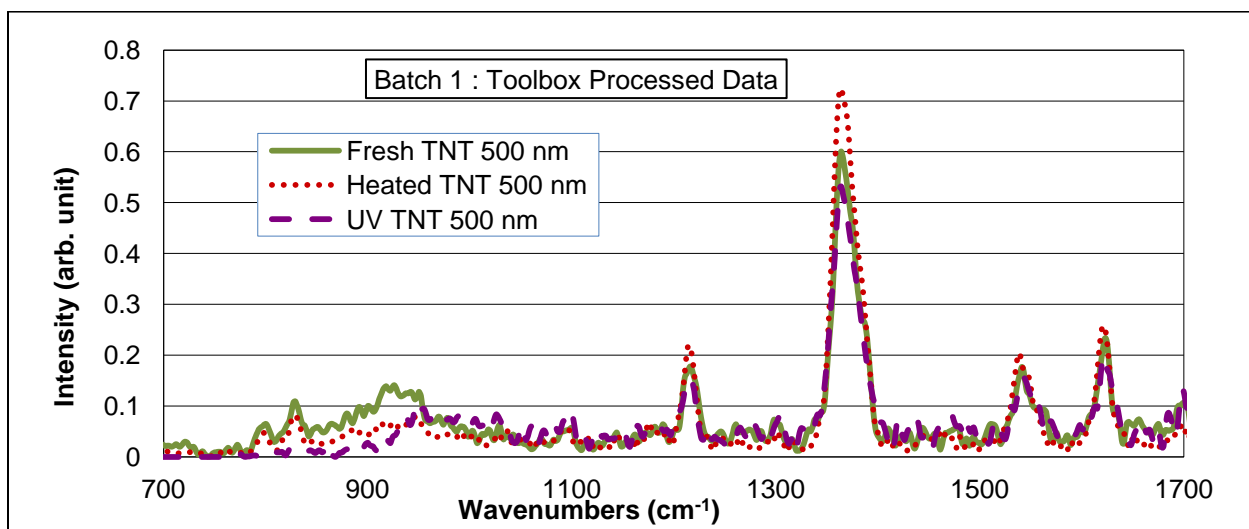
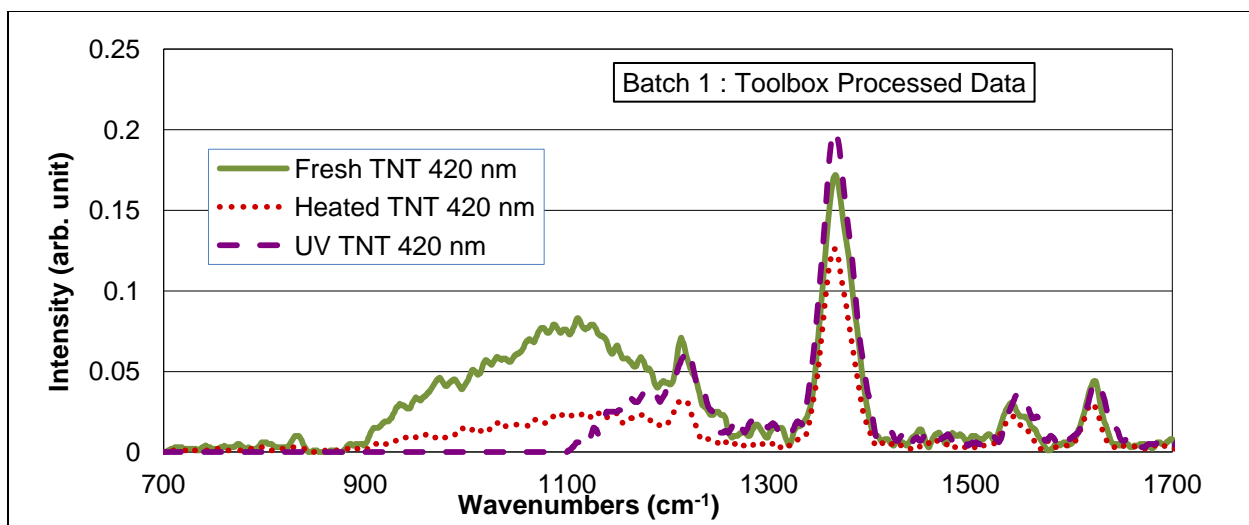
- 12) K.M. Dontsova, J.C. Pennington, C. Hayes, J. Simunek, C. W. Willford "Dissolution and Transport of 2,4-DNT and 2,6-DNT from M1 propellant in soil" *Chemosphere* 77, 597 (2009)
- 13) D.S. Moore, "Instrumentation for trace detection of high explosives" *Rev Sci Instrum.* 75, 2499 (2004)
- 14) J. Grun, J. Bowles, D Gilles, P Kunapareddy, R. Lunsford, C. K. Manka, S. Nikitin, Z. Wang "Tunable multi-wavelength resonance-Raman detection of bacteria and chemicals in complex environments." *Proc SPIE* 7687, 768706 (2010)
- 15) G. Comanescu, C.K. Manka, J. Grun, S. Nikitin, D. Zabetakis, "Identification of Explosives with Two-Dimensional Ultraviolet Resonance Raman Spectroscopy" *Appl. Spectrosc.* 62, 883 (2008)
- 16) C.K. Manka, S. Nikitin, R. Lunsford, P. Kunapareddy, J. Grun, "Wavelength-dependent amplitude of Teflon Raman lines" *J Raman Spectrosc.* 42, 685 (2011)
- 17) J Grun, C.K. Manka, S Nikitin, D. Zabetakis, G. Comanescu, D. Gillis, J. Bowles, "Identification of bacteria from two-dimensional resonant-Raman spectra" *Anal. Chem.* 79, 5489 (2007)
- 18) D.S. Moore, K. Lee, "Raman spectroscopy as a tool for long-term energetic material stability studies" *J Raman Spectroscopy*, 38, 1221 (2007)
- 19) K. Raha, P.S. Makashir, E.M Kurian, "Studies of the Thermal Decomposition of N-2,4,6 Tetranitro-N-Methyl Aniline" *Journal of Thermal Analysis*, 35, 1173, (1989)
- 20) S. Taylor, J.H. Lever, J. Fadden, N. Perron, B. Packer, "Outdoor Weathering and dissolution of TNT and Tritonal" *Chemosphere* 77, 1338 (2009)
- 21) M. E. Sitzmann, "Chemical Reduction of 2,4,6-Trinitrotoluene-Initial Products" *J.Chem and Engineering Data* 19, 179 (1974)
- 22) R.M. Karlsson, "NRL samples GC_LC_MS.pdf", Internal Report, Swedish Defence Research Agency, Stockholm Sweden, June 2013
- 23) R.M. Karlsson, "NRL samples NMR_IR_TGA_DSC.pdf", Internal Report, Swedish Defence Research Agency, Stockholm Sweden, June 2013

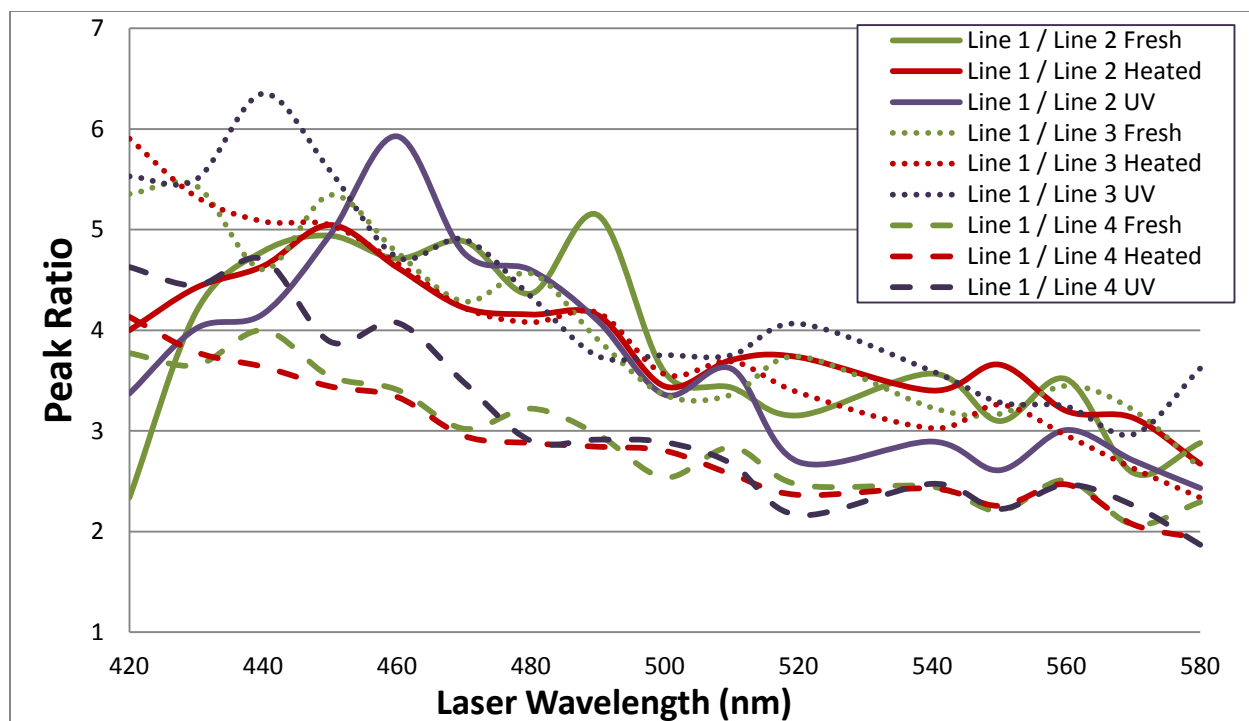
Appendix

Sample Batch 1: HDF Toolbox Processing for TNT Fresh, Heated and UV Aged Respectively



The above 2D graphs are the average of the samples from Batch 1 after automated SWORRD Toolbox processing. Residual fluorescence effects can be seen in the lower wavenumber region of the Fresh TNT graph. These effects are more pronounced in the 420nm lineout on the following page



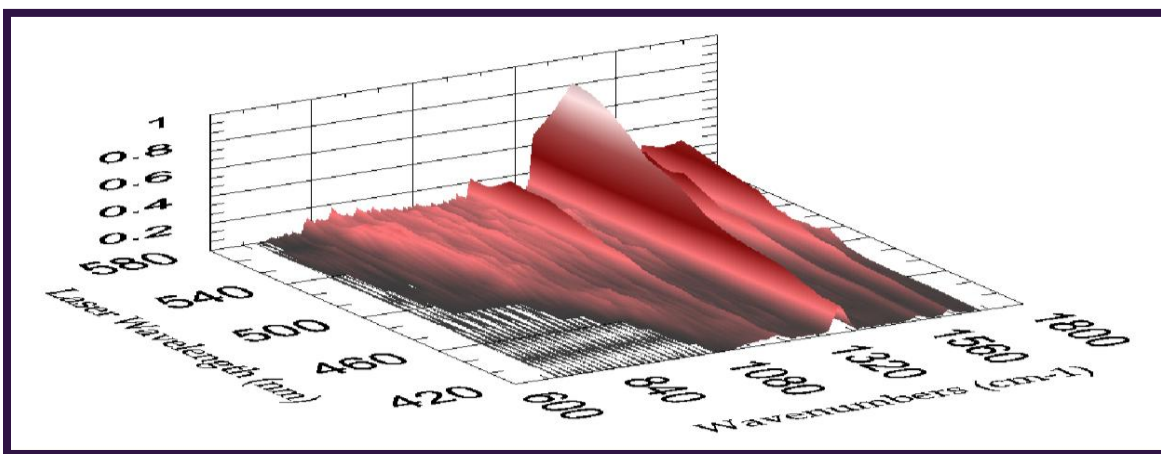
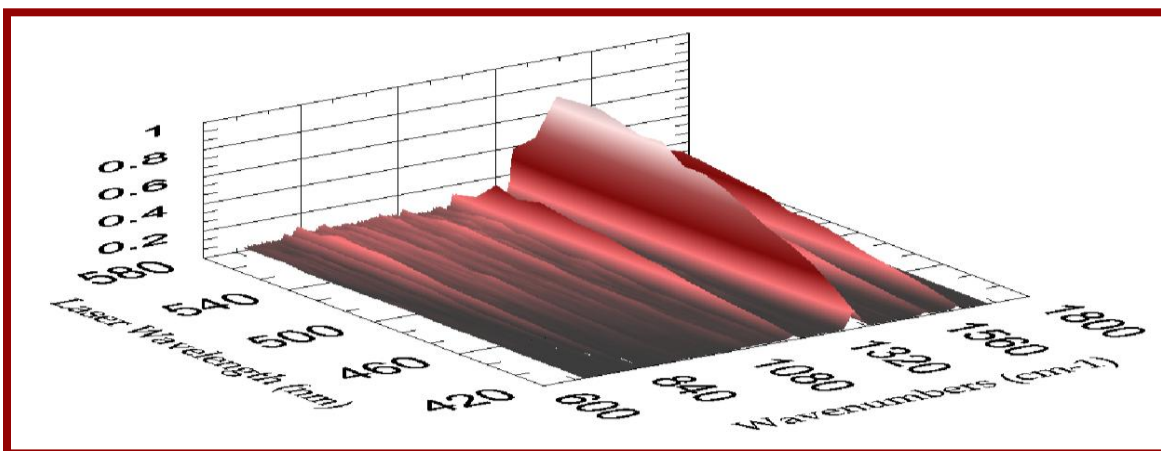
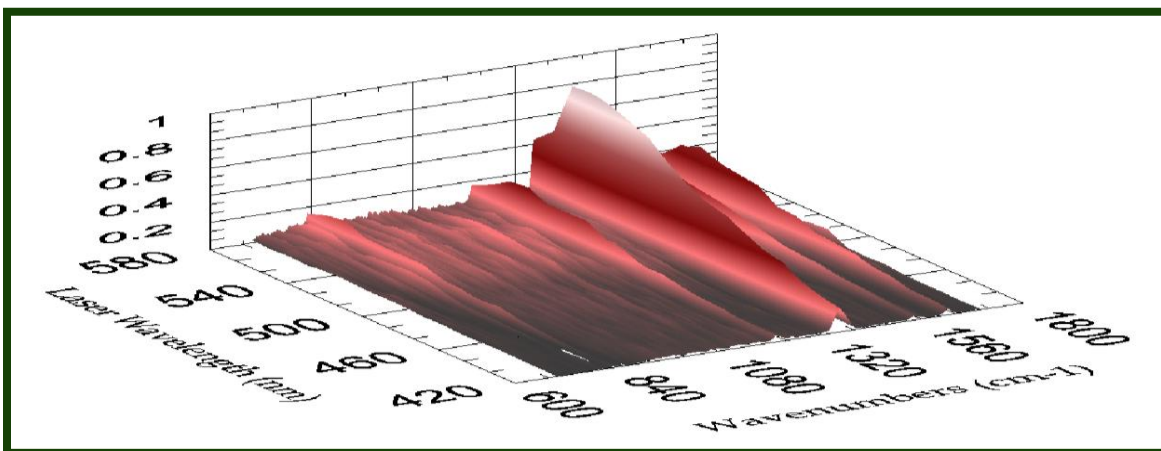


Peak Ratios for TNT Graphs: The Primary Peak ($\sim 1363 \text{ cm}^{-1}$) has been labeled Peak 1 and then the other peaks are labeled 2, 3, and 4 in order of increasing wavenumber.

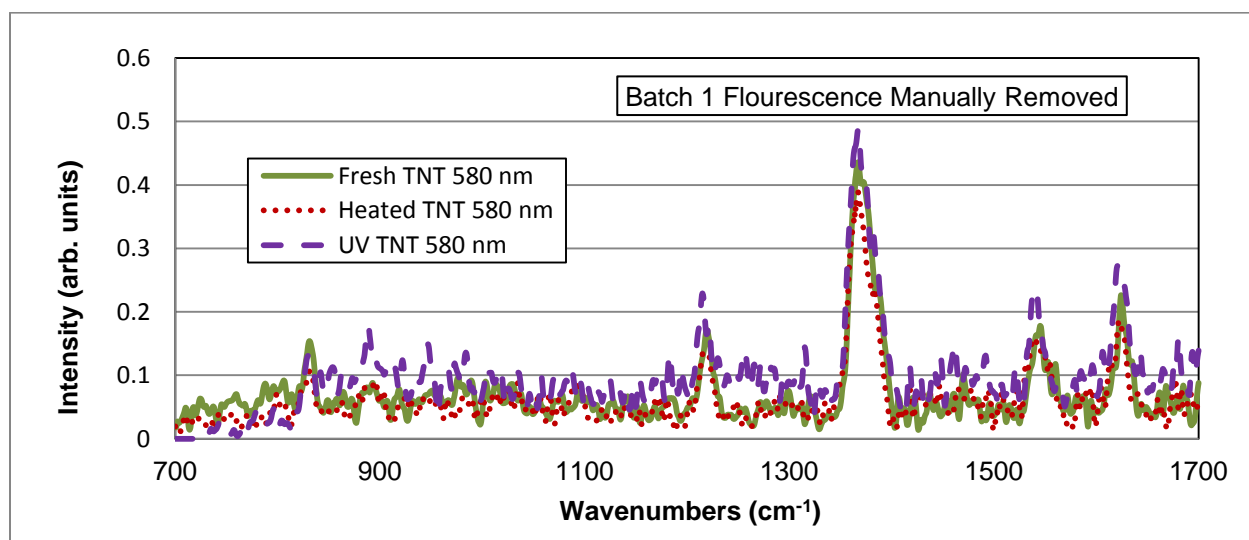
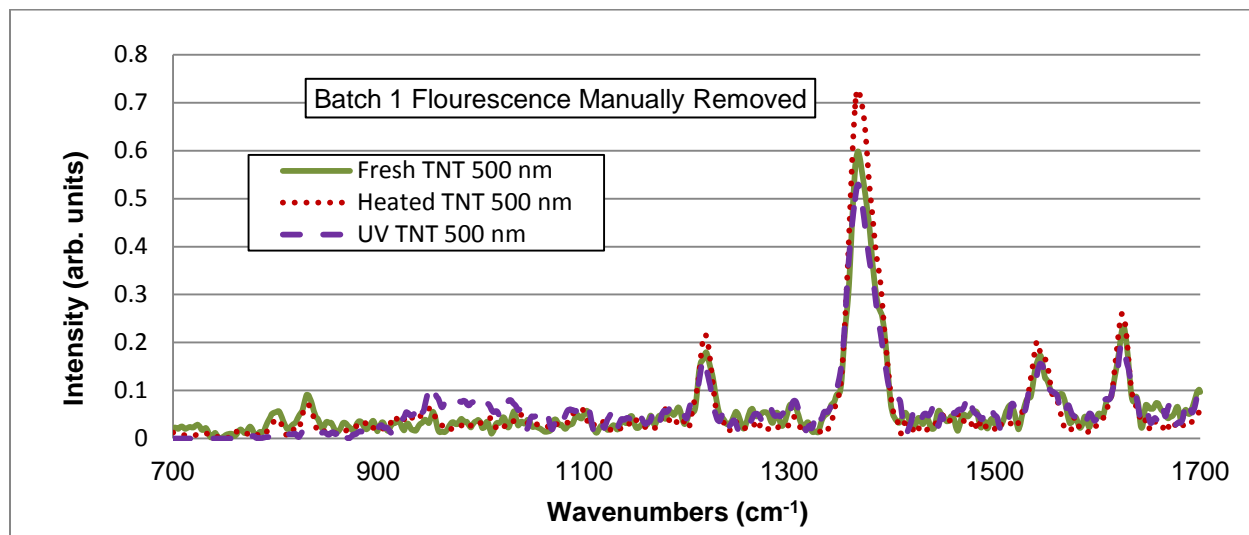
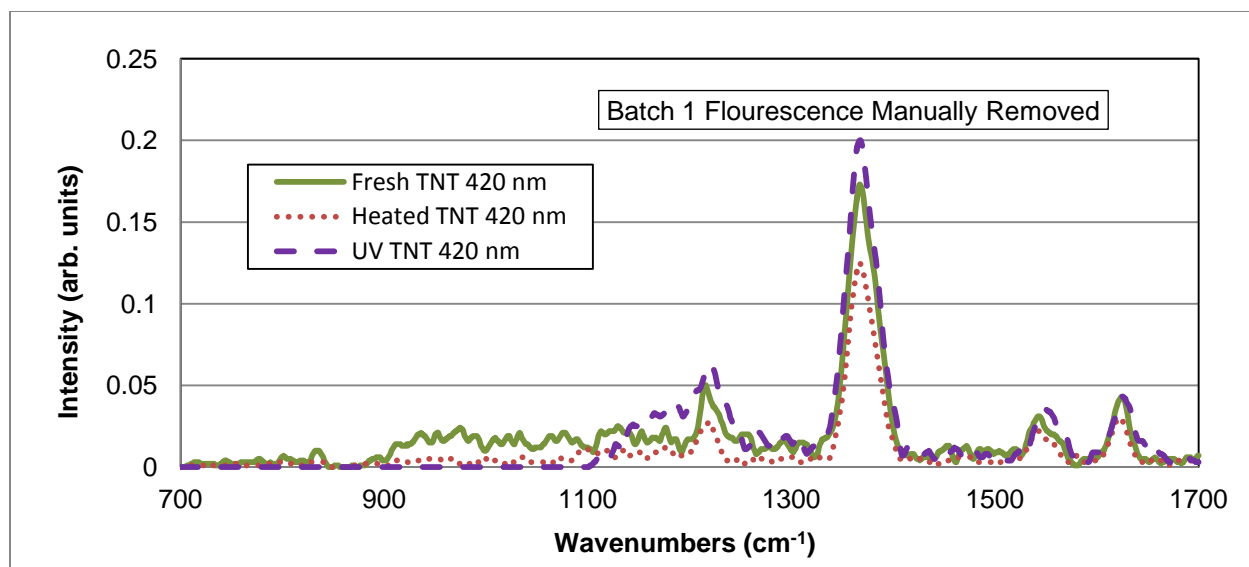
Single Signature Name	Fresh Average	Heated Average	UV Average
Fresh_TNT_exVis2_10_21_2010_HDF2_data.txt	0.9619	0.9362	0.8582
Fresh_TNT_exVis3_10_21_2010_HDF2_data.txt	0.9162	0.7936	0.6901
Fresh_TNT_exVis4_10_21_2010_HDF2_data.txt	0.9217	0.787	0.7068
Fresh_TNT_exVis_10_21_2010_HDF2_data.txt	0.9454	0.9699	0.8957
HeatedTNT_exVis2_10_21_2010_HDF2_data.txt	0.8946	0.9616	0.8946
HeatedTNT_exVis3_10_21_2010_HDF2_data.txt	0.8373	0.9561	0.934
HeatedTNT_exVis4_10_21_2010_HDF2_data.txt	0.9524	0.9677	0.8711
HeatedTNT_exVis_10_21_2010_HDF2_data.txt	0.9003	0.9685	0.898
UVTNT_exVis2_10_21_2010_HDF2_data.txt	0.751	0.8396	0.934
UVTNT_exVis3a_10_21_2010_HDF2_data.txt	0.8144	0.9081	0.9535
UVTNT_exVis4_10_21_2010_HDF2_data.txt	0.8307	0.8879	0.9346
UVTNT_exVis_10_21_2010_HDF2_data.txt	0.7959	0.8817	0.9565

Correlation Crosstable for signature detection : The Sample was correctly identified in 11 of the 12 cases

Sample Batch 1: Baseline Removal Processing

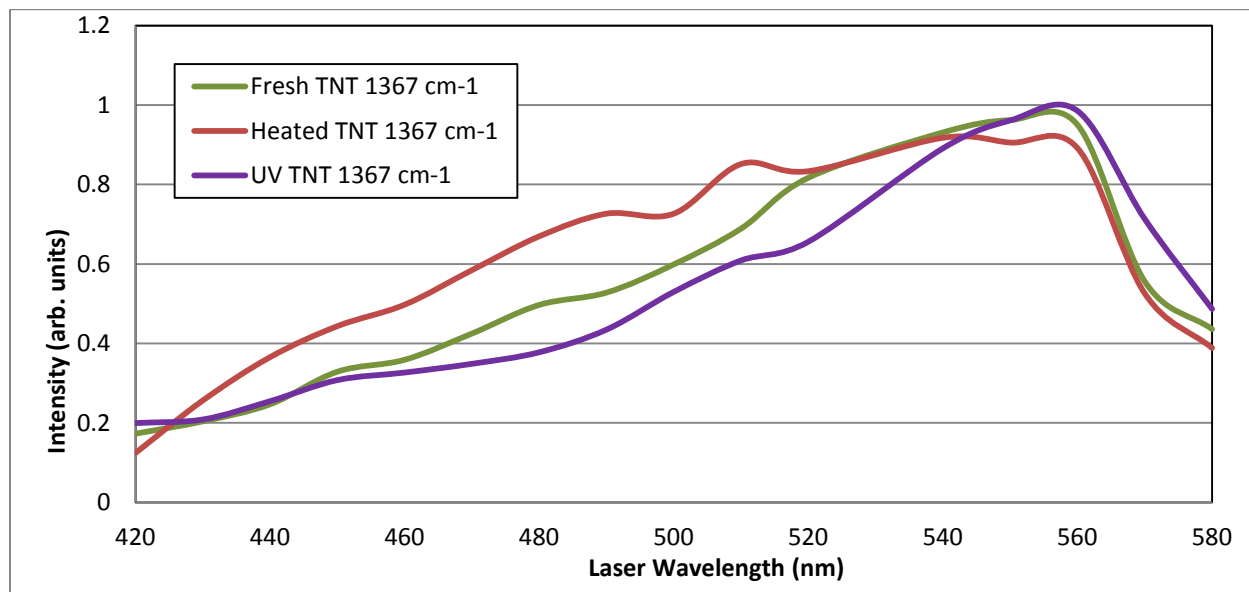


The above 2D Graphs are batch 1 TNT files in which additional baseline features have been manually removed



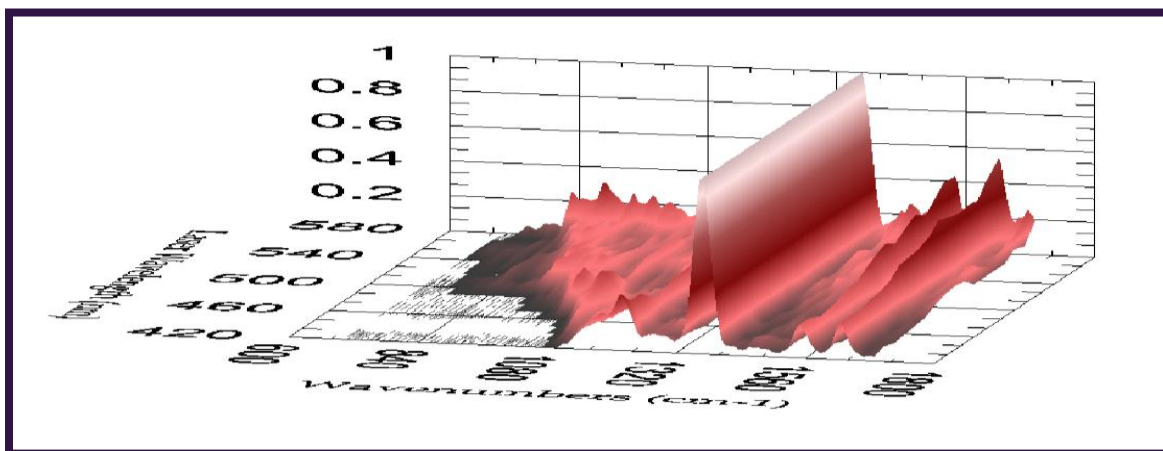
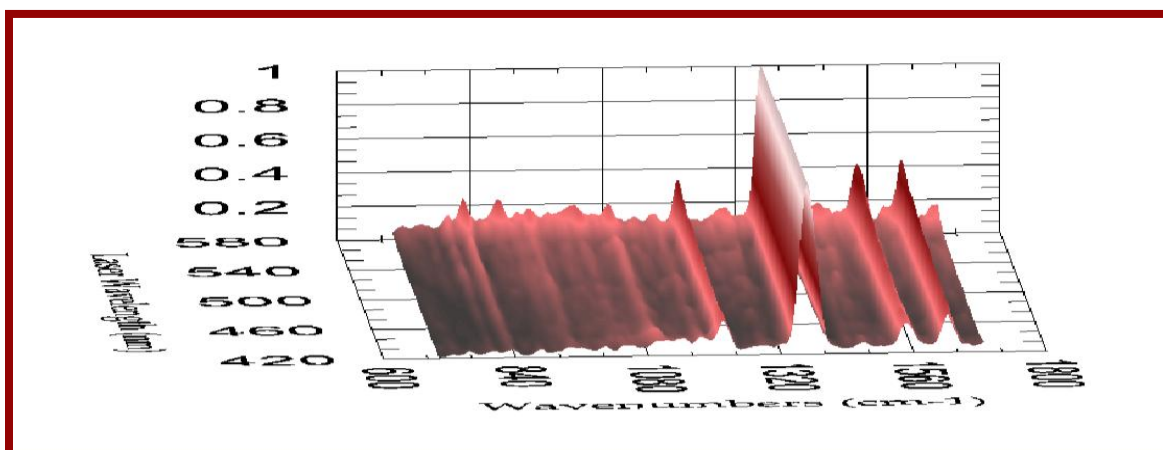
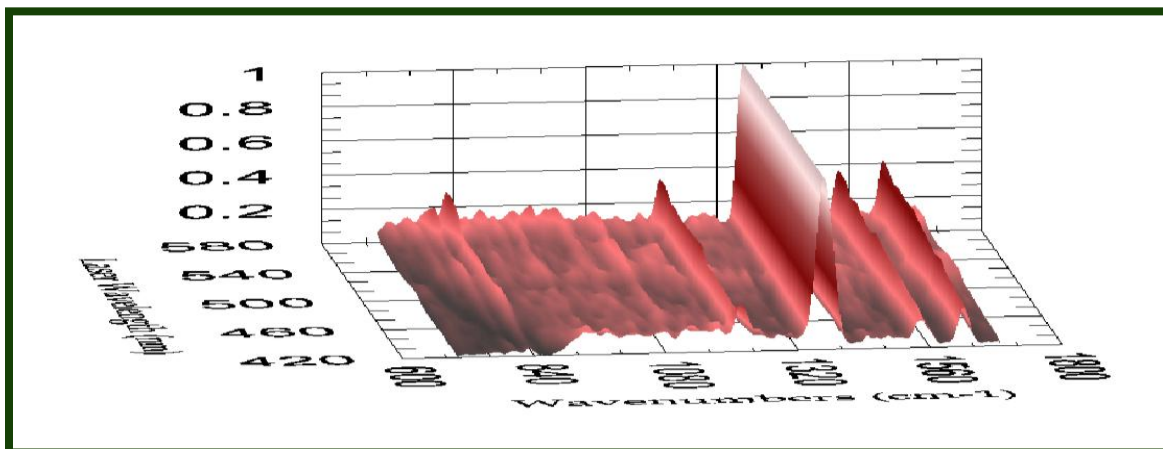
Single Signature Name	Fresh Average	Heated Average	UV Average
Fresh_TNT_exVis2_10_21_2010_PostPro_data.txt	0.9773	0.9643	0.9274
Fresh_TNT_exVis3_10_21_2010_PostPro_data.txt	0.9646	0.9458	0.9153
Fresh_TNT_exVis4_10_21_2010_PostPro_data.txt	0.9343	0.883	0.8478
Fresh_TNT_exVis_10_21_2010_PostPro_data.txt	0.9842	0.9816	0.9338
HeatedTNT_exVis2_10_21_2010_PostPro_data.txt	0.9515	0.972	0.9115
HeatedTNT_exVis3_10_21_2010_PostPro_data.txt	0.9415	0.9735	0.9441
HeatedTNT_exVis4_10_21_2010_PostPro_data.txt	0.9705	0.9841	0.9223
HeatedTNT_exVis_10_21_2010_PostPro_data.txt	0.9735	0.9834	0.9292
UVTNT_exVis2_10_21_2010_PostPro_data.txt	0.8588	0.8683	0.9476
UVTNT_exVis3a_10_21_2010_PostPro_data.txt	0.9201	0.9275	0.9569
UVTNT_exVis4_10_21_2010_PostPro_data.txt	0.9119	0.9138	0.9455
UVTNT_exVis_10_21_2010_PostPro_data.txt	0.891	0.9054	0.9625

Correlation Crosstable for signature detection: While we were now able to identify all 12 signatures from their correlation coefficient, the detection margin has been reduced across the board. The difference between the correct identification and the first wrong answer is now smaller than previously was the case. This is to be expected as the fluorescence feature which was removed resided primarily in the unaged sample signatures.

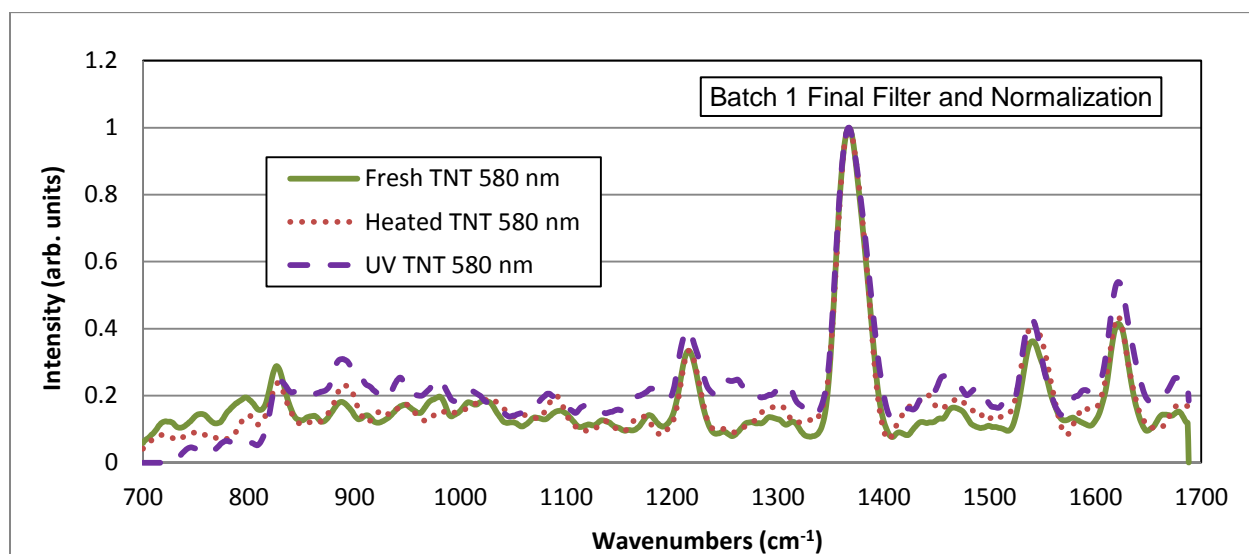
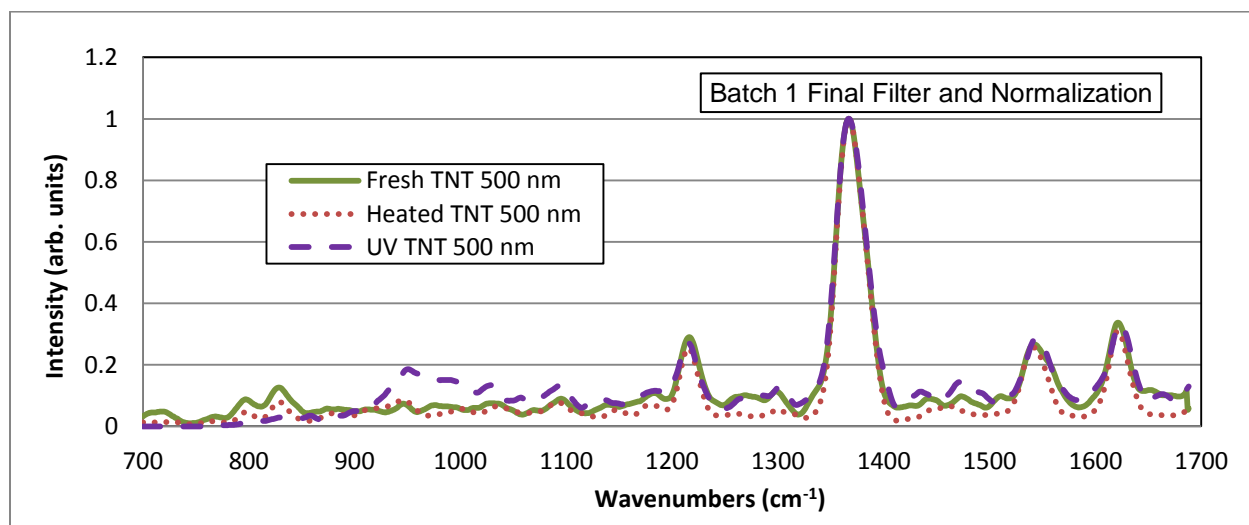
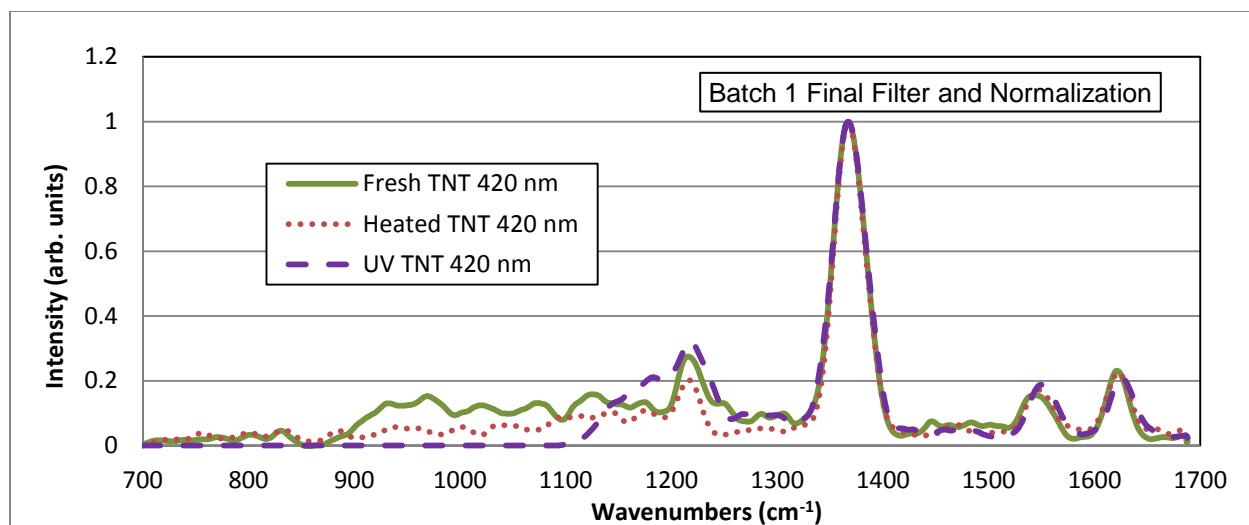


Height of the 1367 cm-1 Raman Peak as a function of wavelength. While the heated peak does appear to increase more rapidly than its fresh counterpart, the difference is slight.

Batch 1 Full Spectrum Normalization



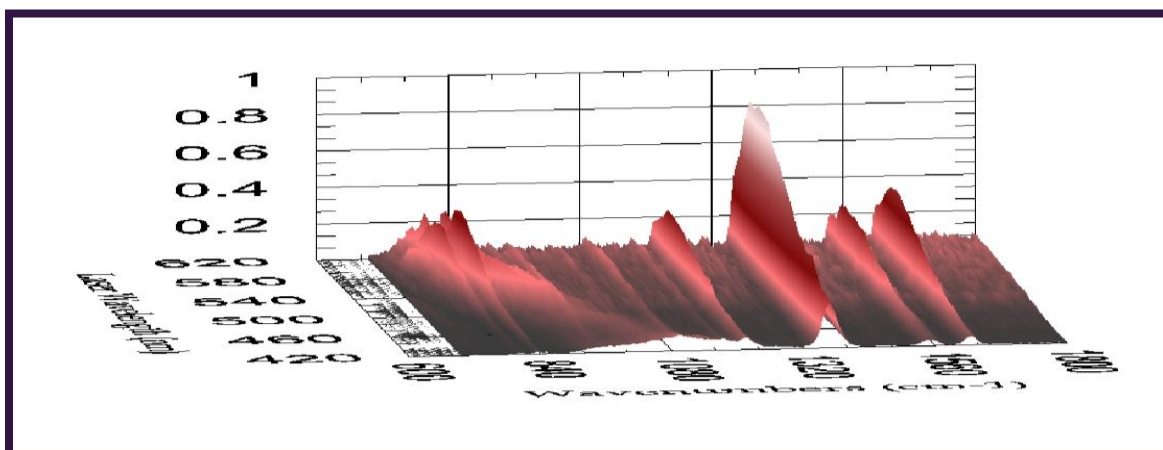
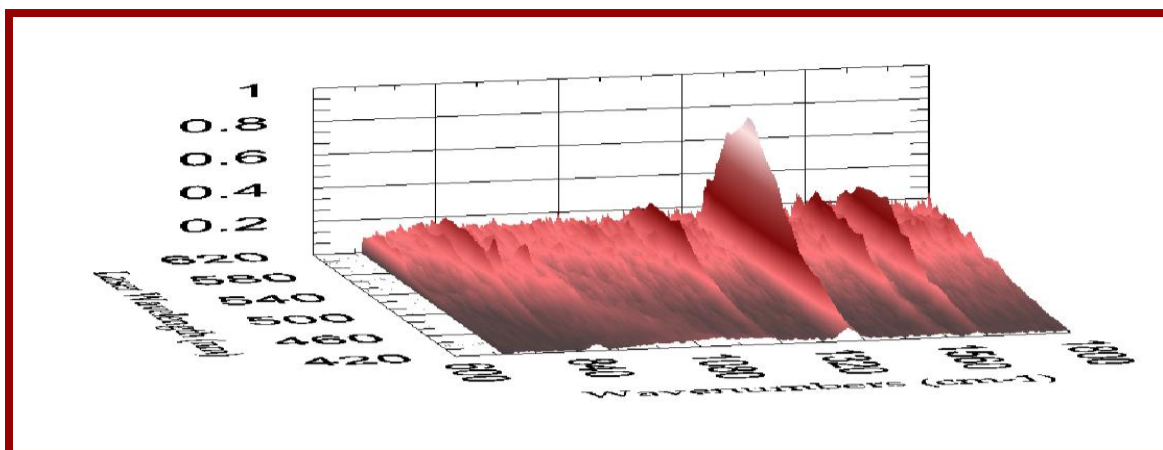
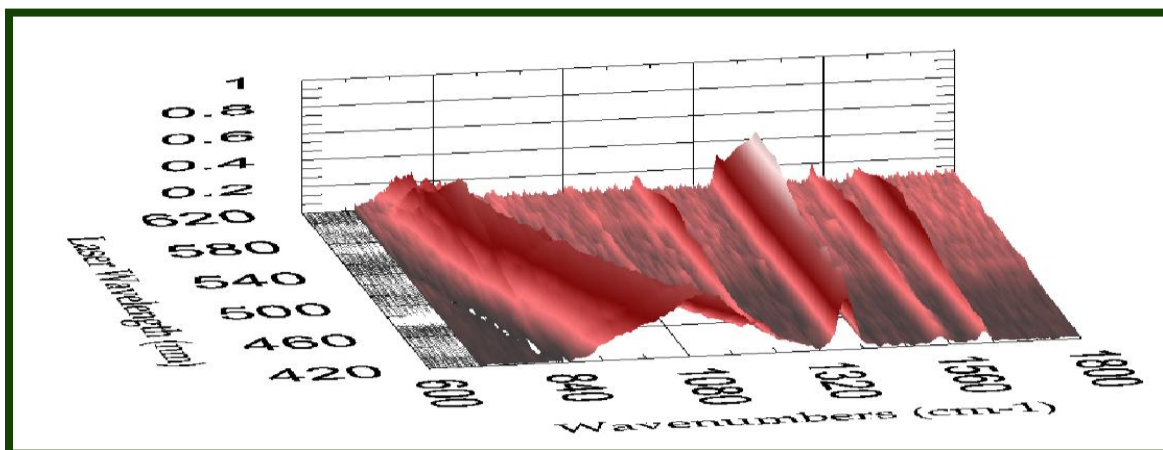
Set 1 Graphs, these graphs have had all baseline features removed and the primary peak at each laser illumination wavelength has been normalized to unity to better illuminate changes in the respective secondary peaks.

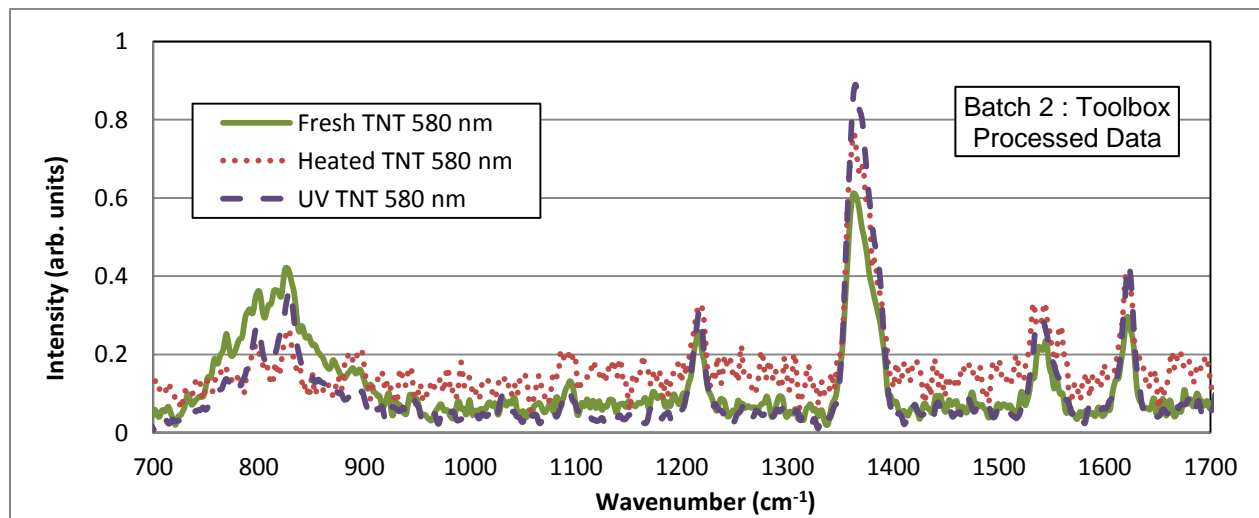
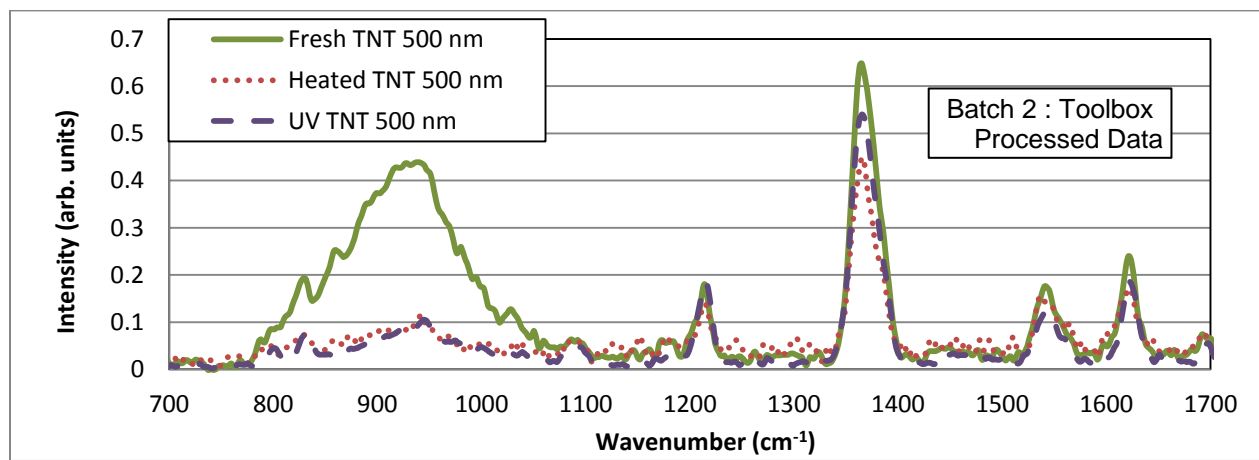
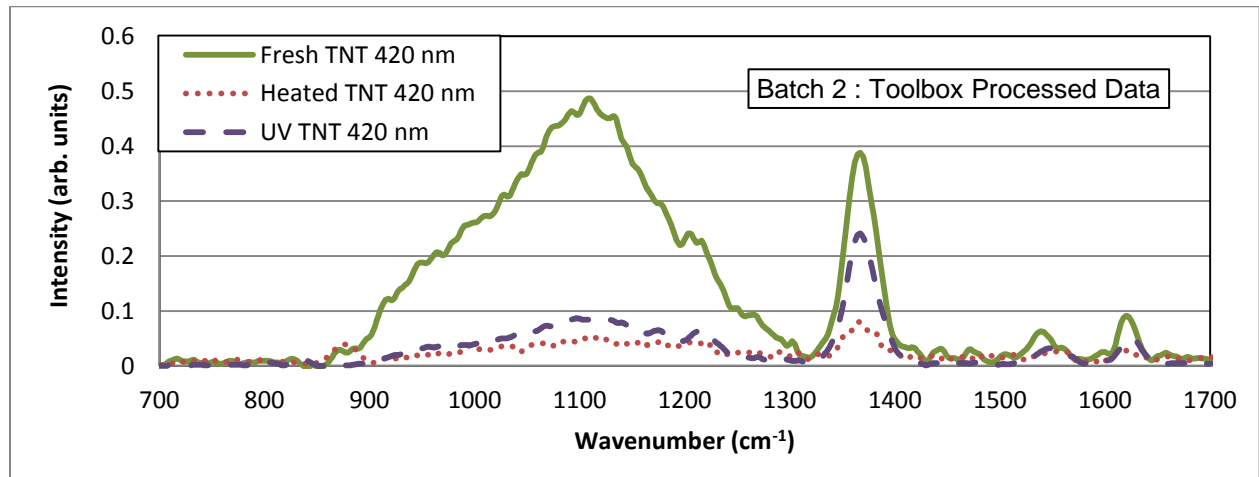


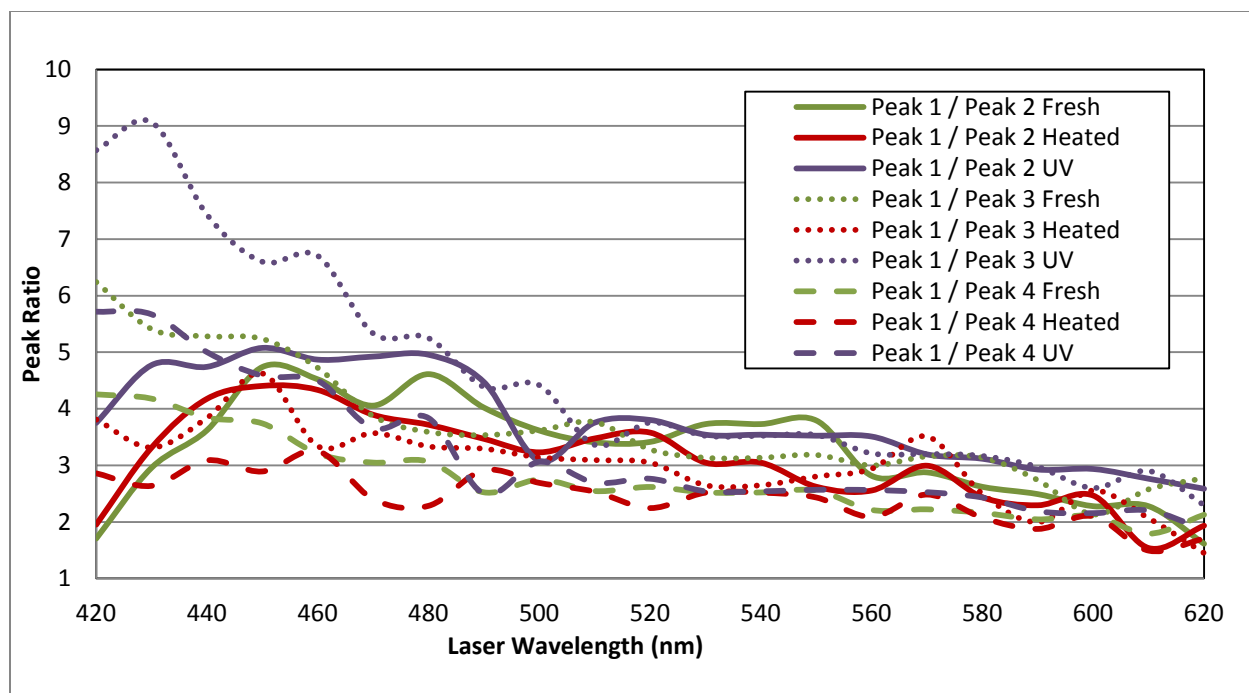
Single Signature Name	Fresh Average	Heated Average	UV Average
Fresh_TNT_exVis2_10_21_2010_FinalData.txt	0.9921	0.9868	0.9497
Fresh_TNT_exVis3_10_21_2010_FinalData.txt	0.9882	0.976	0.9438
Fresh_TNT_exVis4_10_21_2010_FinalData.txt	0.9668	0.9384	0.9057
Fresh_TNT_exVis_10_21_2010_FinalData.txt	0.9901	0.9913	0.9476
HeatedTNT_exVis2_10_21_2010_FinalData.txt	0.9791	0.9887	0.9411
HeatedTNT_exVis3_10_21_2010_FinalData.txt	0.9653	0.9842	0.9705
HeatedTNT_exVis4_10_21_2010_FinalData.txt	0.9833	0.9925	0.9403
HeatedTNT_exVis_10_21_2010_FinalData.txt	0.9871	0.9938	0.948
UVTNT_exVis2_10_21_2010_FinalData.txt	0.893	0.9025	0.9708
UVTNT_exVis3a_10_21_2010_FinalData.txt	0.9499	0.9607	0.9805
UVTNT_exVis4_10_21_2010_FinalData.txt	0.9517	0.9525	0.9707
UVTNT_exVis_10_21_2010_FinalData.txt	0.925	0.9362	0.9814

Correlation Crosstable for signature detection: We again find that the additional smoothing has led to greater correlation scores as well as smaller gaps between the correlation score of correct and incorrect identifications. We again correctly identified 11 of the 12 signatures. We note that the UV aged TNT has consistently shown the largest difference between itself and the other classes of TNT sample, and that while further processing has increased the detection score of the UV aged TNT, it has done more to narrow the gap between the UV aged TNT and the other samples.

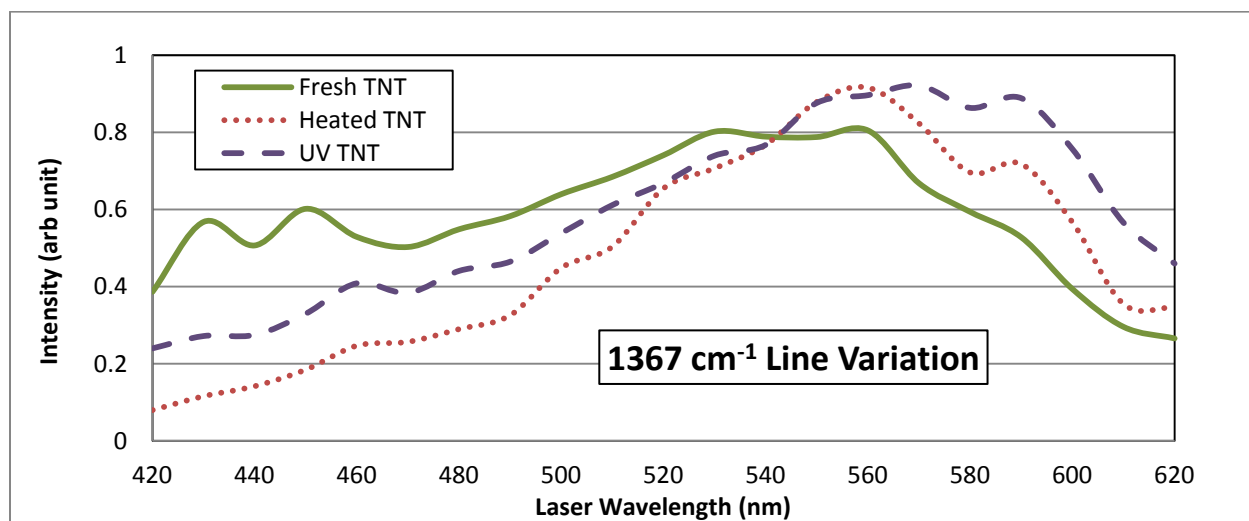
TNT Batch 2 HDF Processing







TNT Peak Ratios for Batch 2: We note that in each of the above peak ratios, the ratio for the UV aged sample is larger than its fresh or heated counterparts. While this is not actionable in and of itself it denotes that there may be differences that are exploitable through alternate metrics.

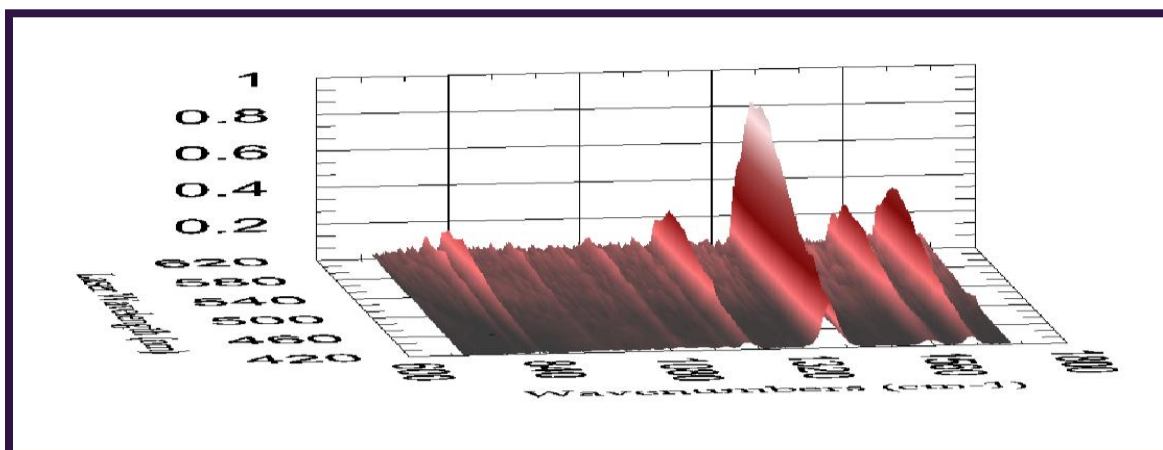
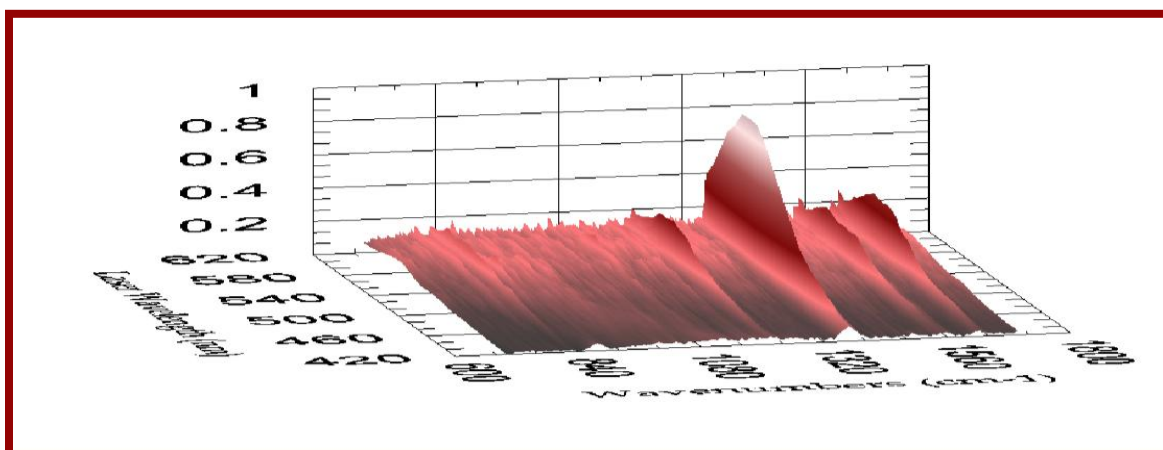
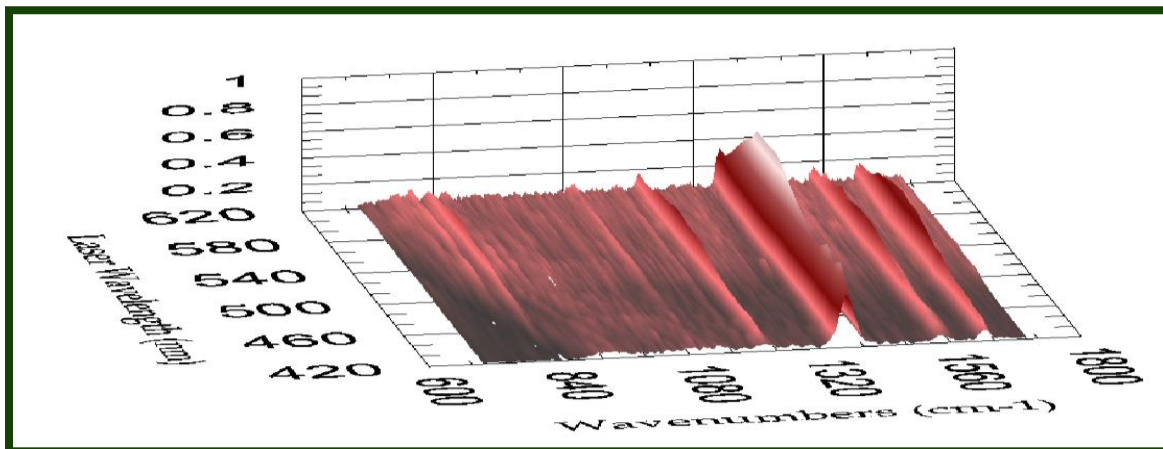


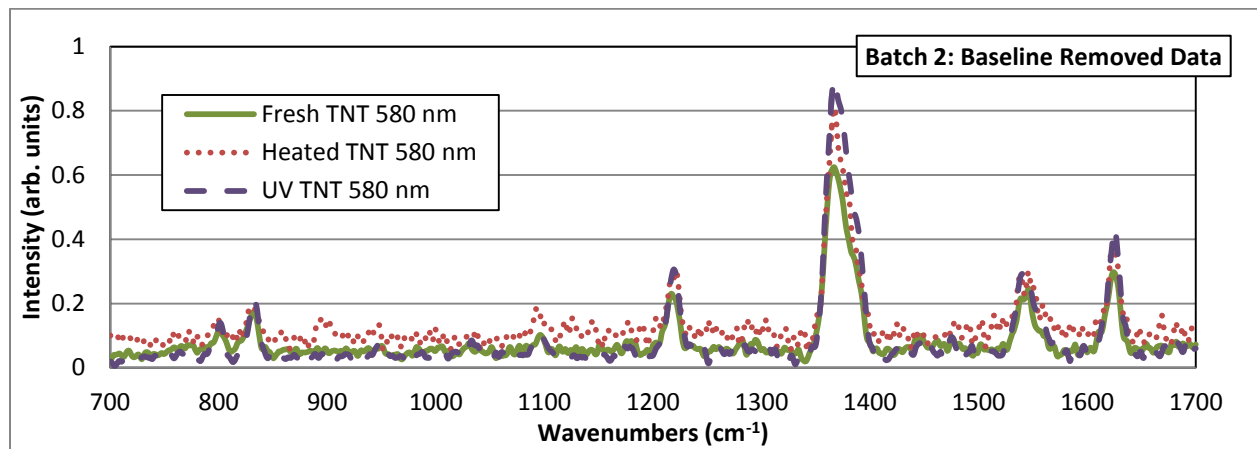
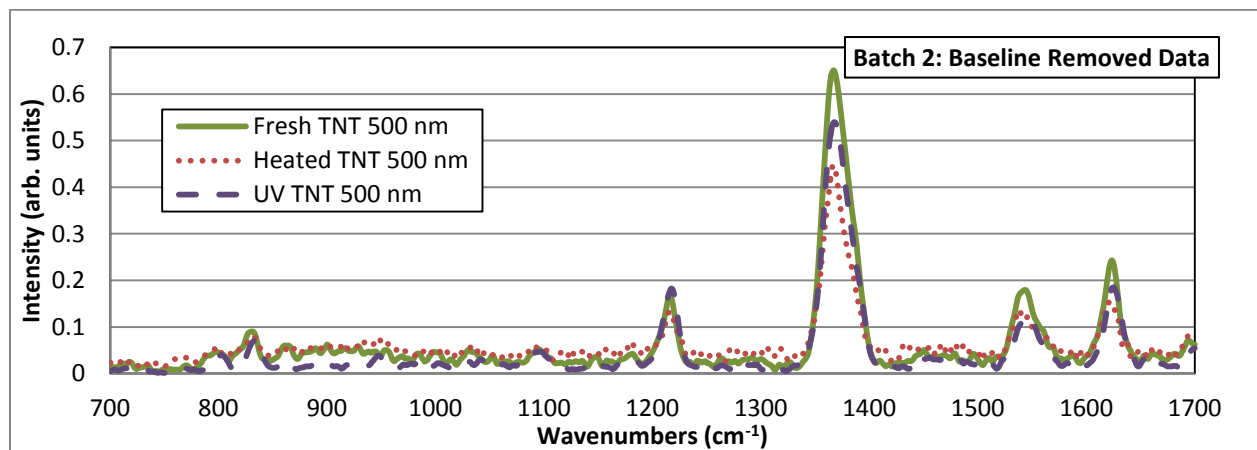
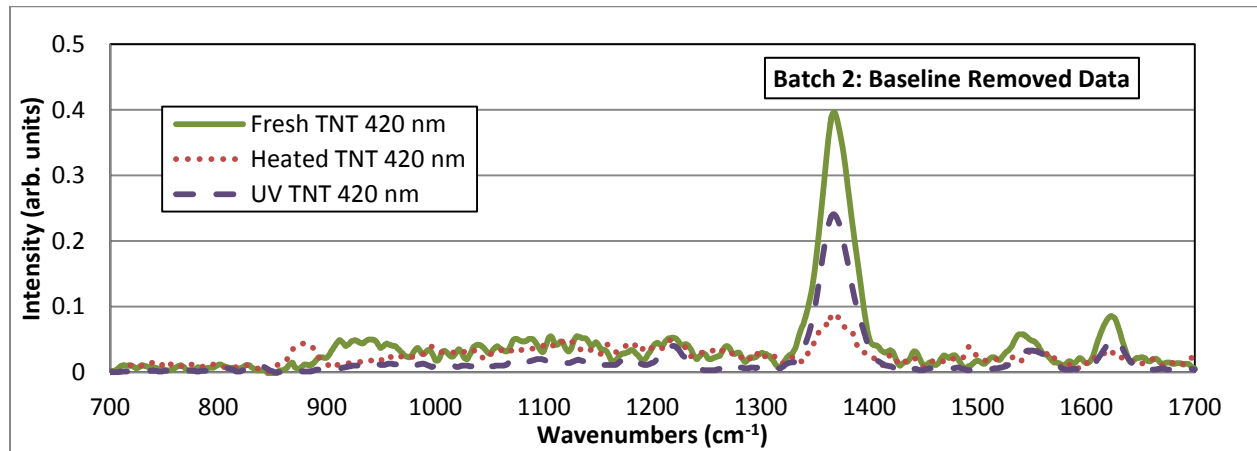
Intensity of 1367 cm^{-1} TNT emission line for Fresh, Heat Aged and UV Aged TNT as laser illumination wavelength is varied. There is a significant difference in both the initial intensity and in the point of maximum intensity for the different classes which was not apparent in the previous batch of explosives examined

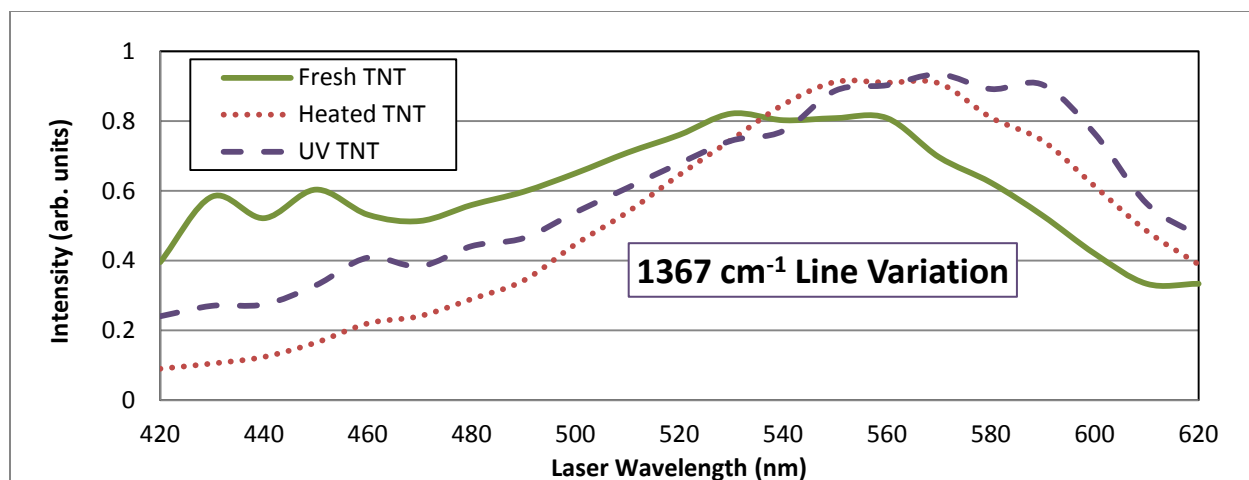
Single Signature Name	Fresh Average	Heated Average	UV Average
FreshTNT_vis_07_20_2011_HDF2_data.txt	0.7545	0.7806	0.7442
FreshTNT_vis_07_20_2011_Run10_HDF2_data.txt	0.9648	0.6374	0.7298
FreshTNT_vis_07_20_2011_Run3_HDF2_data.txt	0.8704	0.759	0.8178
FreshTNT_vis_07_20_2011_Run4_HDF2_data.txt	0.9335	0.6936	0.7202
FreshTNT_vis_07_20_2011_Run5_HDF2_data.txt	0.9237	0.6597	0.6839
FreshTNT_vis_07_20_2011_Run7_HDF2_data.txt	0.9706	0.6716	0.7618
FreshTNT_vis_07_20_2011_Run8_HDF2_data.txt	0.9661	0.6507	0.7467
FreshTNT_vis_07_20_2011_Run9_HDF2_data.txt	0.9687	0.6476	0.7402
HeatedTNT_vis_07_19_2011_HDF2_data.txt	0.4699	0.8027	0.5958
HeatedTNT_vis_07_19_2011_Run2_HDF2_data.txt	0.6102	0.8874	0.814
HeatedTNT_vis_07_19_2011_Run3_HDF2_data.txt	0.7088	0.8991	0.8411
HeatedTNT_vis_07_19_2011_Run4_HDF2_data.txt	0.6974	0.907	0.8922
HeatedTNT_vis_07_19_2011_Run5_HDF2_data.txt	0.7401	0.9045	0.8427
HeatedTNT_vis_07_19_2011_Run6_HDF2_data.txt	0.7563	0.9107	0.8843
UVTNT_vis_07_07_2011_HDF2_data.txt	0.6794	0.8719	0.9603
UVTNT_vis_07_07_2011_Run2_HDF2_data.txt	0.7763	0.8869	0.9798
UVTNT_vis_07_07_2011_Run3_HDF2_data.txt	0.8184	0.8752	0.9375
UVTNT_vis_07_07_2011_Run4_HDF2_data.txt	0.8423	0.8751	0.9356
UVTNT_vis_07_07_2011_Run5_HDF2_data.txt	0.7185	0.842	0.9682
UVTNT_vis_07_07_2011_Run6_HDF2_data.txt	0.8185	0.8247	0.9508

Correlation crosstable for signature identification: We show successful identification of 19 out of 20 signatures

TNT Batch 2 Baseline Removal







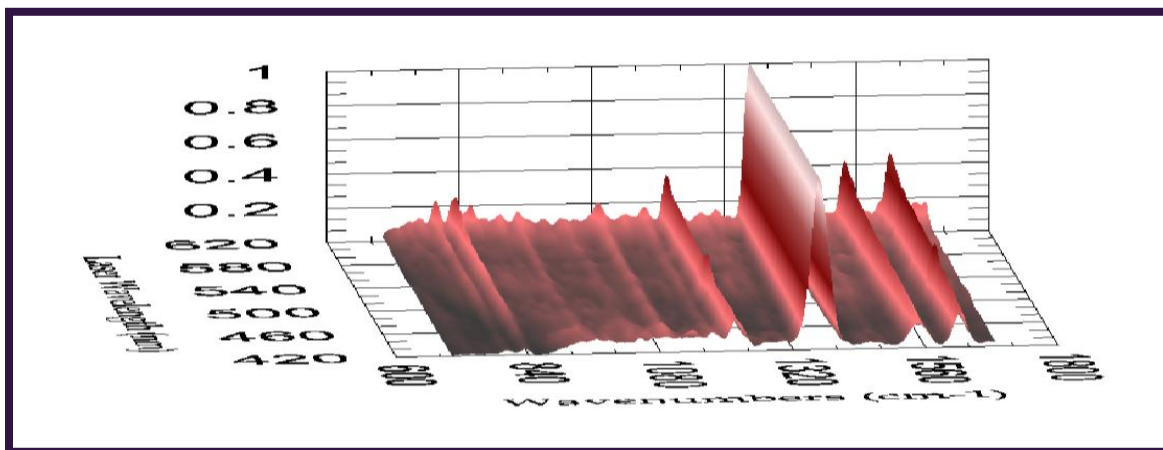
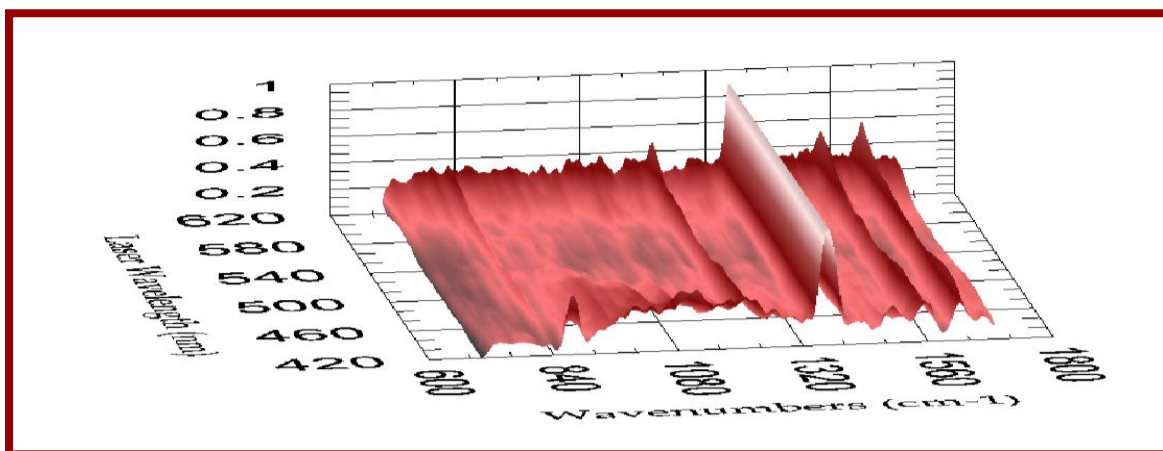
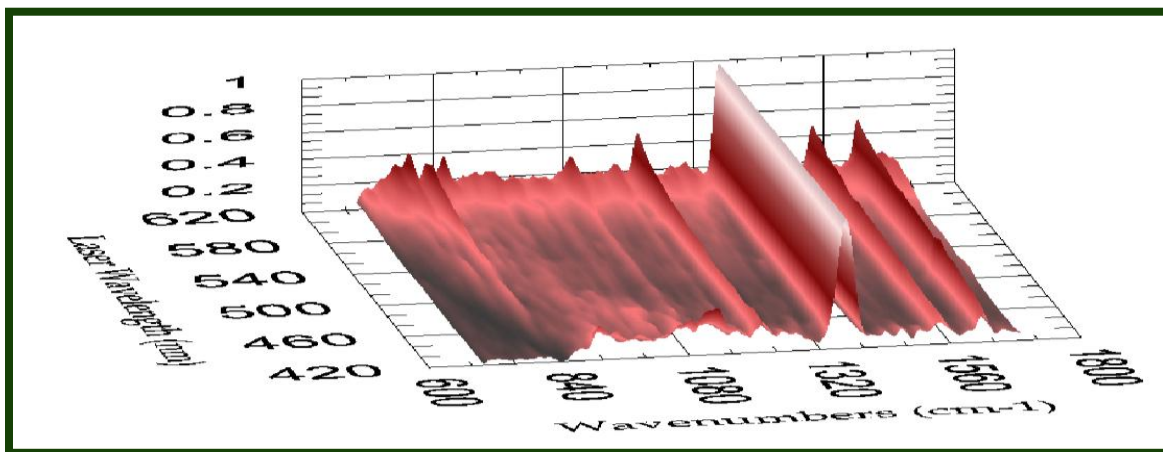
Behavior of the primary TNT line as laser illumination wavelength is varied

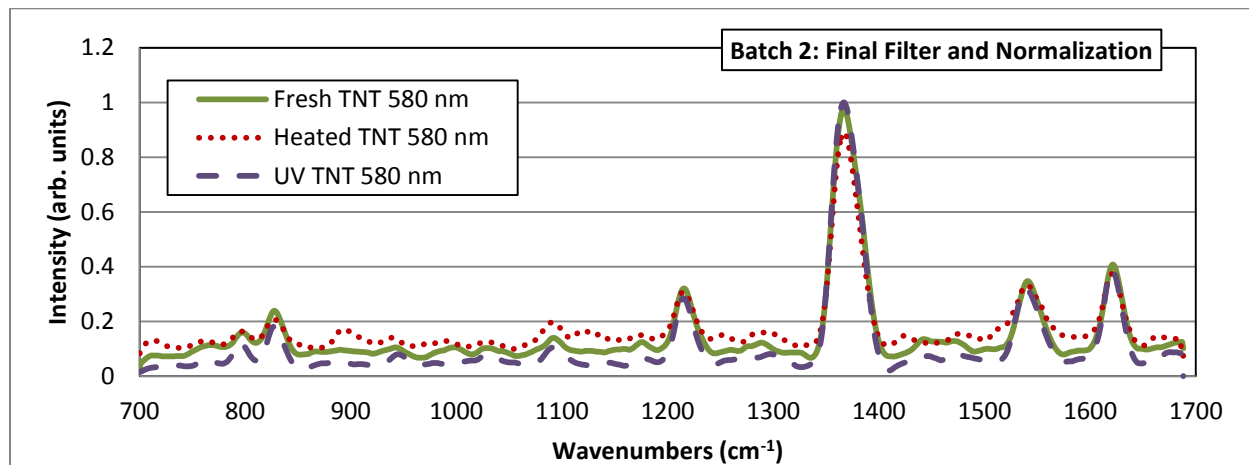
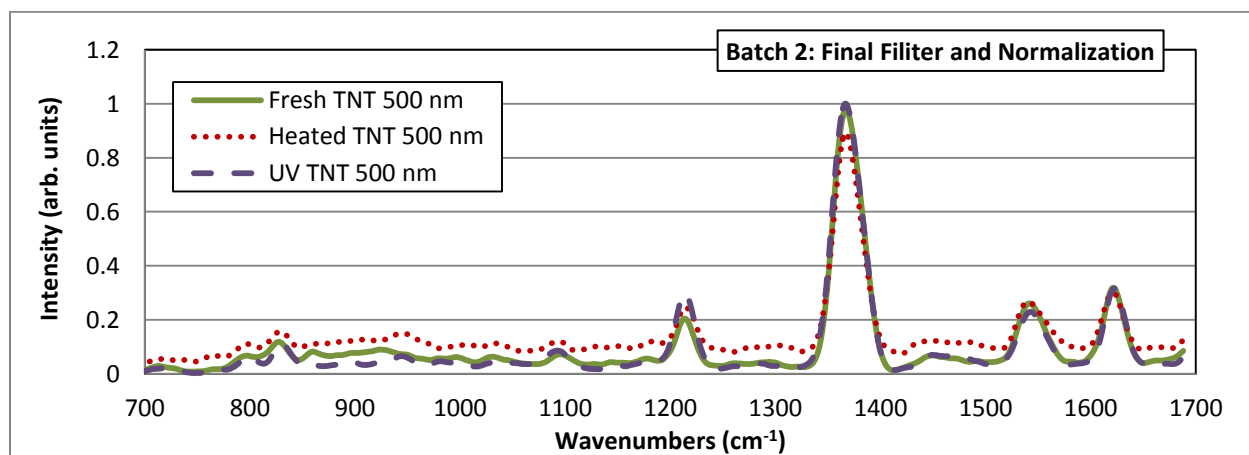
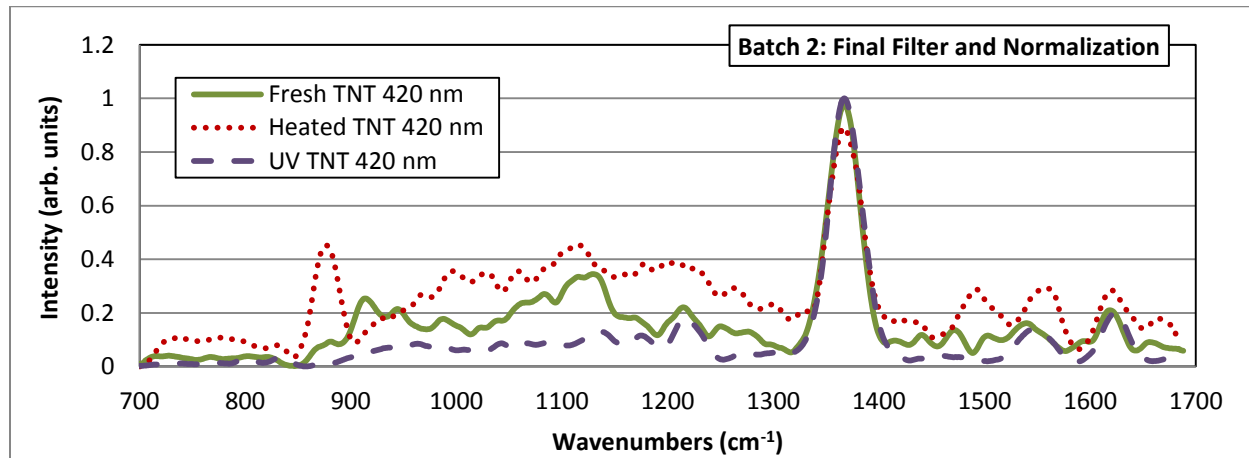
Single Signature Name	Fresh Average	Heated Average	UV Average
FreshTNT_vis_07_20_2011_PostPro_data.txt	0.8932	0.8411	0.8669
FreshTNT_vis_07_20_2011_Run10_PostPro_data.txt	0.9619	0.9135	0.95
FreshTNT_vis_07_20_2011_Run3_PostPro_data.txt	0.9224	0.8982	0.9115
FreshTNT_vis_07_20_2011_Run4_PostPro_data.txt	0.9361	0.9054	0.9133
FreshTNT_vis_07_20_2011_Run5_PostPro_data.txt	0.901	0.8694	0.8809
FreshTNT_vis_07_20_2011_Run7_PostPro_data.txt	0.9602	0.9044	0.9496
FreshTNT_vis_07_20_2011_Run8_PostPro_data.txt	0.9557	0.8988	0.9457
FreshTNT_vis_07_20_2011_Run9_PostPro_data.txt	0.9576	0.9048	0.946
HeatedTNT_vis_07_19_2011_PostPro_data.txt	0.5575	0.6829	0.5553
HeatedTNT_vis_07_19_2011_Run2_PostPro_data.txt	0.847	0.8862	0.8449
HeatedTNT_vis_07_19_2011_Run3_PostPro_data.txt	0.8769	0.8895	0.8773
HeatedTNT_vis_07_19_2011_Run4_PostPro_data.txt	0.9379	0.9419	0.9324
HeatedTNT_vis_07_19_2011_Run5_PostPro_data.txt	0.8734	0.9268	0.8699
HeatedTNT_vis_07_19_2011_Run6_PostPro_data.txt	0.8875	0.9245	0.8852
UVTNT_vis_07_07_2011_PostPro_data.txt	0.9701	0.9256	0.9843
UVTNT_vis_07_07_2011_Run2_PostPro_data.txt	0.9726	0.9336	0.9854
UVTNT_vis_07_07_2011_Run3_PostPro_data.txt	0.9632	0.9294	0.9739
UVTNT_vis_07_07_2011_Run4_PostPro_data.txt	0.9639	0.926	0.975
UVTNT_vis_07_07_2011_Run5_PostPro_data.txt	0.9703	0.923	0.9875
UVTNT_vis_07_07_2011_Run6_PostPro_data.txt	0.9563	0.9072	0.977

Correlation Crosstable for signature identification: Under this processing regime we are correctly able to identify the correct class of all 20 of 20 signatures. Interestingly the correlation score for one of the

Heated TNT samples dropped by over 20 percent between the last level of processing and this one. This is unique as for most other signatures this additional processing removes artifacts and causes the correlation score to increase.

TNT Batch 2 Full Spectrum Normalization



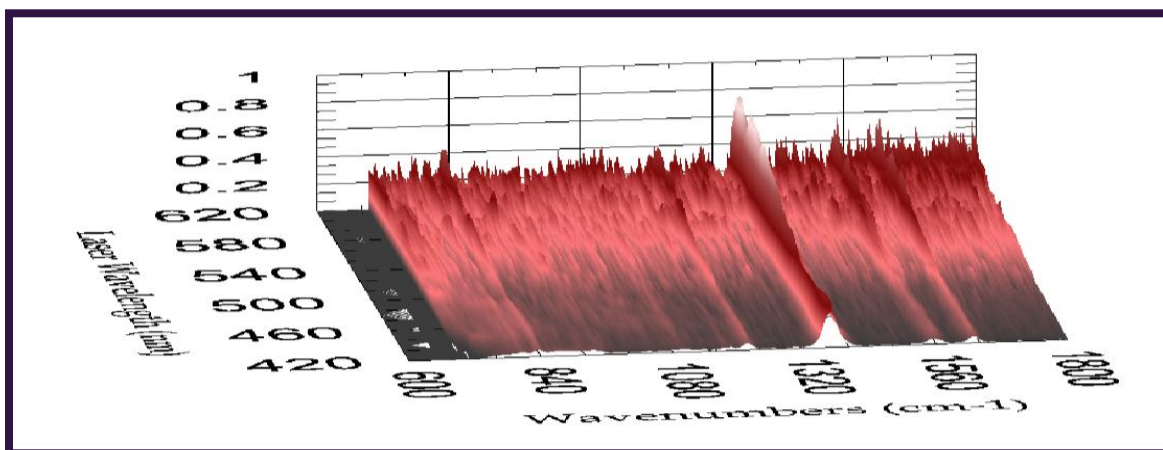
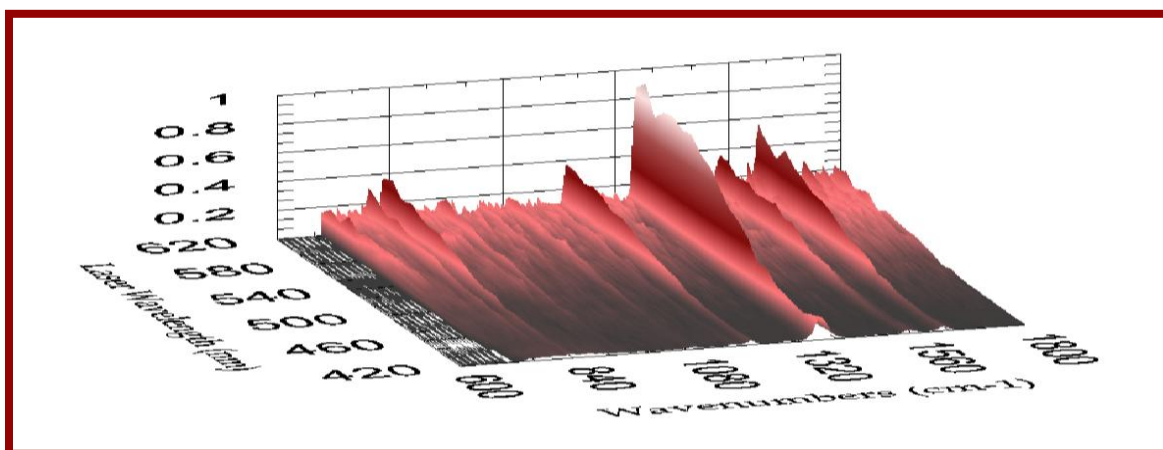
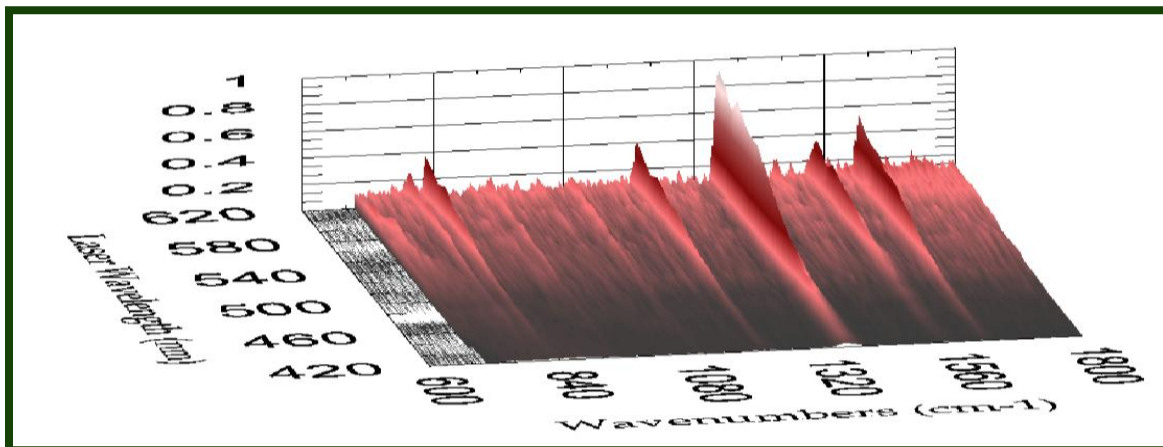


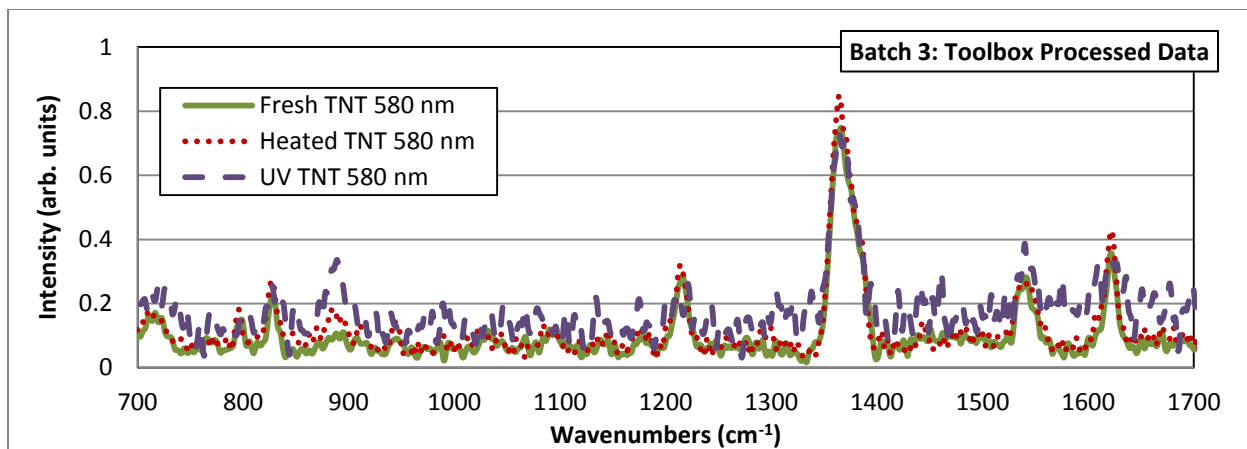
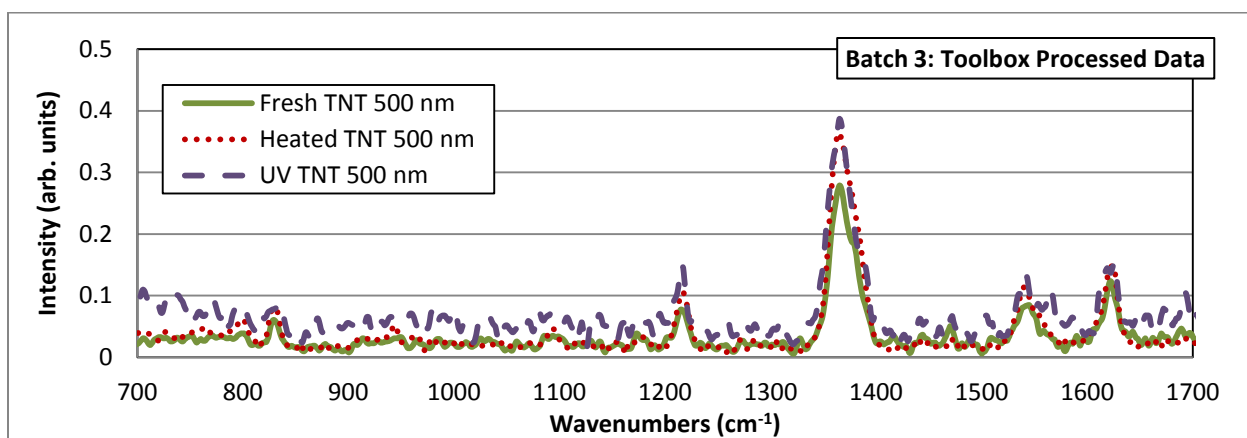
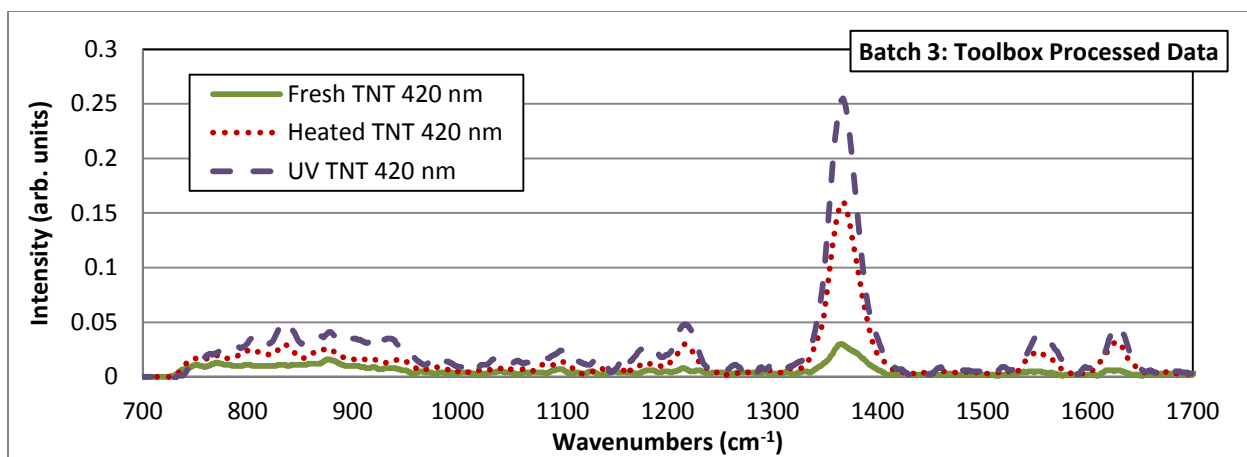
Lineouts for final filter and processed TNT batch 2 files. We note that even with the extensive processing done the Heated TNT retains a higher baseline underneath the signature as a consequence of the noise inherent in the signature as can be seen in the 2D signatures.

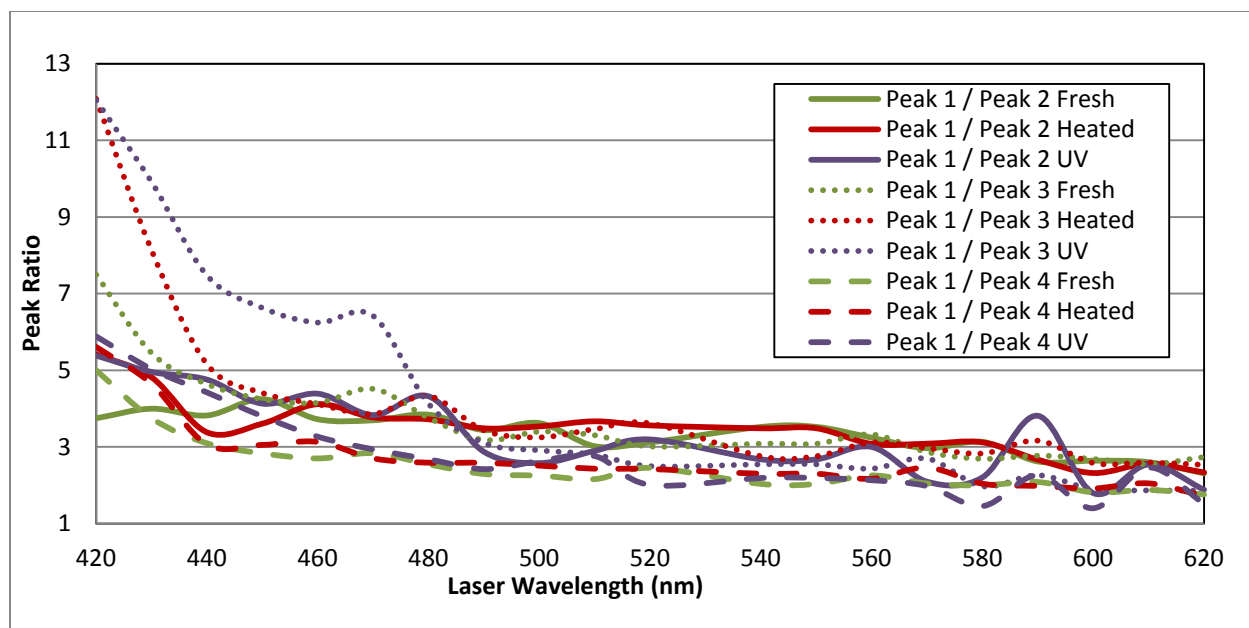
Single Signature Name	Fresh Average	Heated Average	UV Average
FreshTNT_vis_07_20_2011_FinalData.txt	0.9388	0.9142	0.933
FreshTNT_vis_07_20_2011_Run10_FinalData.txt	0.9832	0.9528	0.9786
FreshTNT_vis_07_20_2011_Run3_FinalData.txt	0.9569	0.9456	0.9416
FreshTNT_vis_07_20_2011_Run4_FinalData.txt	0.9647	0.9423	0.9408
FreshTNT_vis_07_20_2011_Run5_FinalData.txt	0.9509	0.9319	0.9274
FreshTNT_vis_07_20_2011_Run7_FinalData.txt	0.9794	0.9454	0.9777
FreshTNT_vis_07_20_2011_Run8_FinalData.txt	0.9732	0.9348	0.9691
FreshTNT_vis_07_20_2011_Run9_FinalData.txt	0.9767	0.9406	0.9725
HeatedTNT_vis_07_19_2011_FinalData.txt	0.6874	0.773	0.6829
HeatedTNT_vis_07_19_2011_Run2_FinalData.txt	0.9266	0.9388	0.9298
HeatedTNT_vis_07_19_2011_Run3_FinalData.txt	0.9244	0.9315	0.9315
HeatedTNT_vis_07_19_2011_Run4_FinalData.txt	0.9732	0.9769	0.9624
HeatedTNT_vis_07_19_2011_Run5_FinalData.txt	0.9256	0.9526	0.905
HeatedTNT_vis_07_19_2011_Run6_FinalData.txt	0.9398	0.9615	0.9341
UVTNT_vis_07_07_2011_FinalData.txt	0.9779	0.9548	0.9931
UVTNT_vis_07_07_2011_Run2_FinalData.txt	0.9836	0.9622	0.9943
UVTNT_vis_07_07_2011_Run3_FinalData.txt	0.9838	0.9675	0.9905
UVTNT_vis_07_07_2011_Run4_FinalData.txt	0.9806	0.9601	0.9909
UVTNT_vis_07_07_2011_Run5_FinalData.txt	0.9771	0.953	0.994
UVTNT_vis_07_07_2011_Run6_FinalData.txt	0.973	0.9474	0.9884

Correlation Crosstable for signature identification: While we do correctly identify all 20 signatures the margin of identification is often only a few tenths of a percent. The fact that these few tenths uniformly allow the correct identification makes it statistically significant however it must be acknowledged that this is closer than the error bounds determined by shot to shot reproducibility.

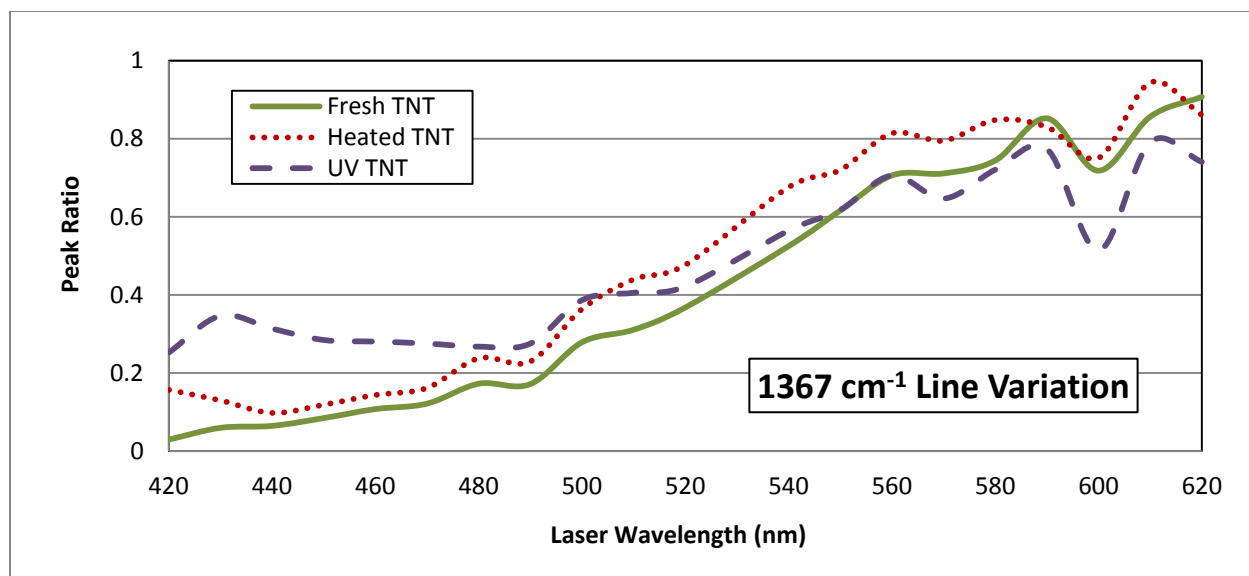
TNT Batch 3 HDF Processed







TNT Peak Ratios for Batch 3: The Ratio of Peak 1 over Peak 3 ($1367\text{cm}^{-1} / 1541\text{ cm}^{-1}$) for the aged variants are significantly larger than their Fresh counterpart at the lower laser illumination wavelengths. This was also true for the UV ratio in batch 2.

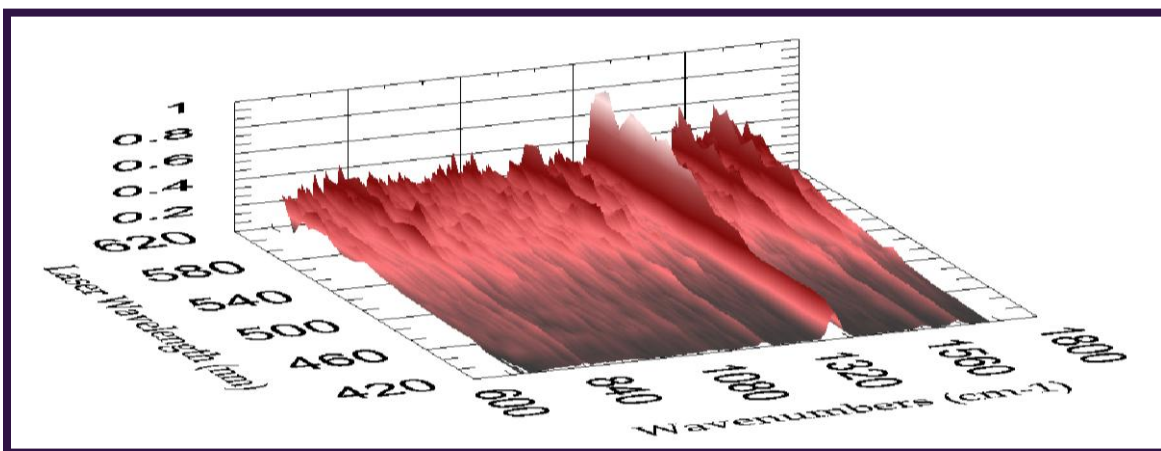
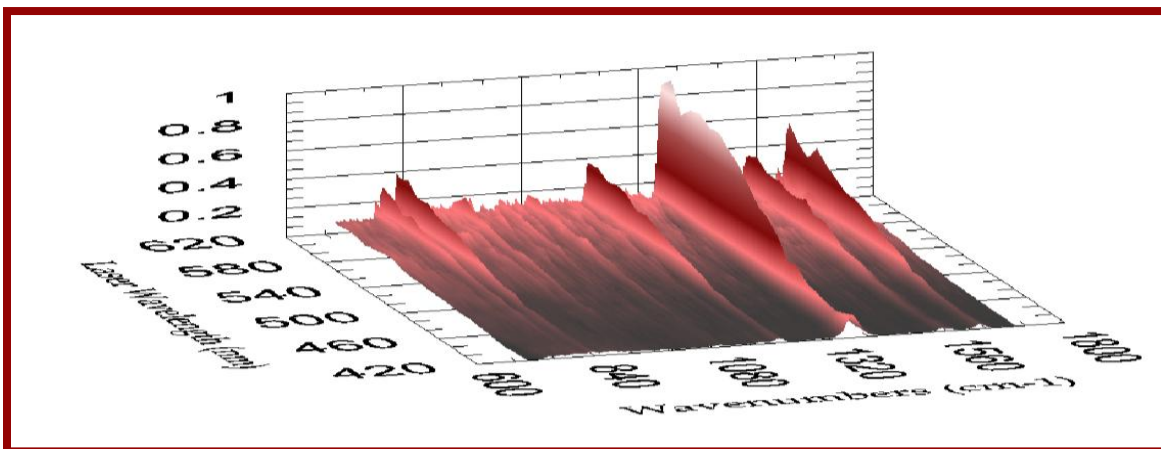
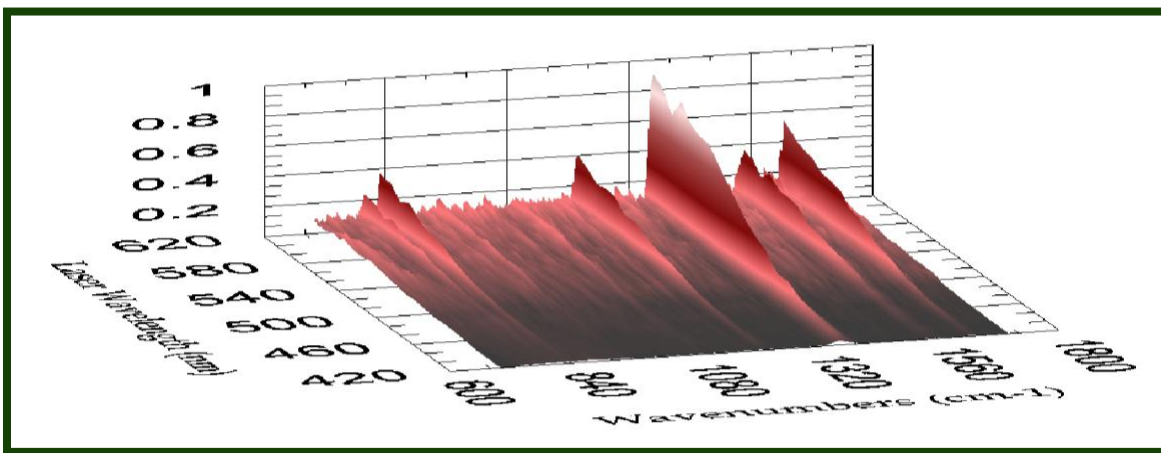


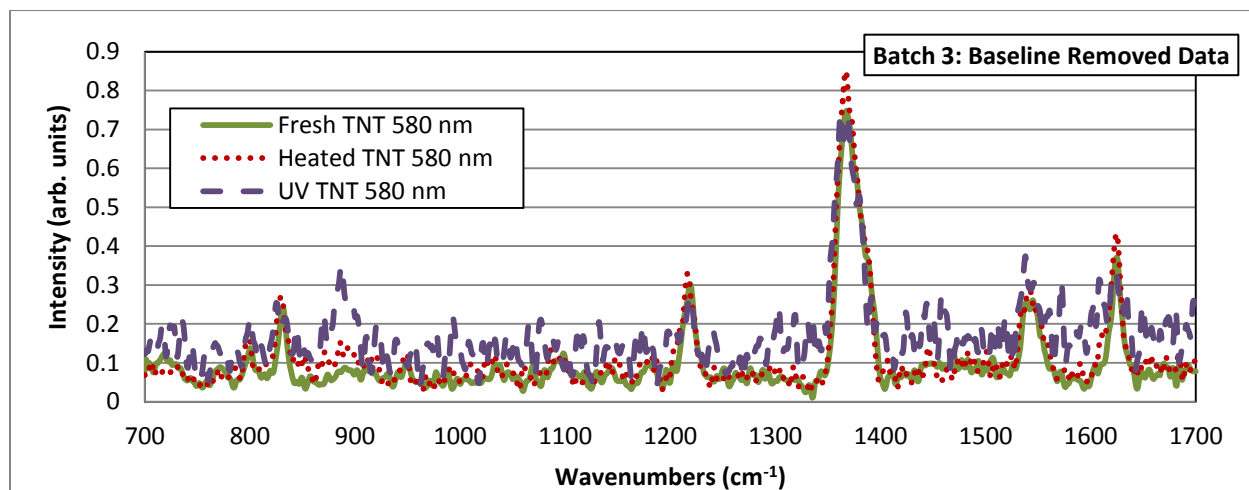
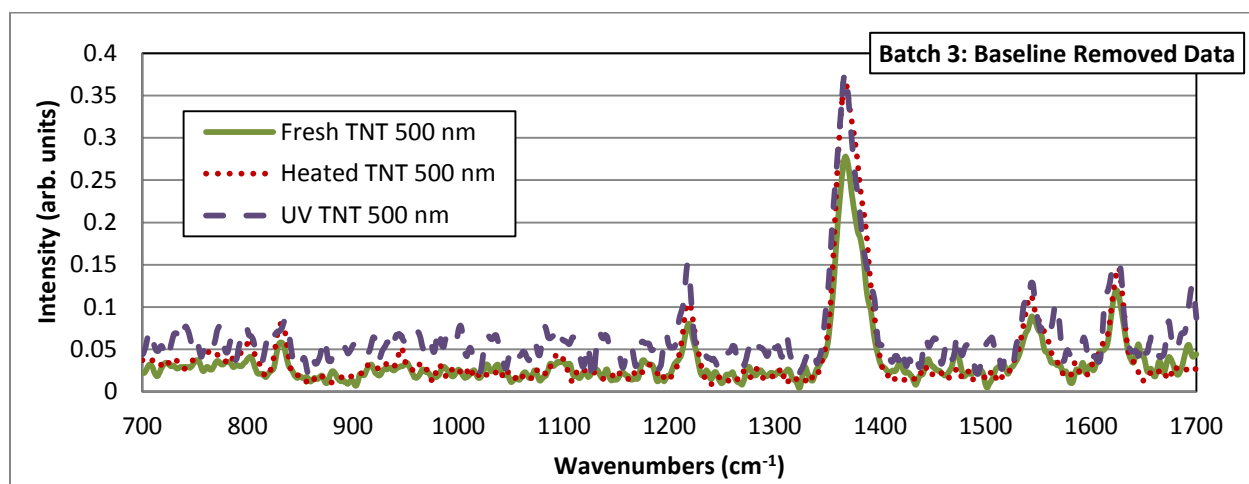
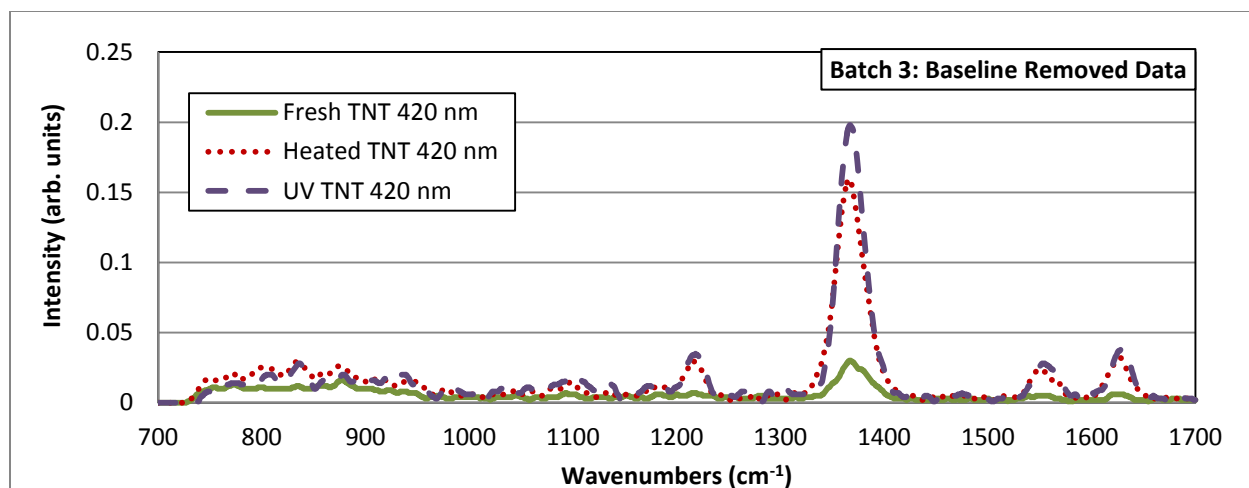
Behavior of the 1367 cm^{-1} line with respect to changes in laser illumination wavelength: As opposed to the first two batches, there does not appear to be a peak in intensity around 560-580 nm for any of the three TNT variants.

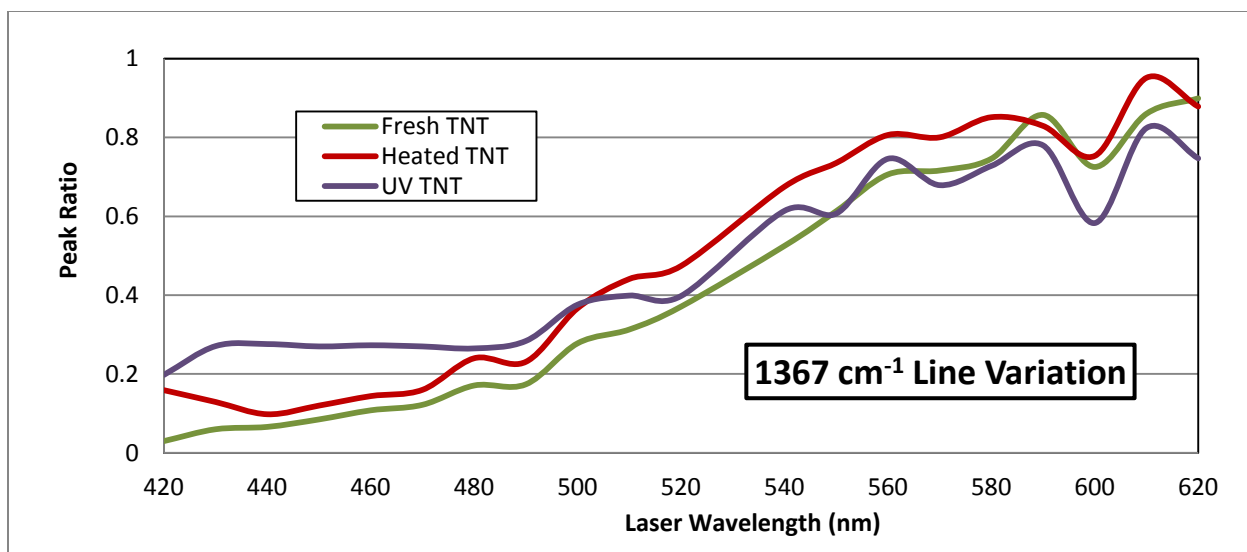
Single Signature Name	Fresh Average	Heated Average	UV Average
FreshTNTVis_10_02_2012_HDF2_data.txt	0.9515	0.9185	0.8333
FreshTNTVis_10_02_2012_Run2_HDF2_data.txt	0.9478	0.9285	0.8308
FreshTNTVis_10_02_2012_Run3_HDF2_data.txt	0.9227	0.8827	0.8157
FreshTNTVis_10_02_2012_Run4_HDF2_data.txt	0.9525	0.9233	0.8469
FreshTNTVis_10_02_2012_Run5_HDF2_data.txt	0.9405	0.9158	0.8408
HeatedTNTVis_10_02_2012_HDF2_data.txt	0.9152	0.9503	0.851
HeatedTNTVis_10_02_2012_Run2_HDF2_data.txt	0.9271	0.9552	0.8575
HeatedTNTVis_10_02_2012_Run3_HDF2_data.txt	0.9184	0.9544	0.8568
HeatedTNTVis_10_02_2012_Run4_HDF2_data.txt	0.8949	0.9216	0.8368
HeatedTNTVis_10_02_2012_Run5_HDF2_data.txt	0.9474	0.9683	0.8437
UVTNTVis_10_03_2012_HDF2_data.txt	0.8661	0.8836	0.8883
UVTNTVis_10_03_2012_Run2_HDF2_data.txt	0.8135	0.824	0.8701
UVTNTVis_10_03_2012_Run3_HDF2_data.txt	0.6282	0.6246	0.7642
UVTNTVis_10_03_2012_Run4_HDF2_data.txt	0.6958	0.7008	0.8672

Correlation Crosstable for sample identification. The correlation coefficient algorithm was correctly able to identify all 14 samples. Due to the reduced data quality in the UV aged samples, the correlation coefficients are all below 90%. This indicates a large amount of noise within the signatures as is visible in both the 2D and 580nm lineout graphs. This is due to the poor quality of the UV aged sample in this particular batch.

Set 3 Baseline Removal





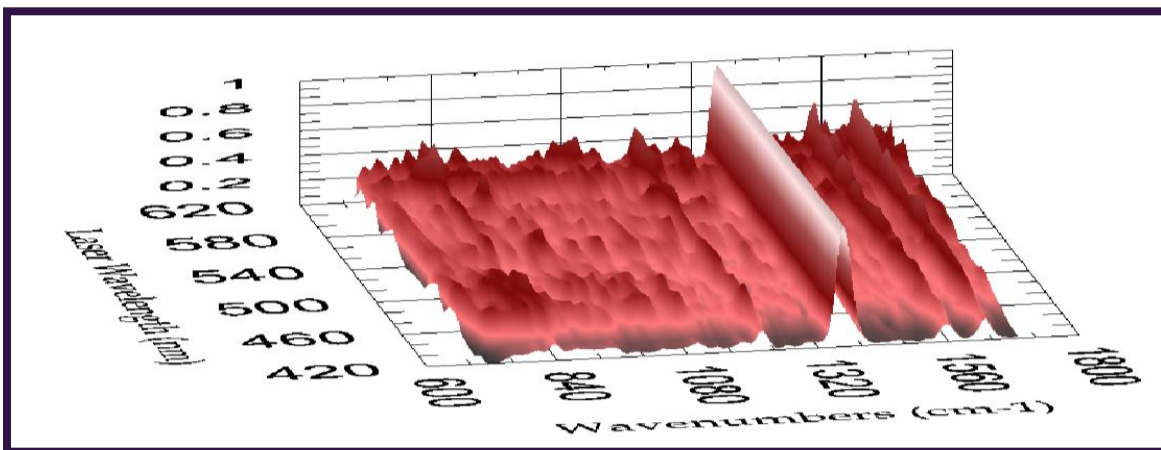
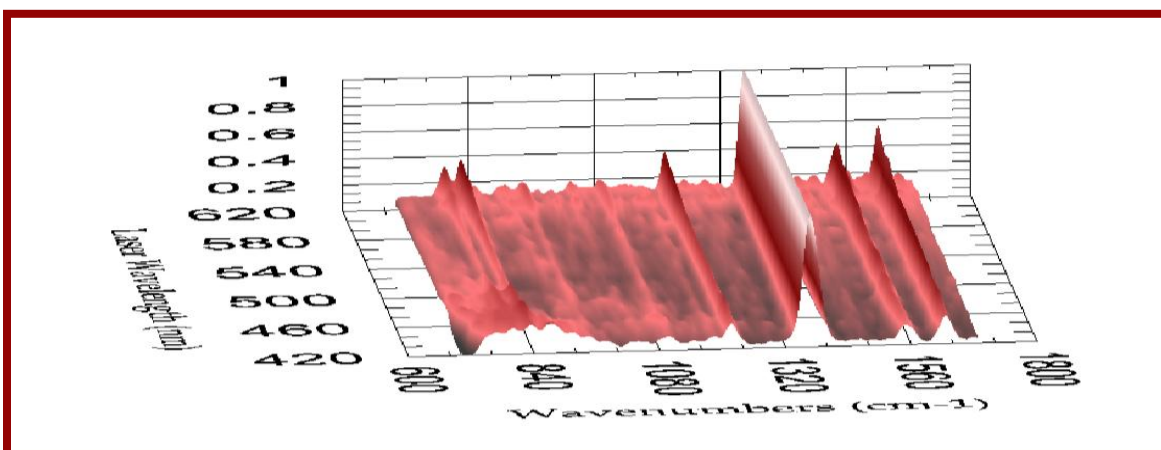
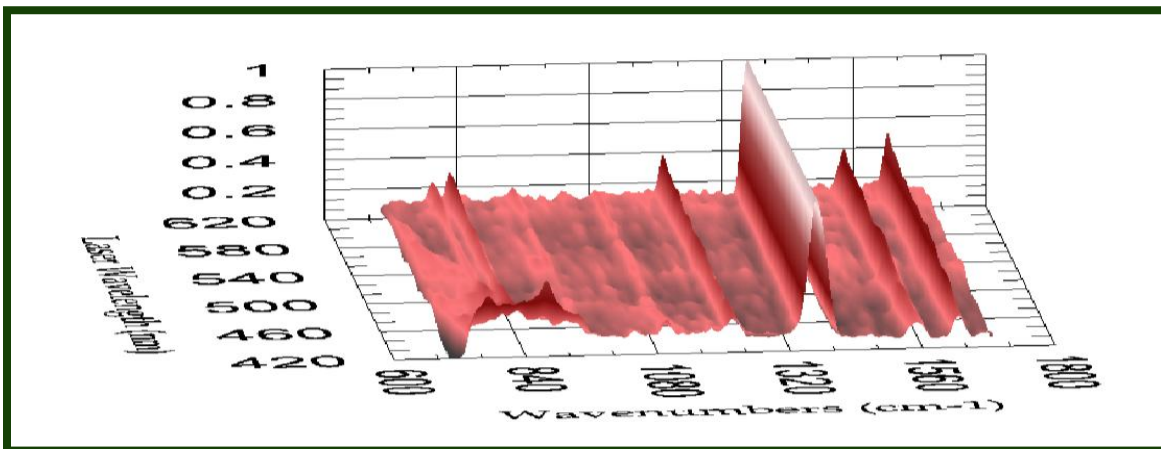


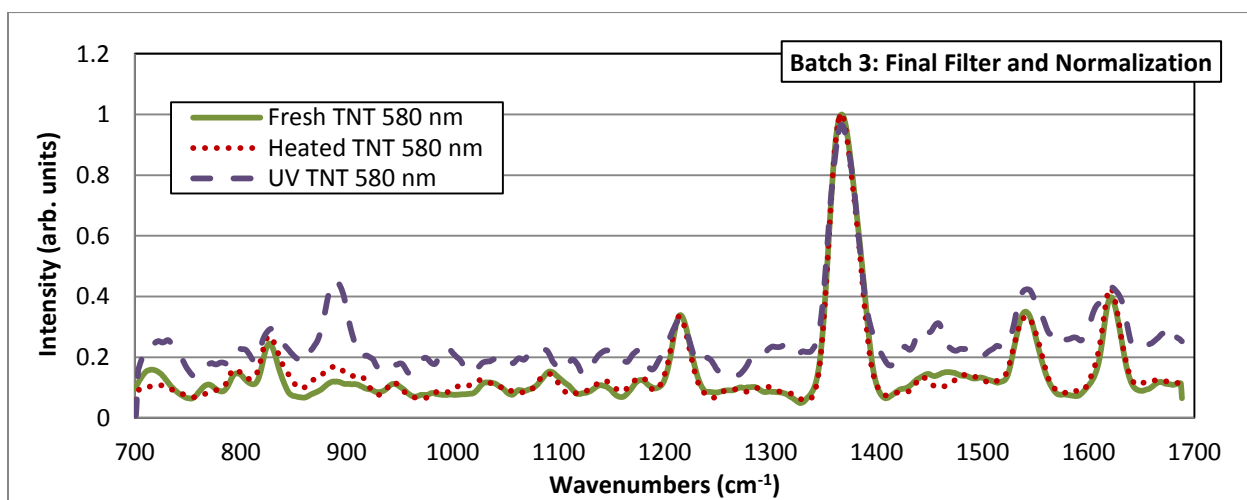
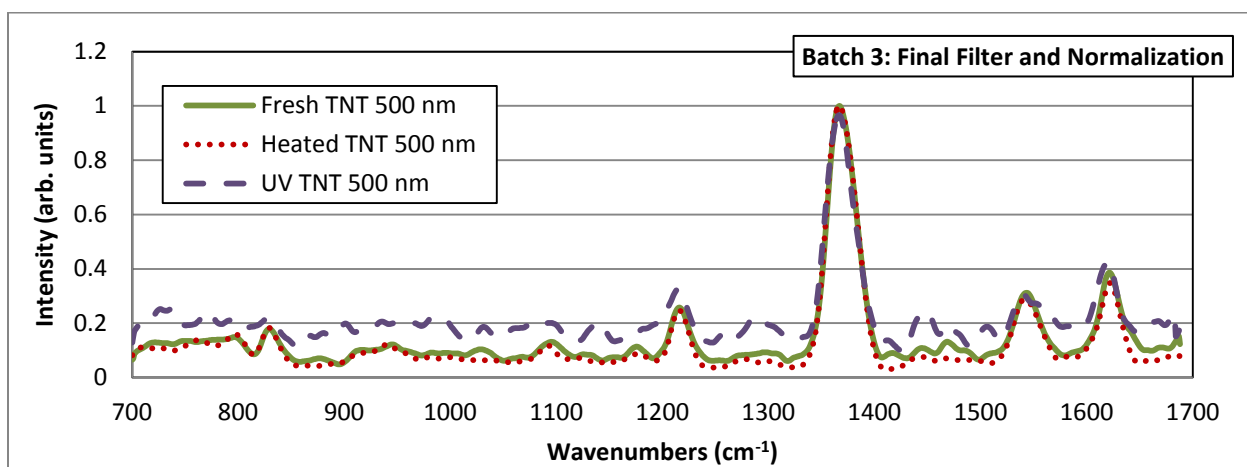
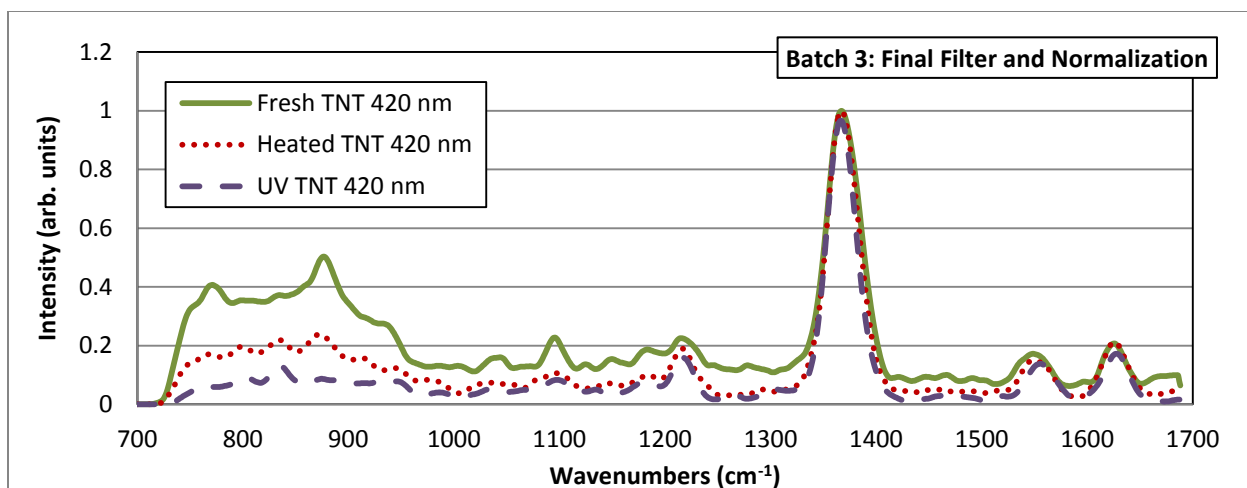
Behavior of the 1367 cm⁻¹ line with respect to changes in laser illumination wavelength

Single Signature Name	Fresh Average	Heated Average	UV Average
FreshTNTVis_10_02_2012_PostPro_data.txt	0.9562	0.9302	0.856
FreshTNTVis_10_02_2012_Run2_PostPro_data.txt	0.958	0.9457	0.8708
FreshTNTVis_10_02_2012_Run3_PostPro_data.txt	0.9282	0.8959	0.8191
FreshTNTVis_10_02_2012_Run4_PostPro_data.txt	0.9589	0.9309	0.8526
FreshTNTVis_10_02_2012_Run5_PostPro_data.txt	0.9462	0.9212	0.8505
HeatedTNTVis_10_02_2012_PostPro_data.txt	0.921	0.9563	0.864
HeatedTNTVis_10_02_2012_Run2_PostPro_data.txt	0.9361	0.9597	0.8739
HeatedTNTVis_10_02_2012_Run3_PostPro_data.txt	0.9249	0.9539	0.8594
HeatedTNTVis_10_02_2012_Run4_PostPro_data.txt	0.9047	0.9267	0.8348
HeatedTNTVis_10_02_2012_Run5_PostPro_data.txt	0.9638	0.9777	0.894
UVTNTVis_10_03_2012_PostPro_data.txt	0.8953	0.9115	0.9018
UVTNTVis_10_03_2012_Run2_PostPro_data.txt	0.816	0.8253	0.8618
UVTNTVis_10_03_2012_Run3_PostPro_data.txt	0.5918	0.6072	0.7075
UVTNTVis_10_03_2012_Run4_PostPro_data.txt	0.5852	0.5957	0.7637

Correlation Crosstable for sample identification: We have correctly identified 13 out of 14 signatures. The correlation scores for the UV aged samples continue to be smaller than the others and we note that the correlation scores for the final two signatures have become even smaller however the spread between the correct and incorrect answers is still greater than 10 percentage points.

Fresh TNT Set 3 Full Spectrum Normalization

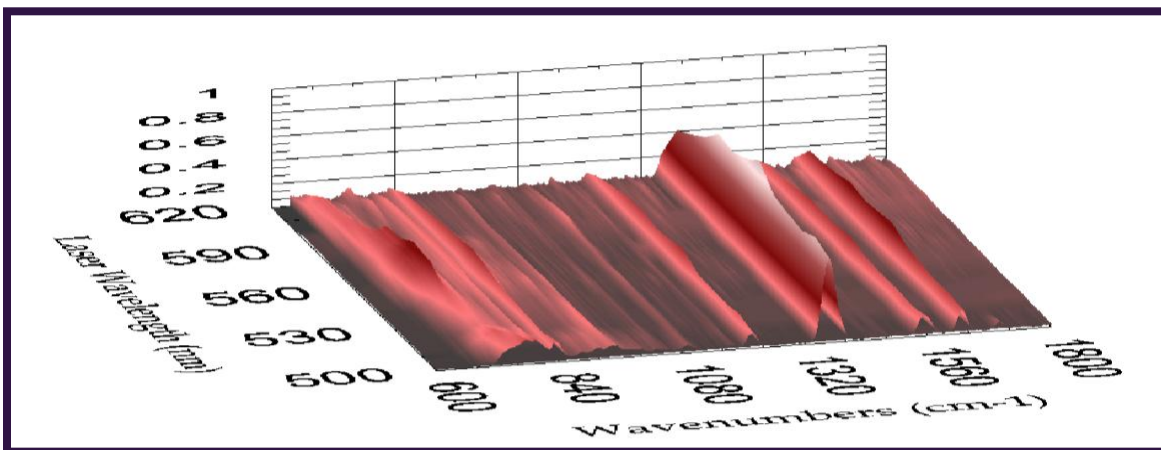
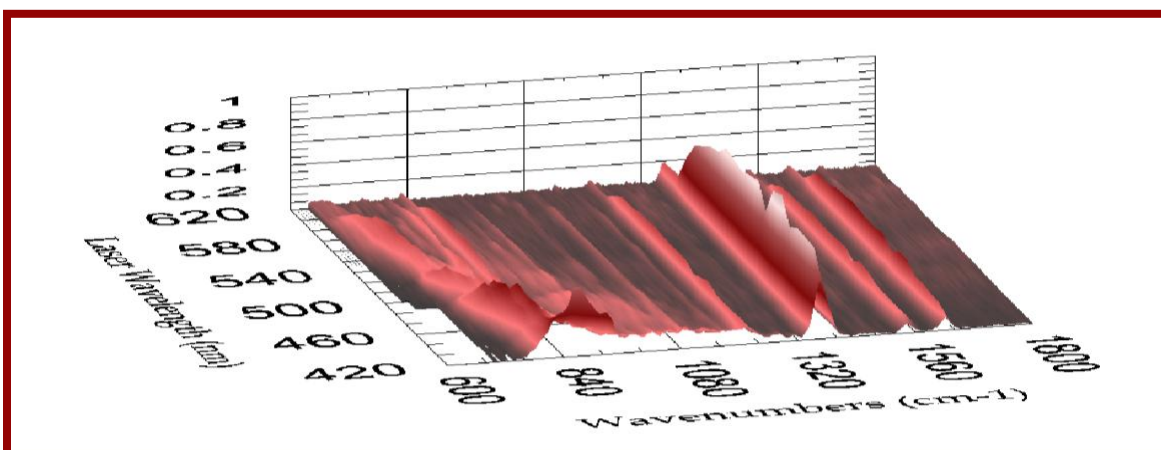
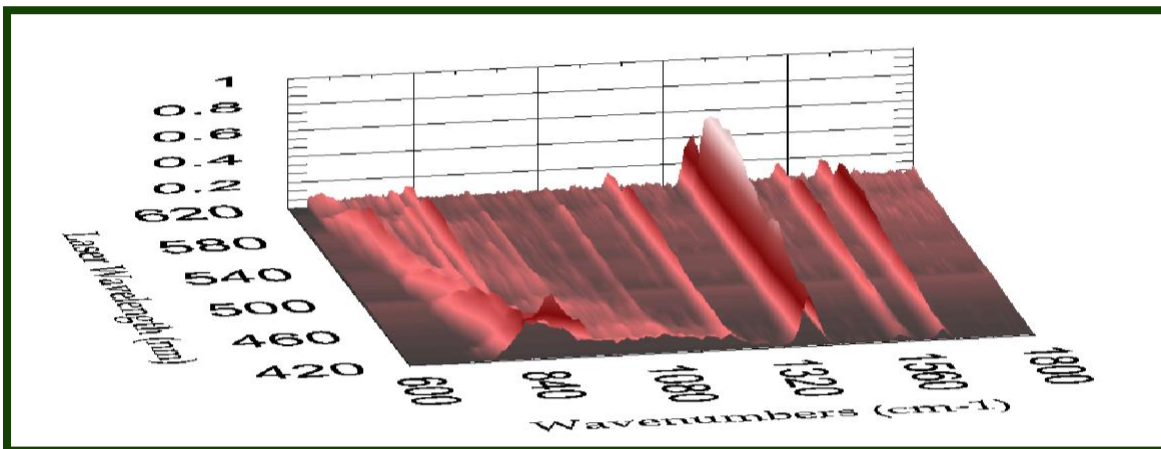


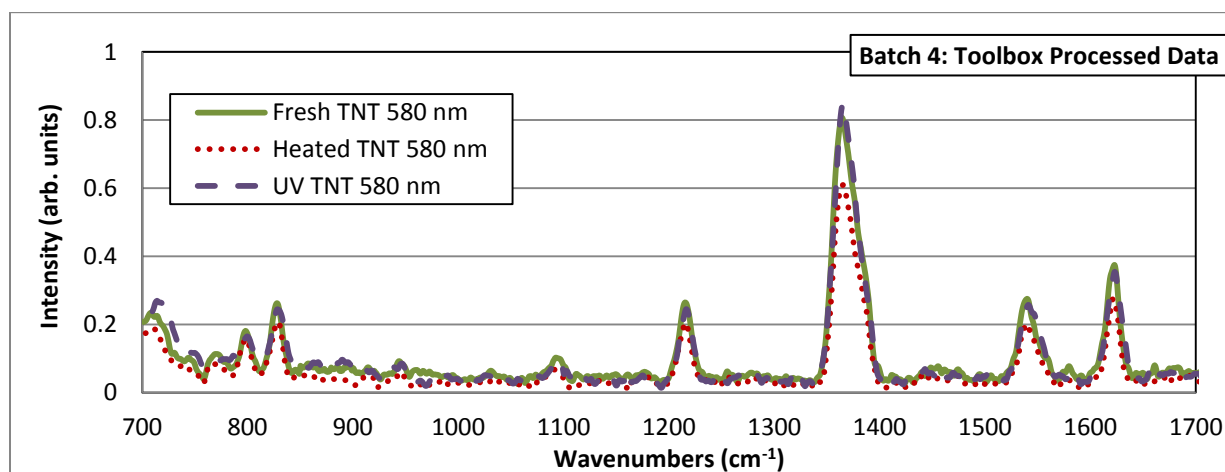
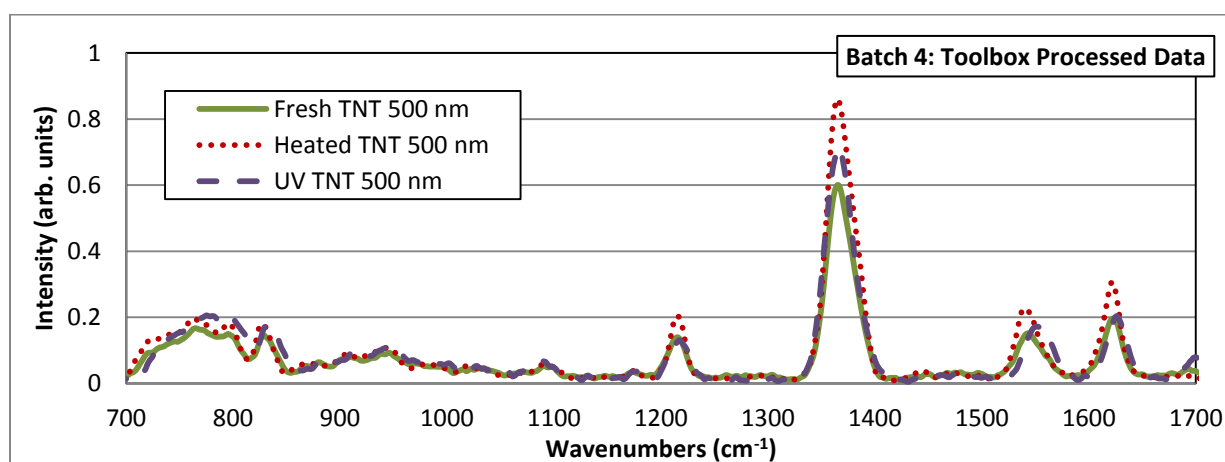
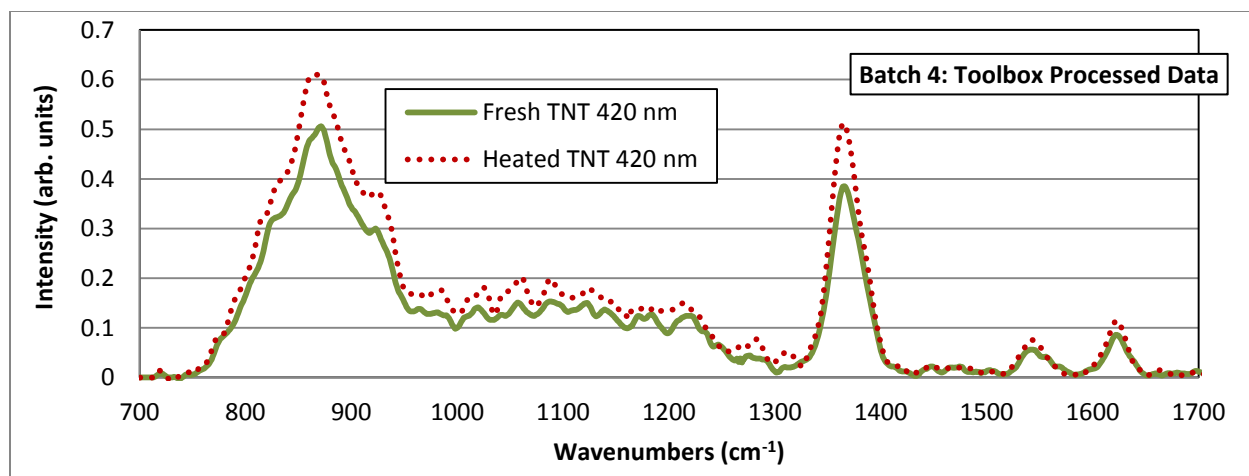


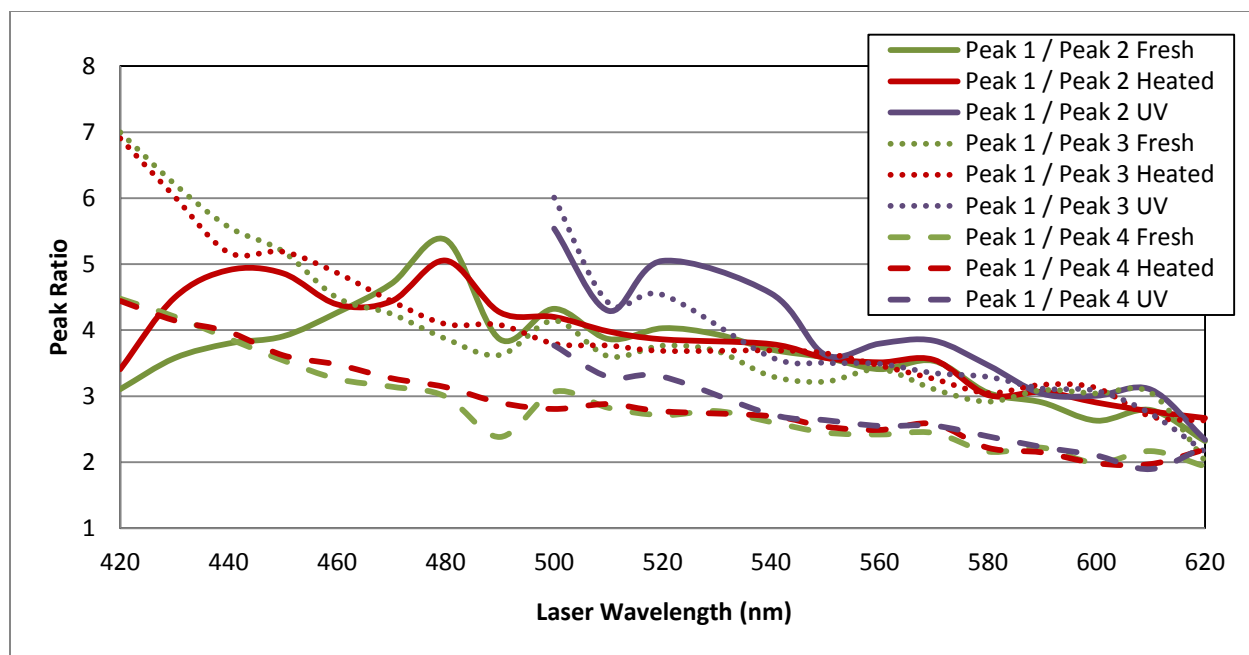
Single Signature Name	Fresh Average	Heated Average	UV Average
FreshTNTVis_10_02_2012_FinalData.txt	0.977	0.9692	0.9108
FreshTNTVis_10_02_2012_Run2_FinalData.txt	0.9787	0.9747	0.9187
FreshTNTVis_10_02_2012_Run3_FinalData.txt	0.9656	0.9487	0.9022
FreshTNTVis_10_02_2012_Run4_FinalData.txt	0.9847	0.973	0.9201
FreshTNTVis_10_02_2012_Run5_FinalData.txt	0.9806	0.9694	0.9186
HeatedTNTVis_10_02_2012_FinalData.txt	0.9681	0.9813	0.9297
HeatedTNTVis_10_02_2012_Run2_FinalData.txt	0.973	0.9844	0.9283
HeatedTNTVis_10_02_2012_Run3_FinalData.txt	0.9676	0.982	0.9318
HeatedTNTVis_10_02_2012_Run4_FinalData.txt	0.9587	0.9699	0.9139
HeatedTNTVis_10_02_2012_Run5_FinalData.txt	0.9814	0.9888	0.9305
UVTNTVis_10_03_2012_FinalData.txt	0.9425	0.9537	0.9198
UVTNTVis_10_03_2012_Run2_FinalData.txt	0.9121	0.9172	0.9322
UVTNTVis_10_03_2012_Run3_FinalData.txt	0.749	0.7621	0.8696
UVTNTVis_10_03_2012_Run4_FinalData.txt	0.7384	0.7483	0.8539

Correlation Crosstable for Batch 3 identification: 13 of 14 were correctly identified. Correlation scores for the UV aged TNT are now all above 85% giving greater confidence in the identification. The ability to identify complex or noisy samples may be aided by the additional processing. We do note however that the additional processing has taken 1 of the aged TNT samples from being correctly identified to the point where the correct identification is now the least likely choice among the options given.

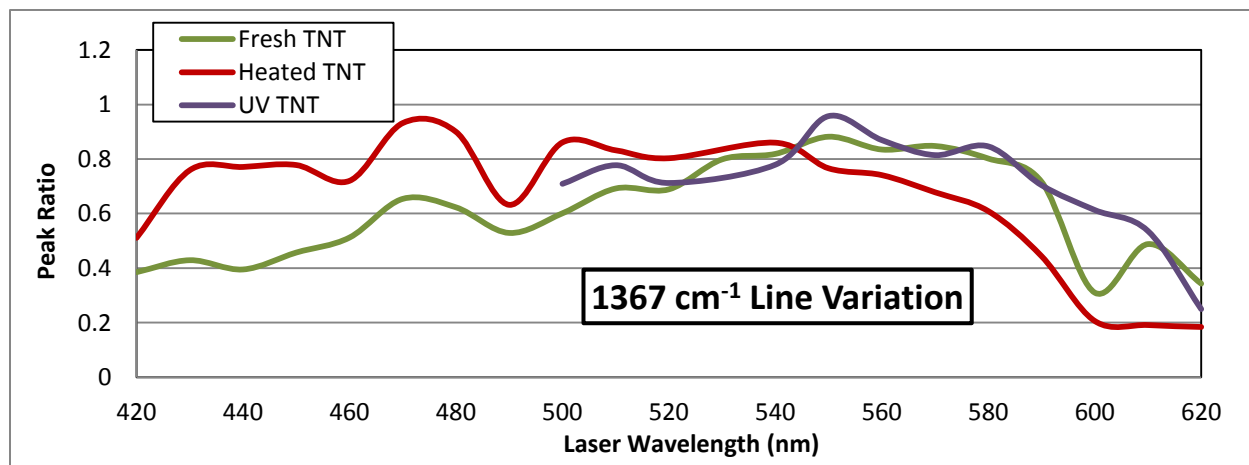
Batch 4 HDF Processed Data







TNT Peak Ratios for Batch 3: The Ratios of all three types are very similar with the UV version being slightly larger from 500 - 540 nm. Due to increased laser absorbance in the UV aged sample we were unable to reliably record Raman signatures under 500nm



Behavior of the 1367 cm⁻¹ line with respect to changes in laser illumination wavelength. The overall 2D behavior of these samples is notably different from the previous 3 batches. The intensity at the lower illumination wavelengths is a factor of at least 2 stronger than in previous iterations. This may be due to a noted sample deterioration during the multiwavelength signature collection. Thus it is not that the lower wavelengths are stronger, but that the upper wavelengths are weaker due to sample degradation.

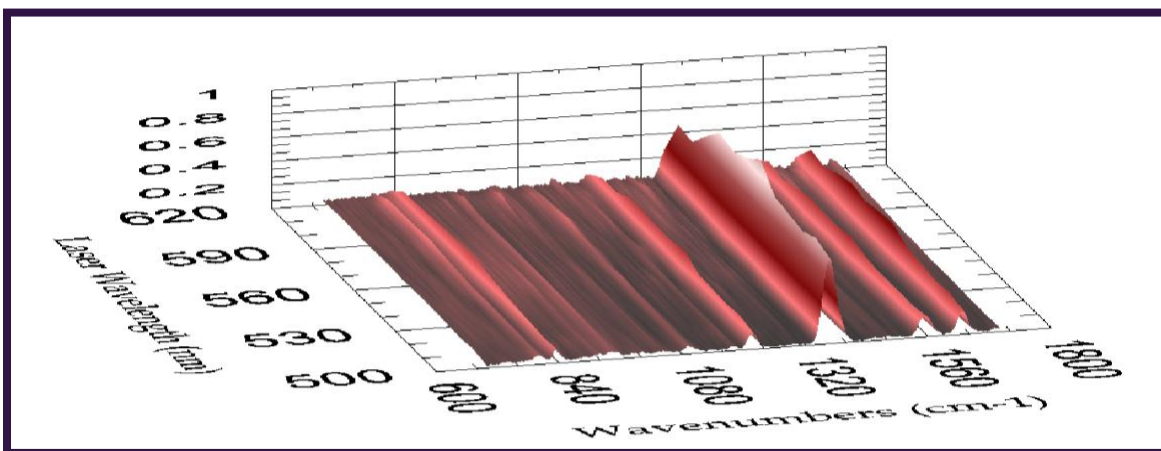
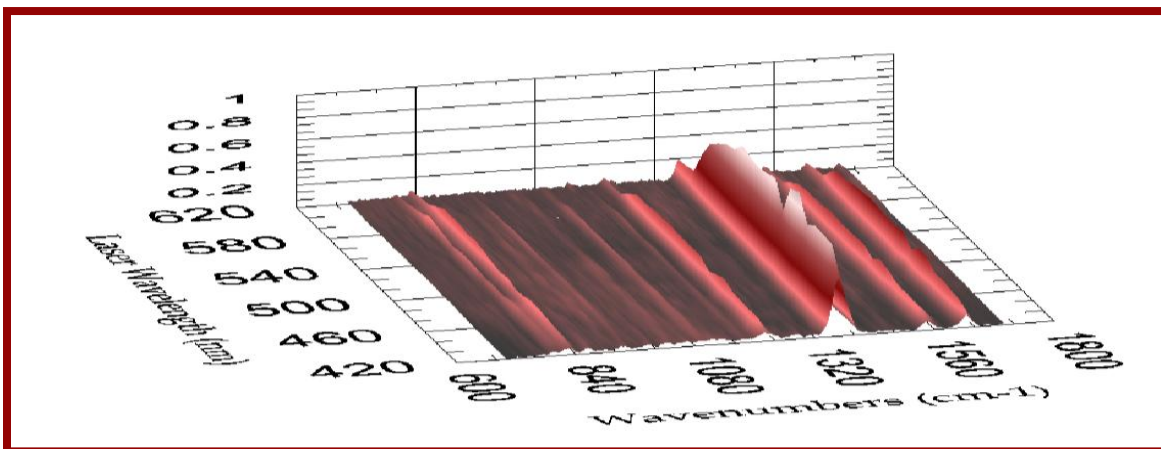
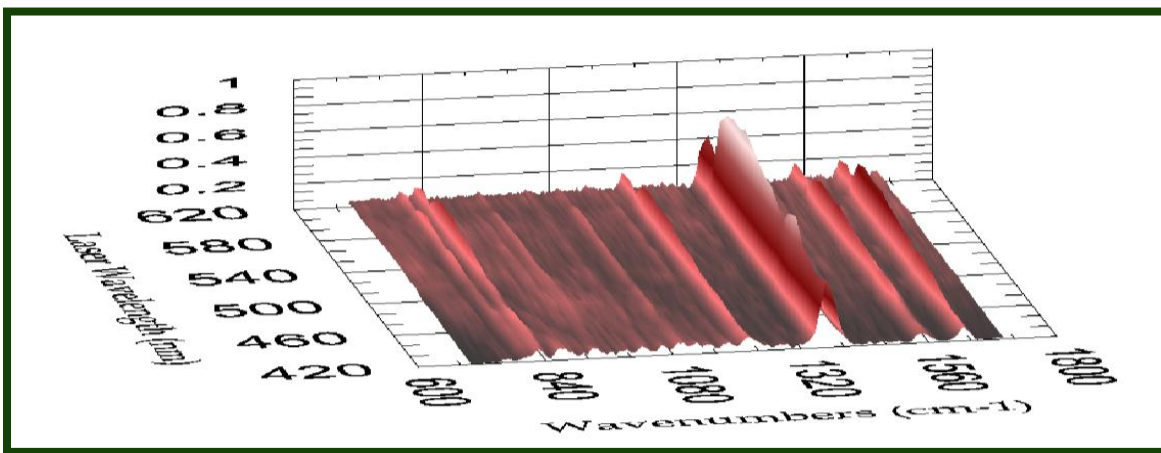
Single Signature Name	Fresh Average	Heated Average	UV Average
FreshTNTVis_01_04_2013_HDF2_data.txt	0.9711	0.9559	0.9473
FreshTNTVis_01_04_2013_Run10_HDF2_data.txt	0.8662	0.8044	0.79
FreshTNTVis_01_04_2013_Run2_HDF2_data.txt	0.9529	0.9387	0.9309
FreshTNTVis_01_04_2013_Run3_HDF2_data.txt	0.9294	0.9306	0.9258
FreshTNTVis_01_04_2013_Run4_HDF2_data.txt	0.9624	0.955	0.9418
FreshTNTVis_01_04_2013_Run5_HDF2_data.txt	0.9572	0.9607	0.9462
FreshTNTVis_01_04_2013_Run6_HDF2_data.txt	0.9569	0.9412	0.9269
FreshTNTVis_01_04_2013_Run7_HDF2_data.txt	0.9616	0.9593	0.9447
FreshTNTVis_01_04_2013_Run8_HDF2_data.txt	0.9664	0.9547	0.9362
FreshTNTVis_01_04_2013_Run9_HDF2_data.txt	0.9109	0.8863	0.864
FreshTNTVis_01_08_2013_HDF2_data.txt	0.8818	0.8686	0.7886
FreshTNTVis_01_08_2013_Run2_HDF2_data.txt	0.9111	0.8921	0.8455
FreshTNTVis_01_08_2013_Run3_HDF2_data.txt	0.9101	0.9018	0.8197
FreshTNTVis_01_08_2013_Run4_HDF2_data.txt	0.6758	0.6139	0.4543
FreshTNTVis_01_08_2013_Run5_HDF2_data.txt	0.8262	0.7724	0.678
FreshTNTVis_01_09_2013_HDF2_data.txt	0.9287	0.9722	0
FreshTNTVis_01_09_2013_Run2_HDF2_data.txt	0.9279	0.9286	0.8122
FreshTNTVis_01_09_2013_Run3_HDF2_data.txt	0.9218	0.9598	0.9118
FreshTNTVis_01_24_2013_Run1b_HDF2_data.txt	0.9649	0.9562	0.9461
FreshTNTVis_01_24_2013_Run2b_HDF2_data.txt	0.9205	0.9091	0.9259
FreshTNTVis_01_24_2013_Run3b_HDF2_data.txt	0.9636	0.9485	0.9476
FreshTNTVis_01_24_2013_Run4b_HDF2_data.txt	0.9604	0.9387	0.9318
FreshTNTVis_01_24_2013_Run5b_HDF2_data.txt	0.9587	0.9453	0.9468
FreshTNTVis_01_24_2013_Run6b_HDF2_data.txt	0.9618	0.9423	0.9413

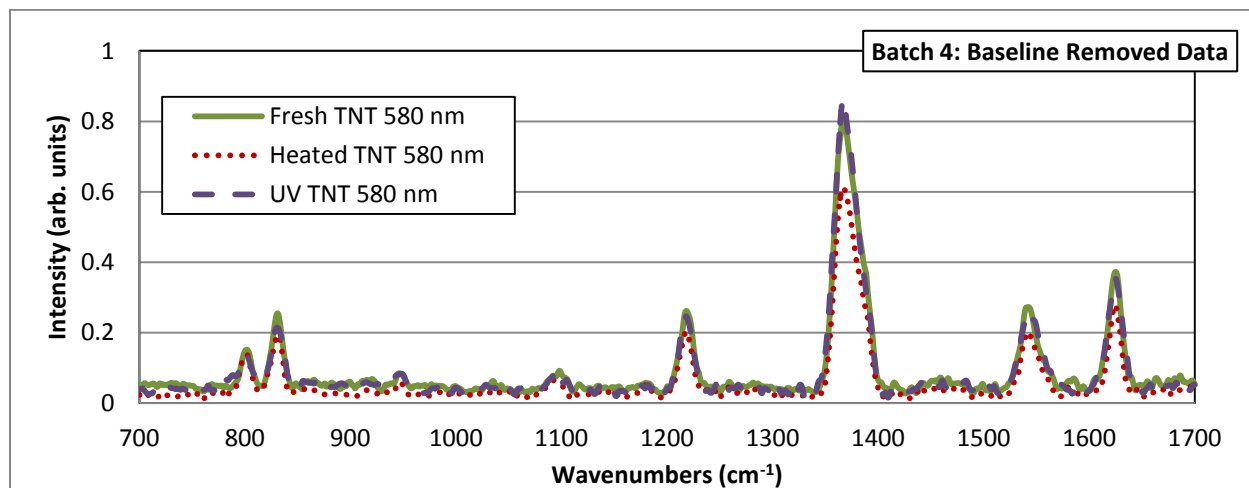
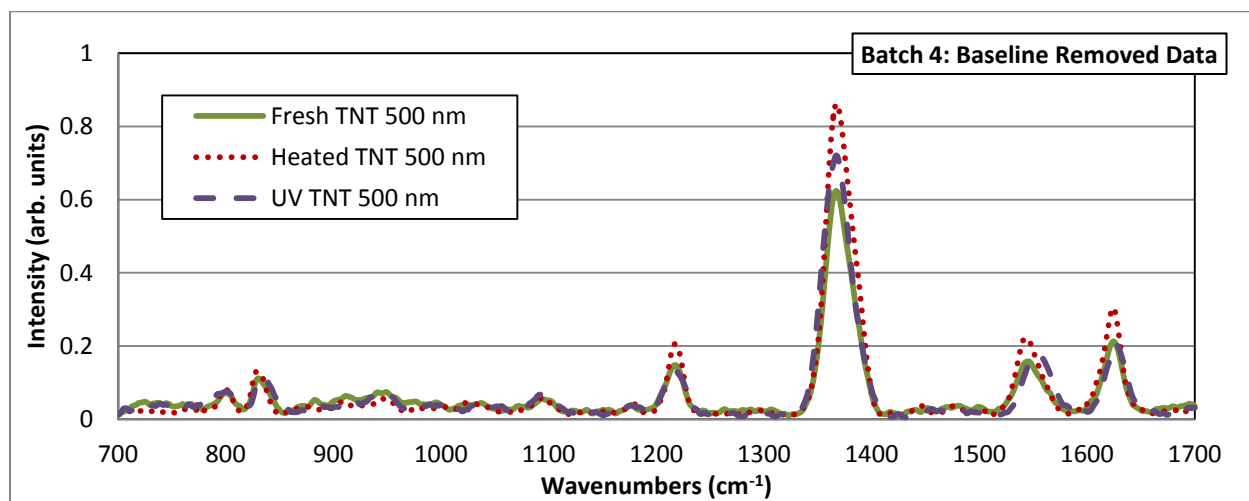
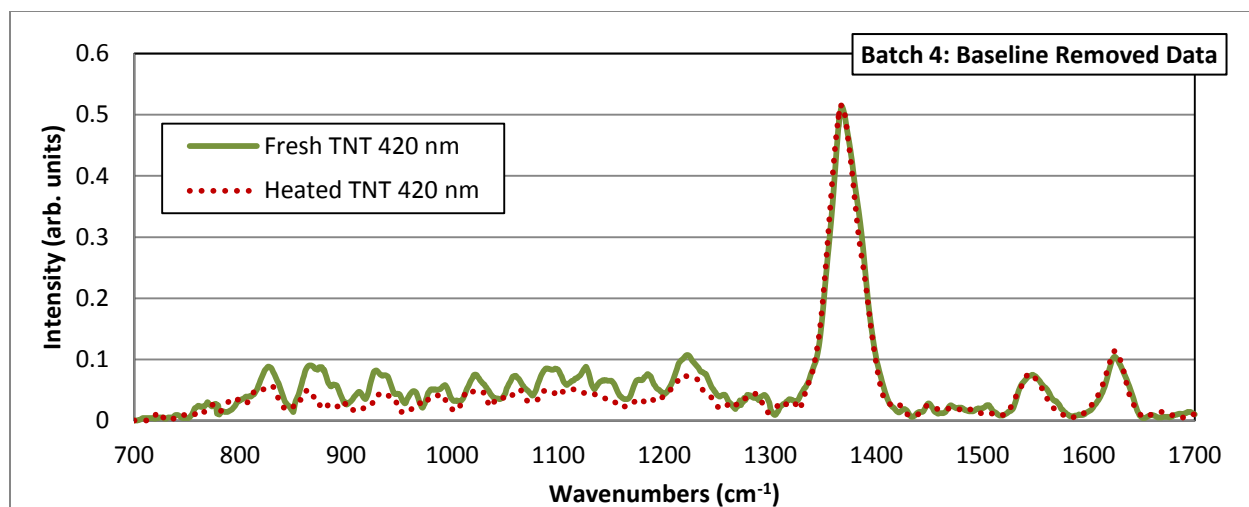
Correlation Crosstable for identification (Heated and UV crosstable located on following page). We have correctly identified 47 of the 54 samples. Note that for one of the Fresh samples the correlation the UV average is zero. This is because the Fresh sample was only illuminated from 420 to 490 nm while the UV average was generated from samples illuminated from 500 - 620 nm thus there is no wavelength crossover.

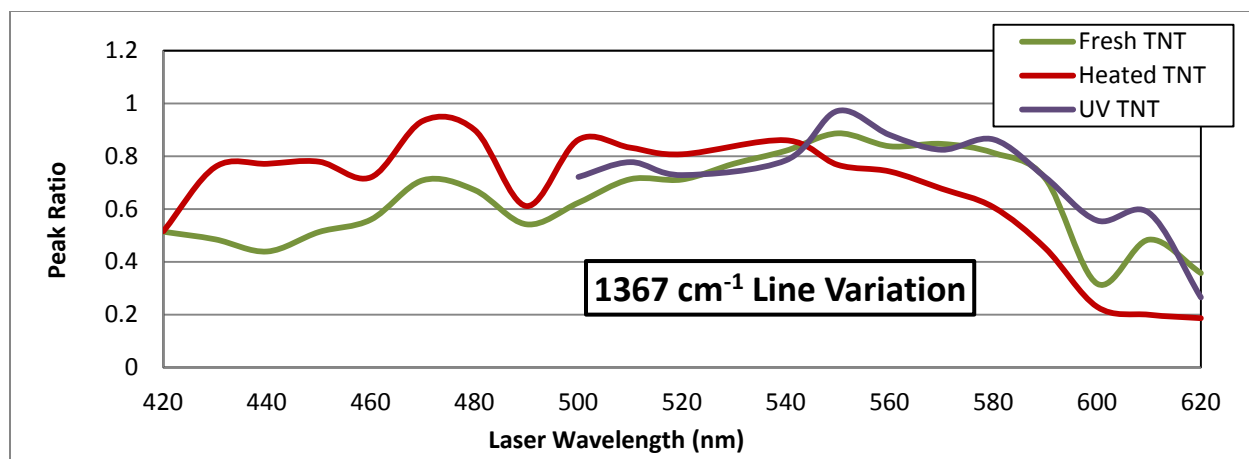
Single Signature Name	Fresh Average	Heated Average	UV Average
HeatedTNTVis_01_15_2013_HDF2_data.txt	0.9232	0.9654	0.9136
HeatedTNTVis_01_15_2013_Run10_HDF2_data.txt	0.9686	0.9806	0.9115
HeatedTNTVis_01_15_2013_Run2_HDF2_data.txt	0.9454	0.9243	0.8856
HeatedTNTVis_01_15_2013_Run3_HDF2_data.txt	0.9266	0.97	0.9091
HeatedTNTVis_01_15_2013_Run4_HDF2_data.txt	0.9348	0.9405	0.8742
HeatedTNTVis_01_15_2013_Run5_HDF2_data.txt	0.9459	0.9812	0.9202
HeatedTNTVis_01_15_2013_Run6_HDF2_data.txt	0.9509	0.9636	0.8607
HeatedTNTVis_01_15_2013_Run7_HDF2_data.txt	0.9433	0.9787	0.9157
HeatedTNTVis_01_15_2013_Run8_HDF2_data.txt	0.9415	0.9742	0.8823
HeatedTNTVis_01_15_2013_Run9_HDF2_data.txt	0.909	0.9568	0.882
HeatedTNTVis_01_16_2013_Run10b_HDF2_data.txt	0.8897	0.924	0.9035
HeatedTNTVis_01_16_2013_Run1b_HDF2_data.txt	0.9598	0.9704	0.9455
HeatedTNTVis_01_16_2013_Run2b_HDF2_data.txt	0.9446	0.9685	0.9432
HeatedTNTVis_01_16_2013_Run3b_HDF2_data.txt	0.9529	0.9735	0.9451
HeatedTNTVis_01_16_2013_Run4b_HDF2_data.txt	0.9545	0.9677	0.9422
HeatedTNTVis_01_16_2013_Run5b_HDF2_data.txt	0.9518	0.9496	0.9304
HeatedTNTVis_01_16_2013_Run6b_HDF2_data.txt	0.957	0.974	0.9502
HeatedTNTVis_01_16_2013_Run7b_HDF2_data.txt	0.9604	0.9712	0.9486
HeatedTNTVis_01_16_2013_Run8b_HDF2_data.txt	0.9403	0.9568	0.9347
HeatedTNTVis_01_16_2013_Run9b_HDF2_data.txt	0.8893	0.93	0.9187

Single Signature Name	Fresh Average	Heated Average	UV Average
UVTNTVis_01_23_2013_Run10b_HDF2_data.txt	0.8408	0.8463	0.9026
UVTNTVis_01_23_2013_Run1b_HDF2_data.txt	0.9482	0.9347	0.9529
UVTNTVis_01_23_2013_Run2b_HDF2_data.txt	0.9552	0.9588	0.9687
UVTNTVis_01_23_2013_Run3b_HDF2_data.txt	0.9563	0.9566	0.9725
UVTNTVis_01_23_2013_Run4b_HDF2_data.txt	0.9451	0.9544	0.9746
UVTNTVis_01_23_2013_Run5b_HDF2_data.txt	0.9273	0.9415	0.9645
UVTNTVis_01_23_2013_Run6b_HDF2_data.txt	0.8118	0.8127	0.8556
UVTNTVis_01_23_2013_Run7b_HDF2_data.txt	0.9423	0.9311	0.9496
UVTNTVis_01_23_2013_Run8b_HDF2_data.txt	0.9434	0.9376	0.9592
UVTNTVis_01_23_2013_Run9b_HDF2_data.txt	0.9165	0.9244	0.951

Batch 4 Baseline Removed







Behavior of the 1367 cm^{-1} line with respect to changes in laser illumination wavelength. Of note, the line height for the fresh and heated variants is the same at 420 nm but the heated samples has almost a factor of 2 greater intensity at 440 nm.

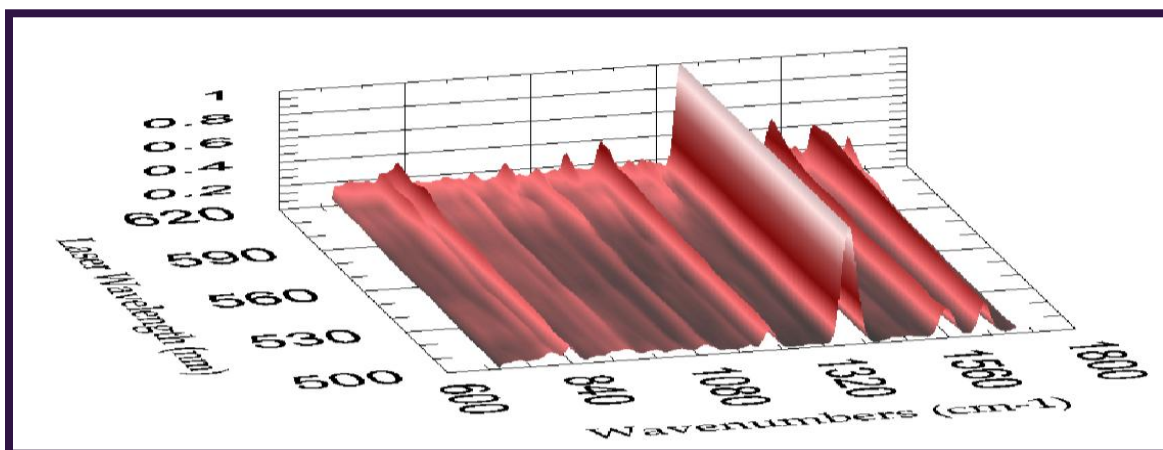
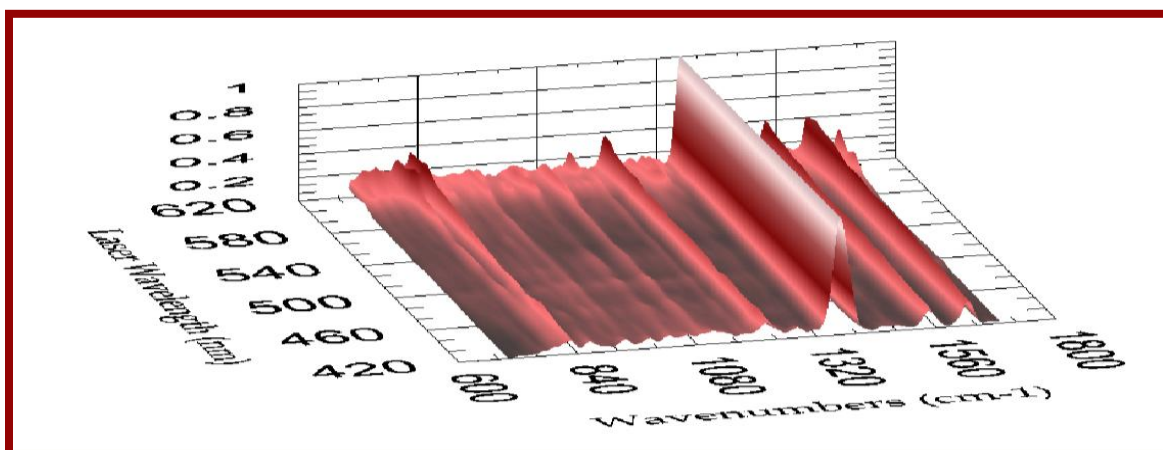
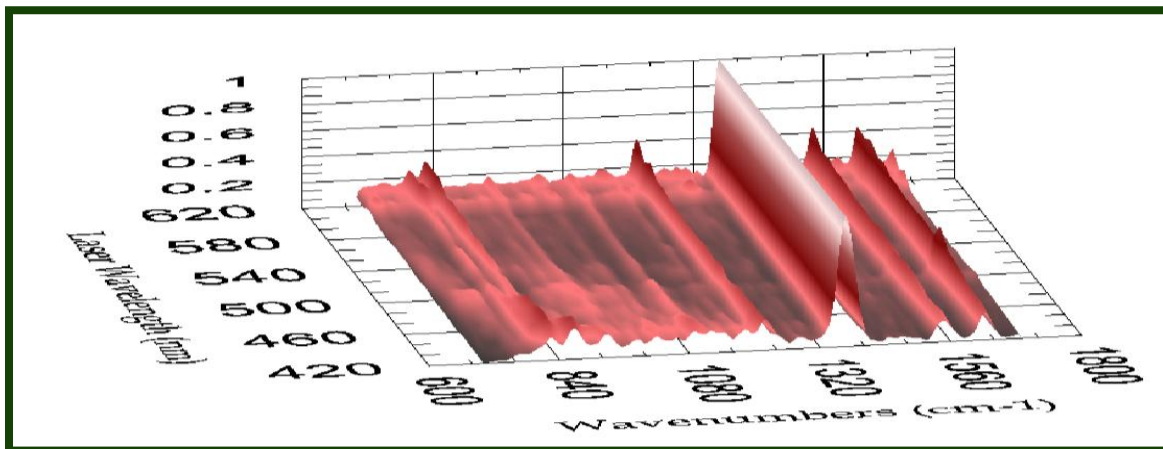
Single Signature Name	Fresh Average	Heated Average	UV Average
FreshTNTVis_01_04_2013_PostPro_data.txt	0.9717	0.9634	0.9632
FreshTNTVis_01_04_2013_Run10_PostPro_data.txt	0.8145	0.7736	0.8235
FreshTNTVis_01_04_2013_Run2_PostPro_data.txt	0.9693	0.9593	0.9591
FreshTNTVis_01_04_2013_Run3_PostPro_data.txt	0.958	0.9461	0.9468
FreshTNTVis_01_04_2013_Run4_PostPro_data.txt	0.9677	0.9575	0.9586
FreshTNTVis_01_04_2013_Run5_PostPro_data.txt	0.9546	0.948	0.9424
FreshTNTVis_01_04_2013_Run6_PostPro_data.txt	0.9577	0.945	0.9459
FreshTNTVis_01_04_2013_Run7_PostPro_data.txt	0.9735	0.9657	0.9641
FreshTNTVis_01_04_2013_Run8_PostPro_data.txt	0.9657	0.9581	0.9479
FreshTNTVis_01_04_2013_Run9_PostPro_data.txt	0.9353	0.9175	0.9192
FreshTNTVis_01_08_2013_PostPro_data.txt	0.9555	0.9518	0.9121
FreshTNTVis_01_08_2013_Run2_PostPro_data.txt	0.9466	0.938	0.9012
FreshTNTVis_01_08_2013_Run3_PostPro_data.txt	0.9669	0.9644	0.9359
FreshTNTVis_01_08_2013_Run4_PostPro_data.txt	0.8214	0.7859	0.7208
FreshTNTVis_01_08_2013_Run5_PostPro_data.txt	0.935	0.9088	0.8597
FreshTNTVis_01_09_2013_PostPro_data.txt	0.9856	0.9912	0
FreshTNTVis_01_09_2013_Run2_PostPro_data.txt	0.9562	0.9506	0.902
FreshTNTVis_01_09_2013_Run3_PostPro_data.txt	0.9796	0.9867	0.9562
FreshTNTVis_01_24_2013_Run1b_PostPro_data.txt	0.9883	0.9878	0.9846
FreshTNTVis_01_24_2013_Run2b_PostPro_data.txt	0.9626	0.9534	0.9569
FreshTNTVis_01_24_2013_Run3b_PostPro_data.txt	0.977	0.9702	0.9704
FreshTNTVis_01_24_2013_Run4b_PostPro_data.txt	0.9716	0.9648	0.9677
FreshTNTVis_01_24_2013_Run5b_PostPro_data.txt	0.9717	0.9612	0.9644
FreshTNTVis_01_24_2013_Run6b_PostPro_data.txt	0.9714	0.9602	0.9628

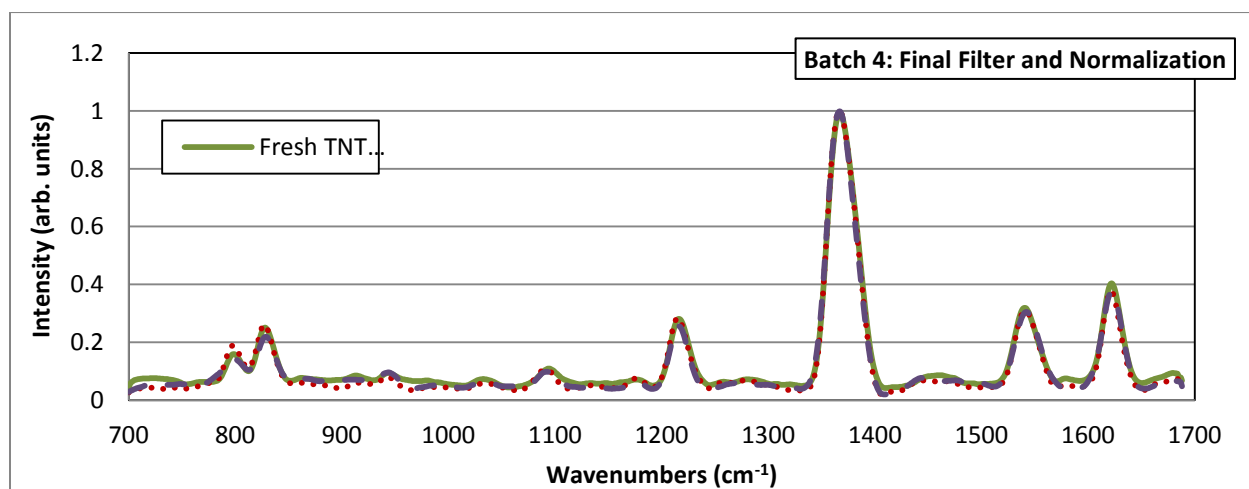
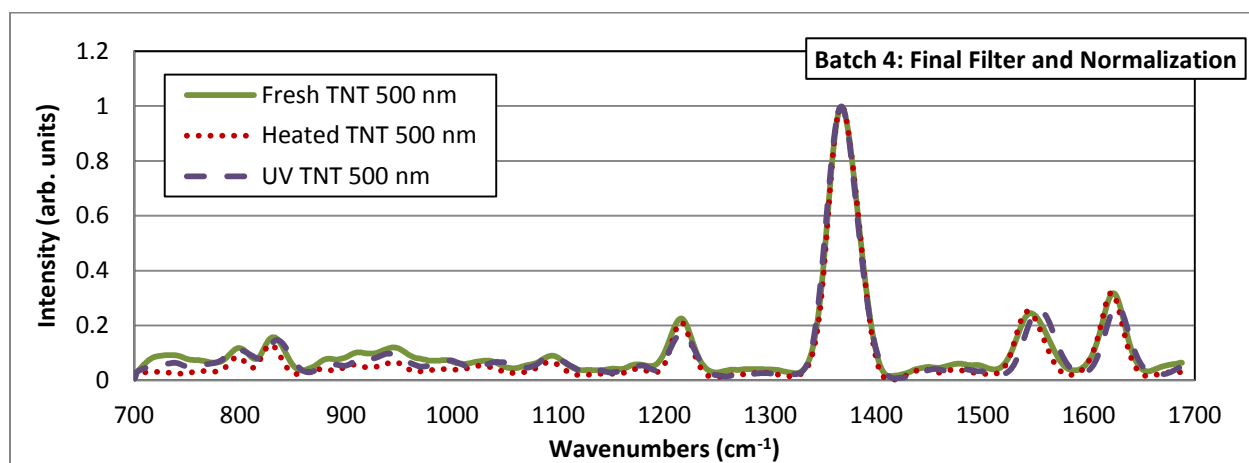
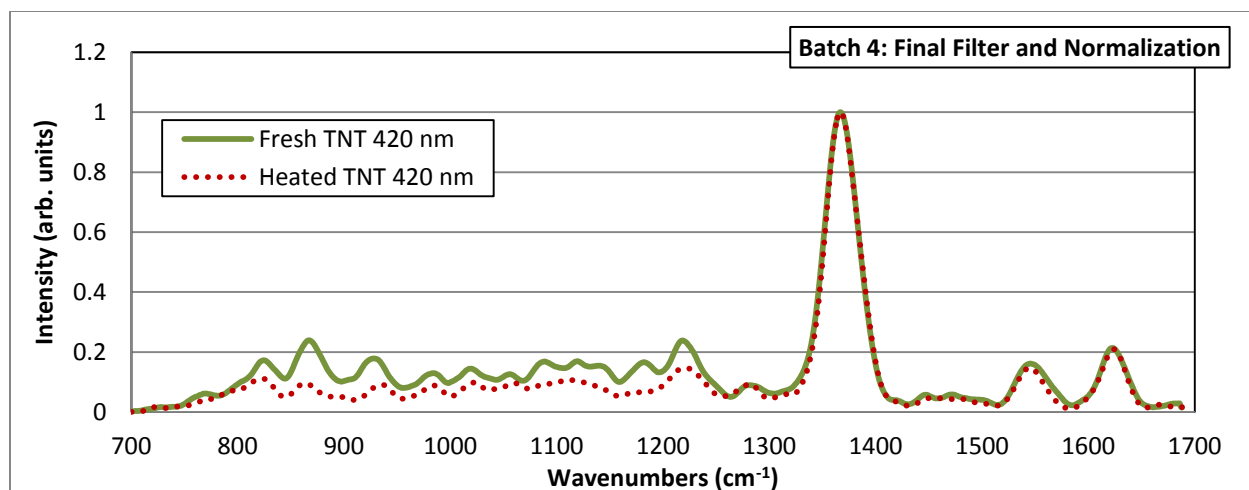
Single Signature Name	Fresh Average	Heated Average	UV Average
HeatedTNTVis_01_15_2013_PostPro_data.txt	0.9834	0.9932	0.9669
HeatedTNTVis_01_15_2013_Run10_PostPro_data.txt	0.9824	0.9889	0.9661
HeatedTNTVis_01_15_2013_Run2_PostPro_data.txt	0.9662	0.9687	0.9425
HeatedTNTVis_01_15_2013_Run3_PostPro_data.txt	0.9801	0.9913	0.9596
HeatedTNTVis_01_15_2013_Run4_PostPro_data.txt	0.969	0.9768	0.9442
HeatedTNTVis_01_15_2013_Run5_PostPro_data.txt	0.9801	0.9924	0.9653
HeatedTNTVis_01_15_2013_Run6_PostPro_data.txt	0.968	0.98	0.9435
HeatedTNTVis_01_15_2013_Run7_PostPro_data.txt	0.9787	0.991	0.9666
HeatedTNTVis_01_15_2013_Run8_PostPro_data.txt	0.9789	0.9894	0.9619
HeatedTNTVis_01_15_2013_Run9_PostPro_data.txt	0.9768	0.9903	0.9619
HeatedTNTVis_01_16_2013_Run10b_PostPro_data.txt	0.9552	0.9618	0.95
HeatedTNTVis_01_16_2013_Run1b_PostPro_data.txt	0.9599	0.9668	0.9524
HeatedTNTVis_01_16_2013_Run2b_PostPro_data.txt	0.952	0.962	0.9419
HeatedTNTVis_01_16_2013_Run3b_PostPro_data.txt	0.9573	0.9727	0.9509
HeatedTNTVis_01_16_2013_Run4b_PostPro_data.txt	0.9612	0.9681	0.9514
HeatedTNTVis_01_16_2013_Run5b_PostPro_data.txt	0.9677	0.9751	0.9602
HeatedTNTVis_01_16_2013_Run6b_PostPro_data.txt	0.9672	0.9732	0.9573
HeatedTNTVis_01_16_2013_Run7b_PostPro_data.txt	0.9674	0.9749	0.958
HeatedTNTVis_01_16_2013_Run8b_PostPro_data.txt	0.9521	0.9594	0.9469
HeatedTNTVis_01_16_2013_Run9b_PostPro_data.txt	0.9426	0.9542	0.9356

Single Signature Name	Fresh Average	Heated Average	UV Average
UVTNTVis_01_23_2013_Run10b_PostPro_data.txt	0.9071	0.8999	0.9292
UVTNTVis_01_23_2013_Run1b_PostPro_data.txt	0.9598	0.9542	0.9664
UVTNTVis_01_23_2013_Run2b_PostPro_data.txt	0.9704	0.9687	0.9699
UVTNTVis_01_23_2013_Run3b_PostPro_data.txt	0.9712	0.9686	0.9735
UVTNTVis_01_23_2013_Run4b_PostPro_data.txt	0.9753	0.9689	0.9811
UVTNTVis_01_23_2013_Run5b_PostPro_data.txt	0.9639	0.9585	0.9724
UVTNTVis_01_23_2013_Run6b_PostPro_data.txt	0.9026	0.8934	0.9269
UVTNTVis_01_23_2013_Run7b_PostPro_data.txt	0.9239	0.918	0.9415
UVTNTVis_01_23_2013_Run8b_PostPro_data.txt	0.9631	0.9587	0.9748
UVTNTVis_01_23_2013_Run9b_PostPro_data.txt	0.9299	0.9264	0.9487

Correlation Crosstables for detection: 50 of 54 signatures correctly identified. Of the 4 incorrect ID's only one had been incorrect under the previous processing regimen

Batch 4 Fully Normalize





Single Signature Name	Fresh Average	Heated Average	UV Average
FreshTNTVis_01_04_2013_FinalData.txt	0.9908	0.9845	0.9874
FreshTNTVis_01_04_2013_Run10_FinalData.txt	0.8896	0.8406	0.9177
FreshTNTVis_01_04_2013_Run2_FinalData.txt	0.9877	0.9823	0.9842
FreshTNTVis_01_04_2013_Run3_FinalData.txt	0.9836	0.9778	0.9801
FreshTNTVis_01_04_2013_Run4_FinalData.txt	0.9877	0.9845	0.9839
FreshTNTVis_01_04_2013_Run5_FinalData.txt	0.9844	0.9792	0.9756
FreshTNTVis_01_04_2013_Run6_FinalData.txt	0.9814	0.9721	0.9745
FreshTNTVis_01_04_2013_Run7_FinalData.txt	0.9888	0.9854	0.9843
FreshTNTVis_01_04_2013_Run8_FinalData.txt	0.9852	0.9819	0.9761
FreshTNTVis_01_04_2013_Run9_FinalData.txt	0.9719	0.9514	0.9676
FreshTNTVis_01_08_2013_FinalData.txt	0.9724	0.9745	0.954
FreshTNTVis_01_08_2013_Run2_FinalData.txt	0.9697	0.9644	0.9487
FreshTNTVis_01_08_2013_Run3_FinalData.txt	0.9797	0.9802	0.9664
FreshTNTVis_01_08_2013_Run4_FinalData.txt	0.8844	0.8383	0.7994
FreshTNTVis_01_08_2013_Run5_FinalData.txt	0.9562	0.9333	0.8984
FreshTNTVis_01_09_2013_FinalData.txt	0.9749	0.9952	0
FreshTNTVis_01_09_2013_Run2_FinalData.txt	0.9701	0.9729	0.9389
FreshTNTVis_01_09_2013_Run3_FinalData.txt	0.9734	0.992	0.967
FreshTNTVis_01_24_2013_Run1b_FinalData.txt	0.9935	0.9955	0.9911
FreshTNTVis_01_24_2013_Run2b_FinalData.txt	0.9863	0.98	0.9837
FreshTNTVis_01_24_2013_Run3b_FinalData.txt	0.9904	0.986	0.9876
FreshTNTVis_01_24_2013_Run4b_FinalData.txt	0.992	0.9871	0.9881
FreshTNTVis_01_24_2013_Run5b_FinalData.txt	0.9886	0.9822	0.9873
FreshTNTVis_01_24_2013_Run6b_FinalData.txt	0.9888	0.9829	0.9857

Single Signature Name	Fresh Average	Heated Average	UV Average
HeatedTNTVis_01_15_2013_FinalData.txt	0.9767	0.9958	0.9799
HeatedTNTVis_01_15_2013_Run10_FinalData.txt	0.9816	0.9944	0.9789
HeatedTNTVis_01_15_2013_Run2_FinalData.txt	0.9749	0.9816	0.9638
HeatedTNTVis_01_15_2013_Run3_FinalData.txt	0.9754	0.9953	0.9771
HeatedTNTVis_01_15_2013_Run4_FinalData.txt	0.9782	0.9864	0.9656
HeatedTNTVis_01_15_2013_Run5_FinalData.txt	0.9754	0.9961	0.9774
HeatedTNTVis_01_15_2013_Run6_FinalData.txt	0.9722	0.9892	0.9607
HeatedTNTVis_01_15_2013_Run7_FinalData.txt	0.9723	0.9948	0.9758
HeatedTNTVis_01_15_2013_Run8_FinalData.txt	0.9758	0.9947	0.9737
HeatedTNTVis_01_15_2013_Run9_FinalData.txt	0.9711	0.9948	0.976
HeatedTNTVis_01_16_2013_Run10b_FinalData.txt	0.9754	0.9816	0.972
HeatedTNTVis_01_16_2013_Run1b_FinalData.txt	0.984	0.9874	0.9807
HeatedTNTVis_01_16_2013_Run2b_FinalData.txt	0.9761	0.9829	0.9718
HeatedTNTVis_01_16_2013_Run3b_FinalData.txt	0.9828	0.9858	0.9804
HeatedTNTVis_01_16_2013_Run4b_FinalData.txt	0.9824	0.9859	0.9773
HeatedTNTVis_01_16_2013_Run5b_FinalData.txt	0.9876	0.9897	0.9845
HeatedTNTVis_01_16_2013_Run6b_FinalData.txt	0.9861	0.9905	0.9808
HeatedTNTVis_01_16_2013_Run7b_FinalData.txt	0.9883	0.9918	0.9829
HeatedTNTVis_01_16_2013_Run8b_FinalData.txt	0.9851	0.9897	0.9808
HeatedTNTVis_01_16_2013_Run9b_FinalData.txt	0.9701	0.9816	0.9658

Single Signature Name	Fresh Average	Heated Average	UV Average
UVTNTVis_01_23_2013_Run10b_FinalData.txt	0.9568	0.9498	0.9668
UVTNTVis_01_23_2013_Run1b_FinalData.txt	0.9863	0.9819	0.9878
UVTNTVis_01_23_2013_Run2b_FinalData.txt	0.9852	0.9854	0.9856
UVTNTVis_01_23_2013_Run3b_FinalData.txt	0.9883	0.9869	0.9893
UVTNTVis_01_23_2013_Run4b_FinalData.txt	0.9888	0.9845	0.9923
UVTNTVis_01_23_2013_Run5b_FinalData.txt	0.9833	0.979	0.9894
UVTNTVis_01_23_2013_Run6b_FinalData.txt	0.9577	0.95	0.9682
UVTNTVis_01_23_2013_Run7b_FinalData.txt	0.9606	0.9568	0.9724
UVTNTVis_01_23_2013_Run8b_FinalData.txt	0.9837	0.9809	0.9896
UVTNTVis_01_23_2013_Run9b_FinalData.txt	0.9669	0.9646	0.9774